Transmission and Reconstruction of Signals Using Functionally Related Zero Crossings

Doctor of Philosophy Thesis

By

Farokh Alim Marvasti

Rensselaer Polytechnic Institute Troy, New York

June 1973

TRANSMISSION AND RECONSTRUCTION OF SIGNALS USING FUNCTIONALLY RELATED ZERO CROSSINGS

by

Farokh Alim Marvasti

A Thesis Submitted to the Graduate
Faculty of Rensselaer Polytechnic Institute
in Partial Fulfillment of the
Requirements for the Degree of
DOCTOR OF PHILOSOPHY
Major Subject: Electrical Engineering

Approved by the
Examining Committee:

Lester A. Gerhardt, Thesis Advisor

Dean Arden, Member

A. Bruce Carlson, Member

Melvin Jaeobsen, Member

Rensselaer Polytechnic Institute
Troy, New York

June 1973

TABLE OF CONTENTS

LIST OF SYMBOLS

$x(t)$	=	The random or baseband signal that has to be recovered at the receiver
$z(t)$	=	The deterministic signal to be intersected with $x(t)$
$y(t)$	=	$x(t) - z(t)$
$F[x(t)]$	=	A function of $x(t)$
n_o	=	The average number of zero crossings
n_c	=	The average number of level crossings at level c
$s(w)$	=	Power spectrum of $x(t)$ when x is Gaussian
$R(0)$	=	Autocorrelation of the signal $x(t)$ at $\tau = 0$
$x_s(t)$	=	A train of nonuniform pulses that are zeros of $y(t)$
T	=	The interval in which there is only one arbitrarily positioned time sample
τ	=	A random variable defined in the region $a \leq \tau < T$
B_{neq}	=	Bandwidth of the n^{th} harmonic term
$E[\ ]$	=	Expectation of a random variable
$\|\ \|^2$	=	Average Power

ACKNOWLEDGEMENTS

I would like to thank my thesis adviser Professor Lester Gerhardt for his liberal attitude and open mindedness without which this dissertation would not have been possible. I also appreciate his guidance and encouragement. I wish to thank the faculty members of systems division at Rensselaer Polytechnic Institute for their criticism and suggestions. I also wish to thank Graphic Sciences, Inc. for letting me use their facilities and especially appreciate Mark Rinaldi for building the Adaptive Quantizer.

Finally, I would like to thank my colleague Bülent Sankur for his help and Priscilla Keene for partially editing and typing my theses. I am especially grateful to Cynthia Lee for her patient and meticulous job in typing most of the first and the final draft of the dissertation.

PART I

INTRODUCTION

The aim of this dissertation is a unified analysis and development of new techniques to eliminate some of the redundancy in digital communication by using different implementations for the source encoder and decoder at the transmitter and receiver respectively. It is our intention to optimize the communication system in terms of transmission rate, bandwidth requirements and quantization noise by developing novel techniques that are practically feasible, by using nonuniform samples at one bit per sample at equal or less than the Nyquist rate with no quantization noise.

Various attempts have been made by others,[1,2,3,4] with partial success, to eliminate the redundancy and optimize the source coding aspects of the communication systems. These techniques, called data compression methods, usually either exploit the time or spatial correlation of samples or design the encoder using the probability density of the signal.

Any digital encoding where the zero crossings convey

information can be represented as the intersection of two signals. One of the signals is a function of the random (baseband) signal, x(t), to be transmitted. The other signal is either a random signal dependent on x(t) or a deterministic signal,z(t). Figure 1-1 is a flow chart for the intersection of two signals of various types. Depending on the types of signals, different modulations and digital encodings are obtained, e.g., the intersection of a random signal, x(t), with a sawtooth periodic waveform, z(t), is pulse position modulation (Section IV-1-a) while delta modulation is the intersection of a random signal, x(t), with another random signal, z(t), dependent on x(t) (Section V-3). A unified time domain and frequency analysis for any digital encoder that can be represented as the intersection of two signals, together with simple reconstruction techniques are the main core of the dissertation.

In the following, Section II will outline the general analysis for the intersection problem. Reconstruction of the nonuniform pulses and the noise analysis is also included. Section III contains the intersection of signals with horizontal waveforms. Section IV discusses the intersection with

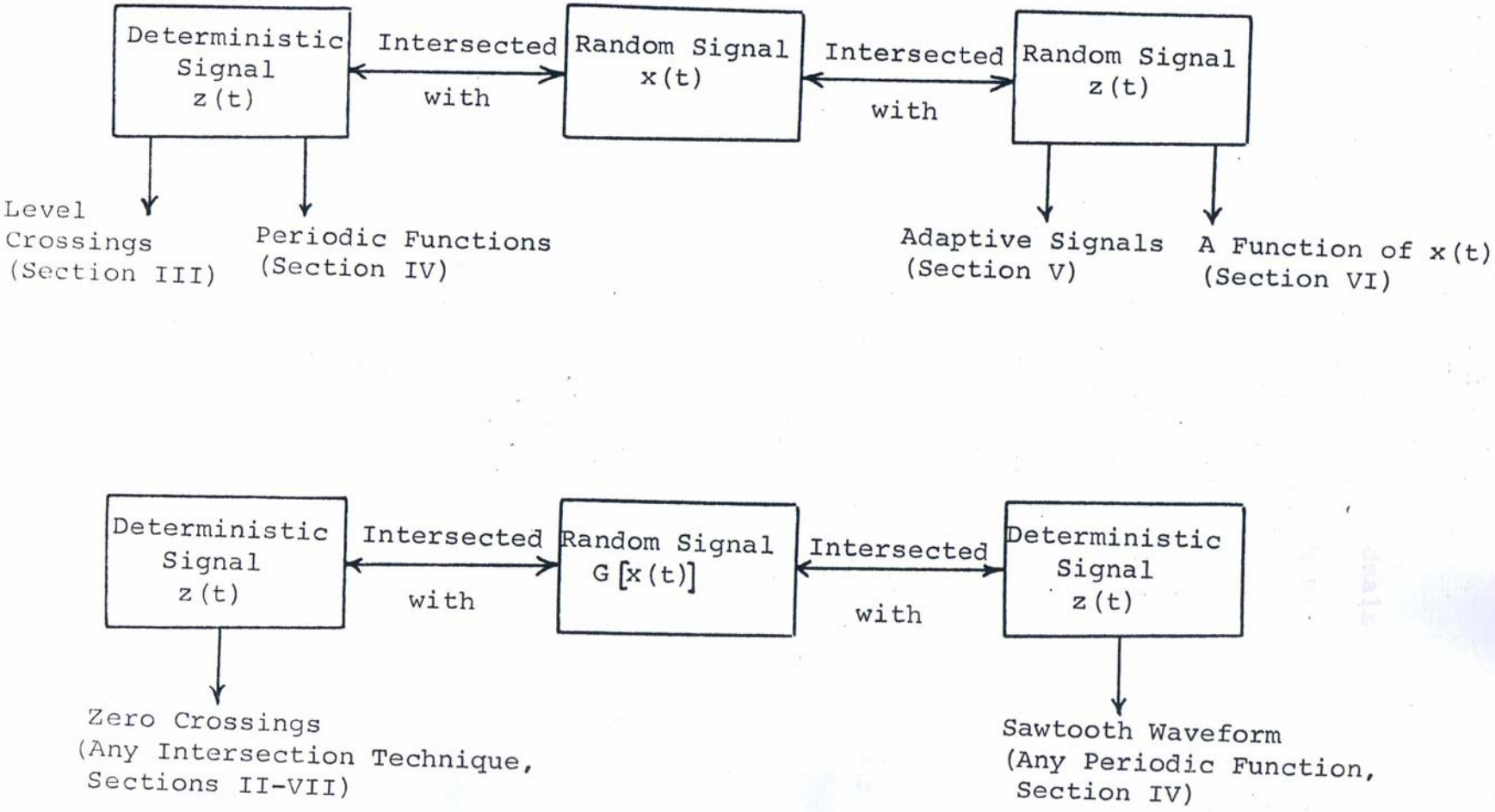

Figure 1-1: The Flow Chart of the Intersection of a Random Signal and a Deterministic Signal

periodic waves, while Section V deals with the adaptive techniques. Sections III through VII are the center or core of this dissertation. Section VI considers other intersection methods. The standard modulation techniques like F.M., P.M., F.S.K. and P.S.K. are discussed in Section VII. Section VIII discusses practical nonuniform sampling reconstruction schemes. The experimental results for the verification of Section IV and V are included in Section IX. The conclusions and recommendations are discussed in Section X.

PART II

GENERAL ANALYSIS

1. The Intersection of Random and Deterministic Signals

Suppose a random signal is intersected with a deterministic signal. The points of intersection of the two signals are transmitted by a pulse waveform at the time of occurrence of the intersection. At the receiver the deterministic signal is generated. Whenever a pulse is received, the deterministic signal is sampled. These pulses, like pulse position modulation, convey the amplitude information in time, and from this time information, the amplitude of the samples are reconstructed on the deterministic signal. Note that for this kind of a system there is no need to transmit the polarity of the samples. That is the transmitted pulses are unipolar, which is one bit per sample. Sampling at the intersection of two signals is equivalent to sampling at the zero crossings of the difference between those two signals. We formulate the above statement as follows

$$y(t) = x(t) - z(t) \qquad 2\text{-}1$$

where $x(t)$ is the random signal and $z(t)$ is the deterministic

signal. The average zero crossings for $y(t)$ is $E[y(t)] = o$. These average zero crossings are only known if $y(t)$ is Gaussian distributed[5] or if $x(t)$ is Gaussian and $z(t)$ is a sine wave[6] or a D.C. level. In other cases the zero crossing problem remains unsolved. The average zero crossings are important because we are interested to see how the average samples per second compare with the Nyquist rate. It is true that the average zero crossings of a random signal are always less than or equal to the Nyquist rate.[5] In order to achieve the Nyquist rate, $y(t)$ has to have a bandwidth higher than that of $x(t)$ (Equation 2-1). Since subtracting in time domain is equivalent to subtracting in frequency domain, $z(t)$ should have the same bandwidth as $y(t)$, and thus, a greater bandwidth than $x(t)$. Note that inherent in the above is that the Fourier transforms of $x(t)$ and $z(t)$ exist. However, a non-periodic signal is not a practical deterministic signal. It is difficult to have two identical non-periodic signals, one at the transmitter and the other at the receiver. Periodic signals, on the other hand, are very easy to reconstruct if their frequencies are known. It is obvious that if the amplitude of the periodic signal, $z(t)$, is large, the average

zero crossings of y(t) in Equation 2-1 will approach twice that of the frequency of the periodic signal (Figure 2-1). If the amplitude of z(t) is low relative to the random signal, x(t), the average zero crossings of y(t) will approach the zero crossings of the random signal, x(t) (Figure 2-2).[5]

Figure 2-1-a -The Random Signal x(t)

Figure 2-1-b The Random Signal subtracted from a Sine Signal. The average zero crossings $\simeq \frac{2}{T}$ when the amplitude of the Sine Wave is large.

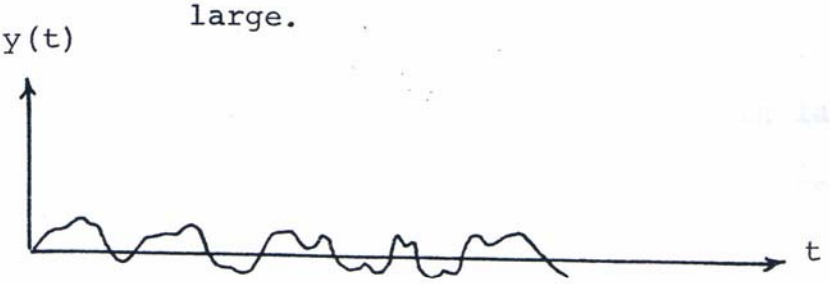

Figure 2-2 The average zero crossings $\simeq$ the average zero crossings of x(t) when the amplitude of the Sine Wave is small.

2. Time and Spectral Domain Analysis

Generation of nonuniform samples at the receiver can be represented as the product of the received nonuniform impulse sequence with the deterministic signal. The random signal can then be reconstructed if the nonuniform sampling theorem is satisfied (See Appendix A). Practical reconstruction of a signal from its nonuniform samples is discussed in Section VIII in detail. However, it is the intention of this section to analyze the nonuniform pulses in the time and frequency domains and to suggest a simpler reconstruction of the random signal, $x(t)$, from the nonuniform pulses, provided that some conditions are satisfied. The general analysis of the intersection of a random signal and a deterministic function is discussed below. Each specific deterministic signal with its particular analysis will be discussed in later sections.

Suppose the random signal, $x(t)$, is intersected with the deterministic signal, $z(t)$ (Figure 2-3).

One bit samples are then obtained at the times of crossings of the deterministic and random signals. The object is to find the conditions for the deterministic signal

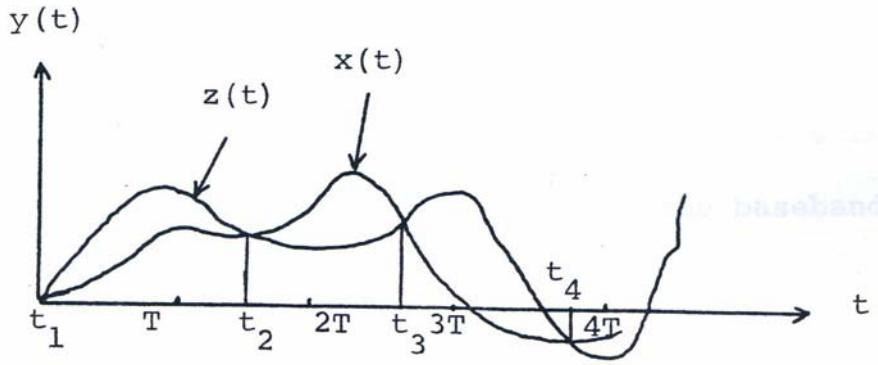

Figure 2-3. Intersection of a Random Signal with a Deterministic Signal

so that x(t) can be reconstructed from the nonuniform samples in a simple way, which is to be described in the next section.

The deterministic signals are divided in two distinct classes, i.e., periodic and nonperiodic signals. The general treatment of periodic signals are discussed in Section IV. Nonperiodic signals that have Fourier transforms are analyzed as follows:

It is assumed that there is only one sample in each interval T. If the above assumption is not satisfied, then the following analysis will not be true and the baseband signal has to be reconstructed from the nonuniform samples using the more complicated procedures as described in Section VIII. The impulses at the intersection points can be written as:

$$x_s(t) = A \sum_{m=1}^{\infty} \delta(t-t_m) \qquad 2\text{-}2$$

where $t_m = (m-1)T + \tau$, $0 \leq \tau < T$, and A is the area of each impulse. An impulse can be represented by:

$$\delta(t-t_m) = |\dot{g}(t_m)|\,\delta[g(t)] \qquad 2\text{-}3$$

where $g(t_m) = 0$, $g(t \neq t_m) \neq 0$, and $\dot{g}(t_m) \neq 0$. $g(t)$ can be

any function satisfying the above conditions. Therefore, we choose:

$$g(t) = t - (m-1)T - \alpha [x(t) - z(t)] - \tau \qquad 2\text{-}4$$

α is a constant such that

$$g(t_m) = o,\ g(t \neq t_m) \neq o$$

and

$$\dot{g}(t_m) = 1 - \alpha [\dot{x}(t_m) - \dot{z}(t_m)] \neq o \qquad 2\text{-}5$$

Substituting Equation 2-3 and 2-4 in Equation 2-2, we get:

$$x_s = A \sum_{m=1}^{\infty} | 1 - \alpha [\dot{x}(t_m) - \dot{z}(t_m)] | \delta \{ t-(m-1)T - \alpha [x(t) - z(t)] - \tau \} \qquad 2\text{-}6$$

If we make another assumption that $1 < \alpha [\dot{x}(t) - \dot{z}(t)]$, equation 2-6 becomes:

$$x_s = A \{ 1 - \alpha [\dot{x}(t) - \dot{z}(t)] \} \sum_{m=1}^{\infty} \delta \{ t - (m-1)T - \alpha [x(t) - z(t)] - \tau \} \qquad 2\text{-}7$$

Using the following substitution, we get:

$$p = t - \alpha [x(t) - z(t)] - \tau$$

$$x_s = A \{ 1 - \alpha [\dot{x}(t) - \dot{z}(t)] \} \sum_{m=1}^{\infty} \delta [p - (m-1)T] \qquad 2\text{-}8$$

The sum of periodic impulses in Equation 2-8 can be expanded in Fourier series in terms of P (See Appendix B)

$$x_s = \frac{A}{T}\{ 1 - \alpha[\dot{x}(t) - \dot{z}(t)]\} \sum_{n=-\infty}^{\infty} e^{\frac{j2\pi n}{T} P} \qquad 2\text{-}9$$

Substituting the value of P in the above equation, we get:

$$x_s = \frac{A}{T}\{1 - \alpha[\dot{x}(t) - \dot{z}(t)]\} \sum_{n=-\infty}^{\infty} e^{\frac{j2\pi n}{T}\{t - \alpha[x(t)-z(t)] - \tau\}} \qquad 2\text{-}10$$

Equation 2-10 can be rewritten as

$$x_s = \frac{A}{T}\{1 - \alpha[\dot{x}(t) - \dot{z}(t)]\{1 + 2 \sum_{n=1}^{\infty} \cos\{\frac{2\pi nt}{T} - \frac{2\pi n}{T}\}\alpha[x(t) - z(t)] - \tau\}\} \qquad 2\text{-}11$$

The above equation is the Fourier series representation of Equation 2-2. The baseband term of the series is:

$\frac{A}{T}\{ 1 - \alpha[\dot{x}(t) - \dot{z}(t)] \}$ and the principle term is

$$\{ 1 - \alpha[\dot{x}(t) - \dot{z}(t)] \} \cos\{ \frac{2\pi t}{T} - \frac{2\pi\alpha}{T}[x(t) - z(t)] - \frac{2\pi}{T}\tau \}$$

If $x(t) - z(t)$ is bandlimited, the harmonic terms of the Fourier series in the above equation are equivalent to the summation of phase modulated signals with carrier frequency $\frac{2\pi n}{T}$ and index of modulation $\frac{2\pi n \alpha}{T}$. The equivalent bandwidth of the P.M. signal is directly dependent on the index of modulation. Hence, the bandwidth increases with increasing n. Depending on the bandwidth of $x(t)$ and the periodicity T, the frequency spectrum of the nonuniform pulses x_s resembles Figure 2-4, 2-5, and 2-6.

Figure 2-4 shows the case where there is no spectrum overlapping at low frequencies. Figure 2-5 is an example of the case where the constant term and the principle term are not aliased. Figure 2-6 resembles the spectrum of an aliased signal.

The practical implications of the assumptions of the Equations 2-6 through 2-9 are mentioned in Part III for each specific deterministic signal.

The analysis for a deterministic periodic signal is slightly different and in fact simplified from the above and is discussed in detail in Section IV. There, a simple reconstruction method is developed provided that the inverse

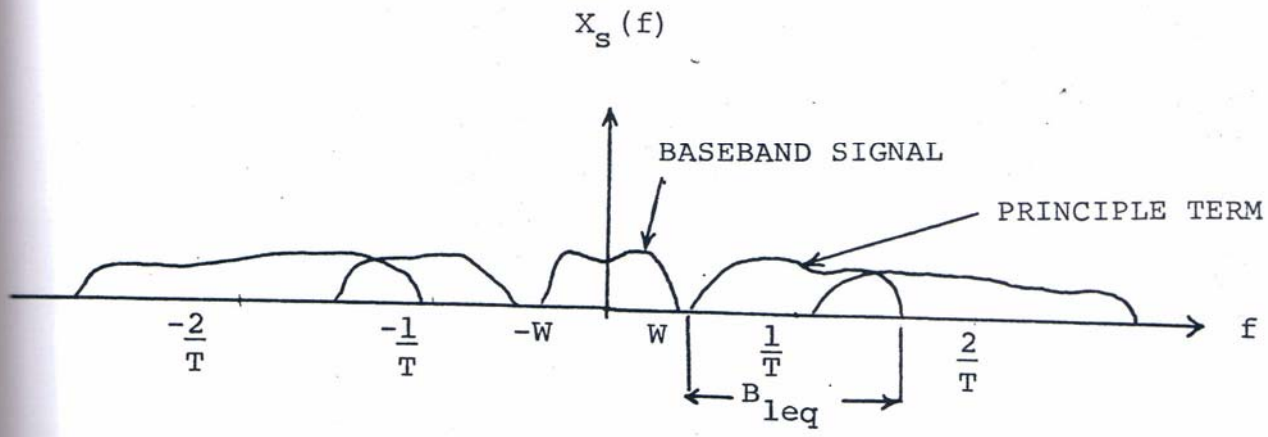

Figure 2-4. The Spectrum of a Recoverable Signal From a Train of Impulses

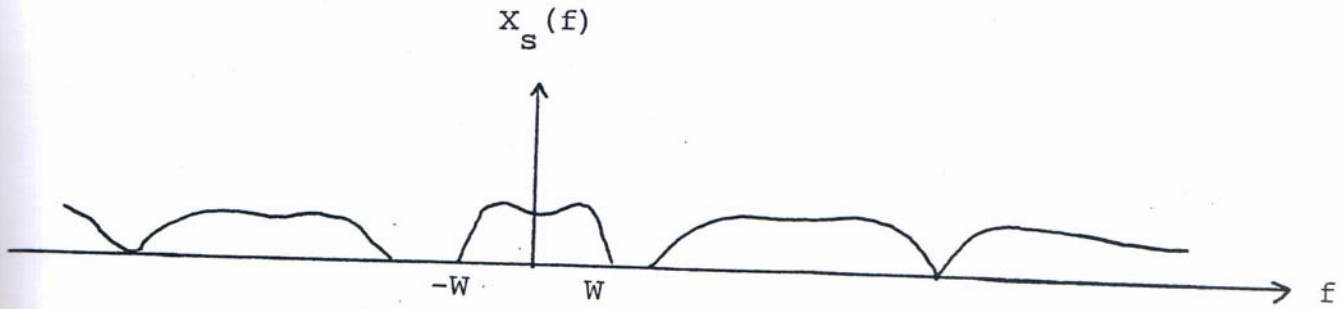

Figure 2-5. The Spectrum of $x_s(t)$.

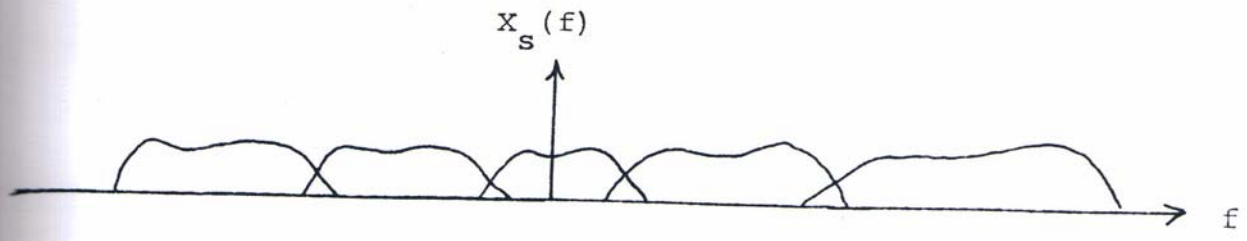

Figure 2-6. The Spectrum of an Aliased $x_s(t)$.

function of the periodic signal exists in each interval and provided that the amplitude and the magnitude of the slope of the periodic signal is greater than the maximum amplitude and magnitude of the slope of the random signal respectively.

The same type of analysis does not hold in general for nonperiodic signals because the inverse function of the nonperiodic signal in each interval (local inverse) may not exist in general, in fact may be different in each interval. Also this periodic analysis does not apply to the adaptive methods developed in the dissertation since the inverse function in each interval depends on the previous intervals. However, each case will be analyzed individually from the intersection point of view with appropriate modifications.

3. Reconstruction

As mentioned before, nonuniform samples can be generated from the deterministic signal, $z(t)$, at the times of received pulses. Practical and theoretical reconstruction of the random signal from the nonuniform samples are discussed in detail in Section VIII and Appendix A respectively.

However, the spectrum analysis in the previous section suggests a simpler reconstruction scheme if some conditions are satisfied. The conditions are summarized below:

1. α in Equation 2-4 should satisfy Equation 2-5.
2. $z(t)$ must be differentiable.
3. $1 > \alpha [\dot{x}(t) - \dot{z}(t)]$
4. $z(t)$ is bandlimited.

If the above conditions are satisfied, the nonuniform pulses can be expanded in Fourier series. The frequency spectra of the pulses are depicted in Figure 2-4 through 2-6. Depending on the bandwidth, W, of $x(t) - z(t)$, and the equivalent bandwidth, B_{neq}, of the n^{th} harmonic term, different spectra are obtained (Figures 2-4, 2-5, and 2-6). If $\frac{1}{T} < W + \frac{B_{leq}}{2}$, the frequency spectrum is aliased (Figure 2-6). Therefore, the random signal, $x(t)$, cannot be reconstructed by frequency

domain analysis. However, $x(t)$ might be reconstructed by the techniques mentioned in Section VIII. Since the bandwidth of a phase modulated signal is always greater than 2W, the condition $\frac{1}{T} < 2W$ means that the Nyquist rate is not satisfied and the nonuniform pulses cannot be reconstructed (See Appendix A).

If $\frac{1}{T} \geq W + \frac{B_{leq}}{2}$, there is no spectrum overlapping in the region $-W \leq f \leq W$ (Figures 2-4 and 2-5). Thus, a low pass filter with a bandwidth of W will eliminate all the harmonic terms. The output of the low pass filter is $\{1 - \alpha[\dot{x}(t) - \dot{z}(t)]\}$. After subtracting 1 and integration, the result is $\alpha[x(t) - z(t)]$. The random signal, $x(t)$, is retrieved by adding $\alpha z(t)$ to $\alpha[x(t) - z(t)]$. This reconstruction scheme is depicted in Figure 2-7.

In the next chapters, we shall discuss the different intersecting waves.

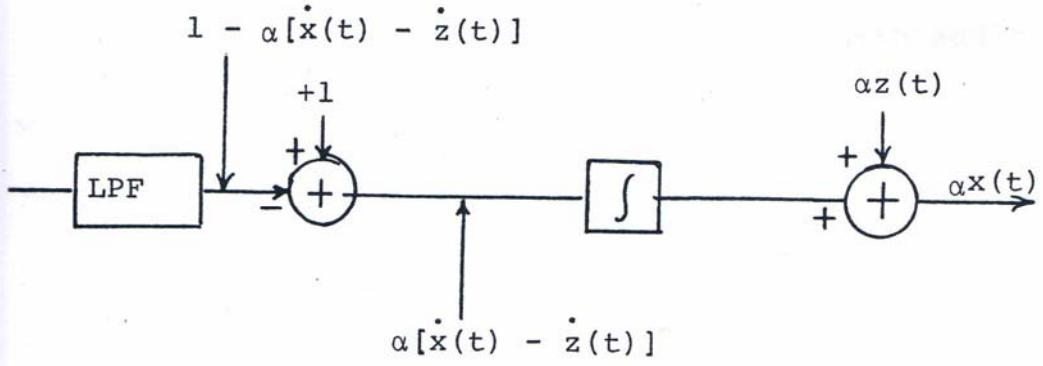

Figure 2-7 - Reconstruction Scheme for the Nonuniform Pulses when $\frac{1}{T} \geq w + \frac{B_{1eq}}{2}$

4. Noise analysis

It is known that pulse time modulation techniques have noise immunity similar to F.M. The noise analysis depends on the means of transmission, i.e. either the nonuniform pulses or a square wave or a P.M. signal that are transmitted to convey the zero crossing information. The effect of noise is also dependent on the type of receiver, i.e., the reconstruction scheme. Each case will be treated briefly for the sake of completeness.

The transmission of nonuniform pulses with additive white noise is considered first. It is assumed that, at the receiving end, there is a threshold level, which extracts pulses from noise. The white noise may deteriorate completely some signal pulses, produce unwanted pulses and break a signal pulse into several pulses of smaller width as shown in Figure 2-9. Assuming that there is one nonuniform pulse in each interval and the threshold level is only sensitive at the positive going transitions, the regenerated pulse train is shown in Figure 2-10. The distortion, due to noise, shifts a signal by a fraction of its width, causes some

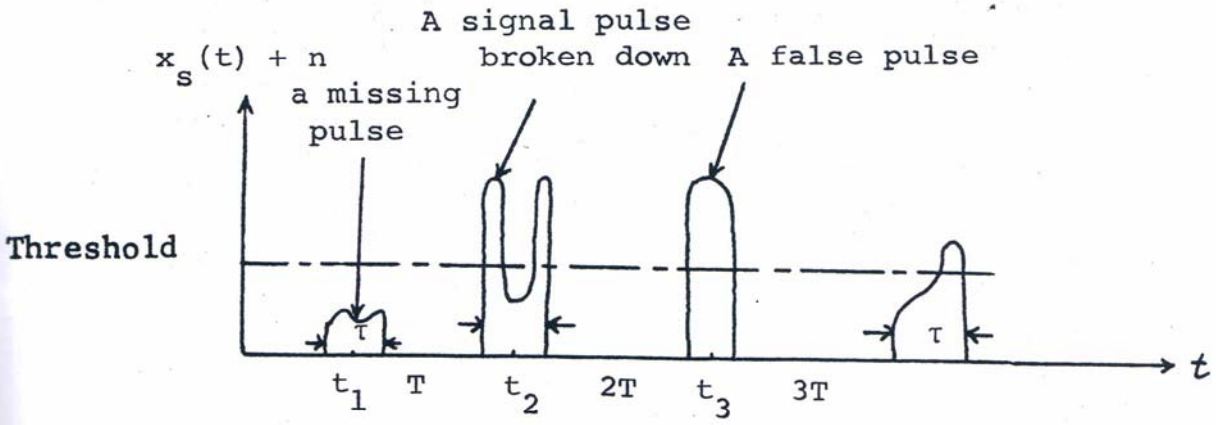

Figure 2-9. A Train of Non-Uniform Pulses plus noise.

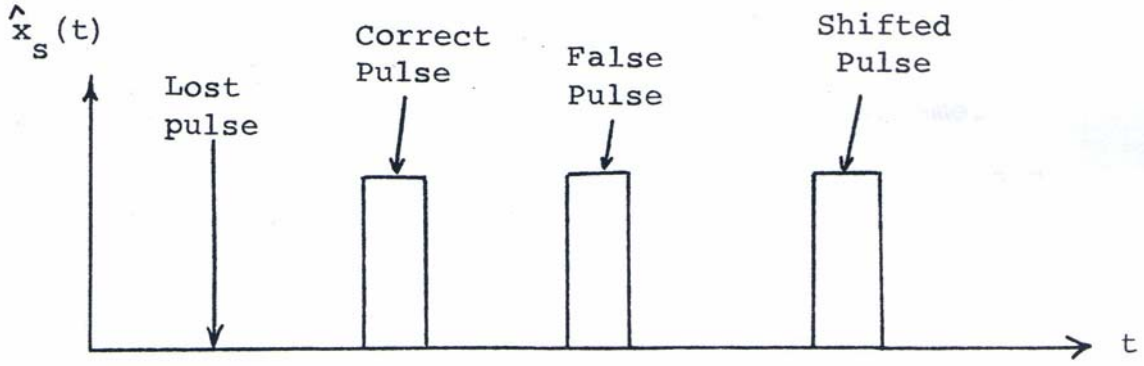

Figure 2-10. The Train of Pulses After the Threshold Detection

pulses to be lost, or causes false pulses. If the signal pulse width, τ, is very small, the pulse shifts are negligible, but small pulse widths require higher bandwidths. Hence, there is a trade-off between bandwidth and phase jitter. Appendix C gives the analysis for phase jitter when the amplitude of noise is small and the errors due to false and missing pulses are ignored. On the contrary, if the amplitude of noise is large, relative to the pulse amplitudes, and if the pulse width, τ, is small, relative to the interval T, phase jitter is negligible. However, the error due to false and missing pulses becomes considerable. The average error per unit time is calculated in Appendix D. The error analysis for a bipolar train of pulses (Section V) is given in Reference 34. The signal to noise ratio at the output of the receiver depends on the reconstruction scheme.

If low pass filtering and integrating of Figure 2-7 is used for reconstruction of the signal, x(t), the signal to noise ratio is found as follows:

$$y(t) = x_s(t) + n(t) \qquad 2\text{-}19$$

Where x_s is the train of pulses and n(t) is a white noise of average power N_o.

After low pass filtering, Equation 2-19 becomes:

$$Y_{LP} = 1 - \dot{F}[x(t)] + n_{LP}(t) \qquad 2\text{-}20$$

Provided that there is no spectrum overlapping, n_{LP} is the white noise after low pass filtering with a bandwidth of W. Subtracting the constant value and integrating yields:

$$Q = F[x(t)] + \int_o^t n_{LP}(P)\,dP \qquad 2\text{-}21$$

The signal to noise ratio at this point is:

$$S/N = \frac{||\dot{F}[x(t)]||^2}{\sigma^2}$$

where σ^2 is the variance of noise that can be found as follows:

$$v = \int_o^t n_{LP}(t)\,dt$$

$$Ev = E\int_o^t n_{LP}(P)\,dP = \int_o^t E[n_{LP}(P)]\,dP = o \qquad 2\text{-}24$$

since $E[n_{LP}] = En = o$.

$$Ev^2 = E\left[\int_o^t n_{LP}(p)\,dp\right]^2 = E\left\{\int_o^t n_{LP}(q)\,dq \int_o^t n_{LP}(p)\,dp\right\} =$$

$$= E\int_o^t\int_o^t n_{LP}(q)\,n_{LP}(p)\,dqdp = \int_o^t\int_o^t E[n_{LP}(p)\,n_{LP}(q)]dpdq =$$

$$= \int_o^t\int_o^t R_{LP}(p-q)\,dpdq \qquad 2\text{-}25$$

where $R_{LP}(p-q)$ is the autocorrelation of $n_{LP}(t)$ that is a sinc function as depicted in Figure 2-11. Substituting the sinc function in the Equation 2-25 yields:

$$Ev^2 = \int_o^t dq \int_o^t 2N_oW\,\mathrm{sinc}(p-q)\,dp = 2N_oW \int_o^t dq \int_o^t \mathrm{sinc}(p-q)\,dp$$

2-26

When W is large, sinc (p-q) approaches $\delta(p-q)$, $Ev^2 = 2N_oWt$ and $\sigma^2 = E(v)^2 - (Ev)^2 = Ev^2$. The variance depends on time, which shows the process is nonstationary as expected.

The inverse function of Equation 2-21 is

$$F^{-1}[Q\ ] = F^{-1}\{F[x(t)] + \int_o^t n_{LP}(p)\,dp\} \qquad 2\text{-}27$$

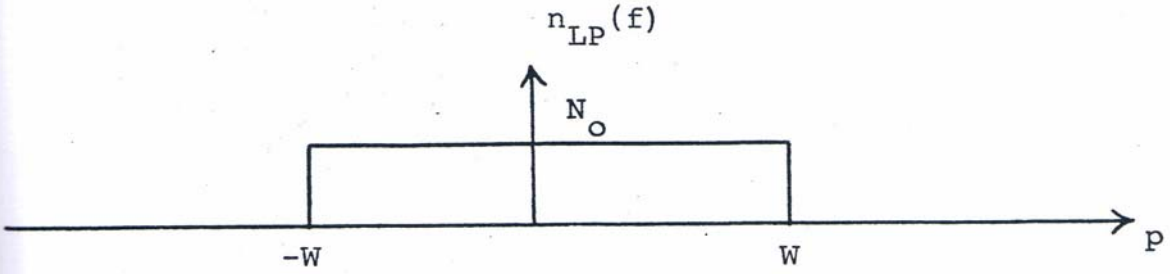

a. The Power Spectrum of a Low Pass Filtered White Noise.

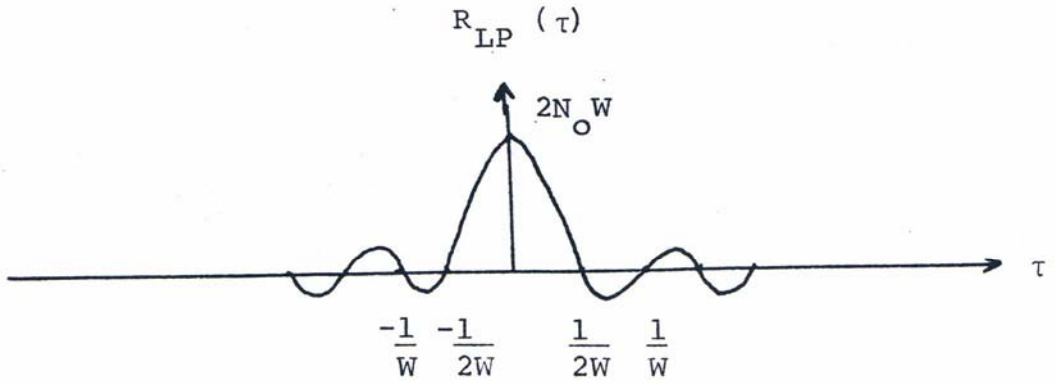

b. The Antocorrelation of a Low Pass Filtered White Noise.

Figure 2-11.

If F is nonlinear, the preceding Equation cannot be written in terms of x(t) plus noise and thus signal to noise ratio is not defined. For a linear operator like a sawtooth wave (Section IV-1-a), $F[x(t)] = t_o x(t)$ and hence, the signal to noise ratio at the output of the receiver becomes:

$$S/N = \frac{||x^2||}{\sigma^2} \qquad 2\text{-}28$$

If bandpass filtering and integrating of Figure 2-8 is used for the reconstruction of the signal x(t), the analysis becomes as follows:

$$y = x_s(t) + n(t) \qquad 2\text{-}29$$

After band pass filtering, Equation 2-29 becomes

$$y_{BP}(t) = \{1 - \dot{F}[x(t)]\} \cos\{wt - wF[x(t)]\} + n_{BP} \qquad 2\text{-}30$$

where n_{BP} is the white noise after bandpass filtering. After integration, we have:

$$G(t) = \int_o^t y_{BP}(h)dh = \frac{1}{W} \sin\{wt - wF[x(t)]\} + \int_o^t n_{BP}dt \qquad 2\text{-}31$$

The above Equation is similar to an F.M. or a P.M. signal plus noise. Therefore, the P.M. noise analysis holds for

this kind of reconstruction. This kind of reconstruction exploits bandwidth to noise reduction of angle modulated signals.

The zero crossings information of nonuniform pulses can also be transmitted by a square wave. Its noise analysis is given in Appendix E.

PART III

LEVEL INTERSECTION WAVEFORM

This chapter deals with the transmission of nonuniform samples at the intersection of a signal with horizontal levels. The average number of samples and an analysis for the reconstruction of the nonuniform samples are given in the following sections.

1. Single level

The zero crossings of a random signal, $x(t)$, can be viewed as the intersection of $x(t)$ with the horizontal axis $z(t) = o$. If certain conditions are satisfied, a signal can be retrieved from its zero crossings.[4] According to the nonuniform sampling theorem, if the average sampling rate satisfies the Nyquist rate, then the signal can be completely reconstructed (Appendix A). For a Gaussian signal, $x(t)$, the average rate of zero crossings is well known[5] to be less than twice the bandwidth of the signal, $x(t)$, i.e., the average number of zero crossings is equal or less than the Nyquist rate. Some transformations on $x(t)$, e.g., differentiation can increase the average rate

of zero crossings. "Level crossings" can be equivalently represented by the intersection of $x(t)$ with $z(t) = c$, where c is a constant. For a Gaussian signal, $x(t)$, the level crossings are related to the zero crossings by Rice's[5] formula

$$n_o^2 = \frac{1}{\pi^2} \frac{\int_{-\infty}^{\infty} w^2 s(w)\,dw}{\int_{-\infty}^{\infty} s(w)\,dw} \qquad 3\text{-}1$$

$$n_c = n_o e^{\frac{-c^2}{2R(o)}} \qquad 3\text{-}2$$

Where n_o is the average rate of zero crossings, n_c is the average number of level crossings at c.

$s(w)$ is the power spectrum of the signal and $R(o)$ is the autocorrelation of the signal at $\tau = o$. Hence, in the case of Gaussian signals, the average number of level crossings are always less than that of the zero crossings rate, For a better understanding of the average zero crossings, the following example is given.

Example 1: Assume x(t) is a white, bandlimited (w_c) Gaussian signal. Therefore, the power spectrum of the signal is

$$s(w) = 1 \text{ for } |w| \leq w_c$$
$$s(w) = 0 \text{ for } |w| > w_c \qquad 3\text{-}3$$

From Equations 3-1 and 3-3, we can deduce that

$$n_o^2 = \frac{1}{\pi^2} \frac{\int_{-w_c}^{w_c} w^2 dw}{\int_{-w_o}^{w_c} dw} = \frac{4f_c^2}{3} \qquad 3\text{-}4$$

thus,

$$n_o = \frac{2f_c}{\sqrt{3}} < 2f_c = \text{The Nyquist rate} \qquad 3\text{-}5$$

The above example shows that the average number of samples per second are not sufficient for the reconstruction of x(t) for this signal.

The level crossings at an arbitrary level c is given by

$$n_c = n_o e^{\frac{-c^2}{2R(o)}} = \frac{2f_c}{\sqrt{3}} e^{\frac{-c^2}{4f_c}} \qquad 3\text{-}6$$

where

$$R(o) = \int_{-f_c}^{f_c} s(f)df = 2f_c \qquad 3\text{-}7$$

To analyze the zero crossing problem, it is assumed in Figure 3-2 that there is only one sample per Nyquist interval. Methods of concern in this dissertation assure this condition. This assumption implies that

$$t_m = (m-t)T + \tau \quad \text{where} \quad o \leq \tau \leq T \qquad 3\text{-}8$$

where t_m is the zero crossing times

$$x_s = A \sum_m \delta(t-t_m) \qquad 3\text{-}9$$

Using the general analysis described in Section II-2, we define

$$g(t) = t - (m-1)T - \tau + ax(t) \qquad 3\text{-}10$$

where $x(t_m) = o$, $g(t_m) = o$ and $g(t \neq t_m) \neq o$. "a" has to be chosen such that

$$[t - (m-1)T - \tau\ ] \neq -ax(t) \qquad 3\text{-}11$$

Note that the inverse of z(t) does not exist in this case

$$\dot{g}(t) = 1 + a\dot{x}(t) \qquad 3\text{-}12$$

$$x_s = A \sum_{m=o}^{\infty} |1+a\dot{x}(t_m)| \; \delta \; [t - (m-1)T - \tau + ax(t)] \qquad 3\text{-}13$$

The Fourier series equivalent is

$$x_s = \frac{1}{T} [1 + a\dot{x}(t)] \sum_{n=-\infty}^{\infty} e^{\frac{jn2\pi}{T}} [t - \tau + ax(t)] \qquad 3\text{-}14$$

where $|a\dot{x}(t)| < 1$.

If spectrum overlapping is ignored, low pass filtering and integration will yield the baseband signal. However, according to Rice, the average zero crossings is always less than the Nyquist rate (Example 1). To avoid spectrum overlapping, the sampling rate has to be at least 2W where W is the bandwidth of the baseband signal, x(t), and the bandwidth of the first harmonic is 2(1+a)W. For the level crossings depicted in Figure 3-3 , we have

$$t_m = (m-1)T + \tau \qquad \text{where} \qquad o \leq \tau < T \qquad 3\text{-}15$$

$$x(t_1) = x(t_2) = \ldots = x(t_m) = A \qquad 3\text{-}16$$

$$x_s = A \sum_{m=-\infty}^{\infty} (t-t_m) \qquad 3\text{-}17$$

$$g(t) = t - (m-1)T - \tau + a(x-A) \qquad 3\text{-}18$$

$$g(t_m) = o, \; g(t \neq t_m) \neq o \Rightarrow [t - (m-1)\; T - \tau \;] \neq - a(x-A) \qquad 3\text{-}19$$

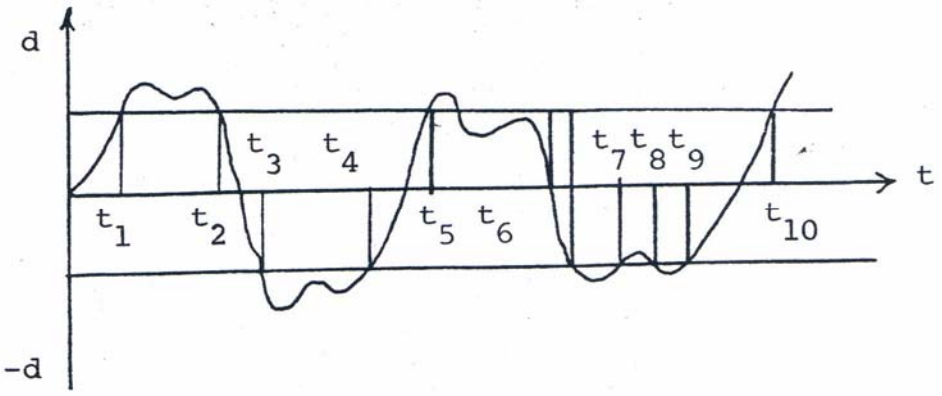

Figure 3-1. Two Level Intersection Transmission

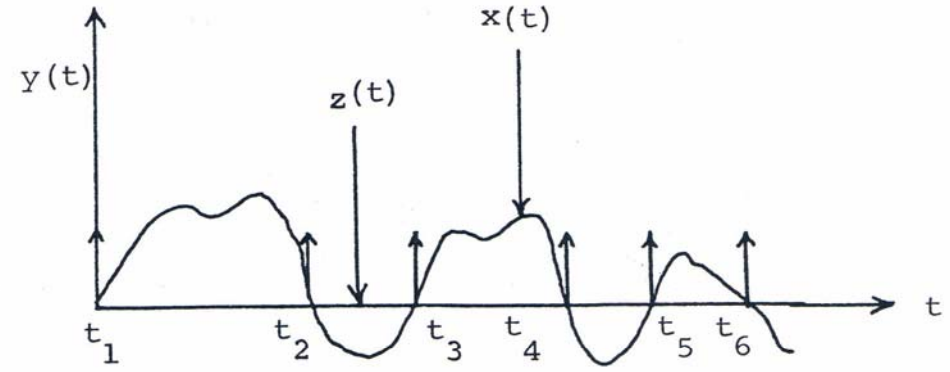

Figure 3-2. Zero Crossing Transmission

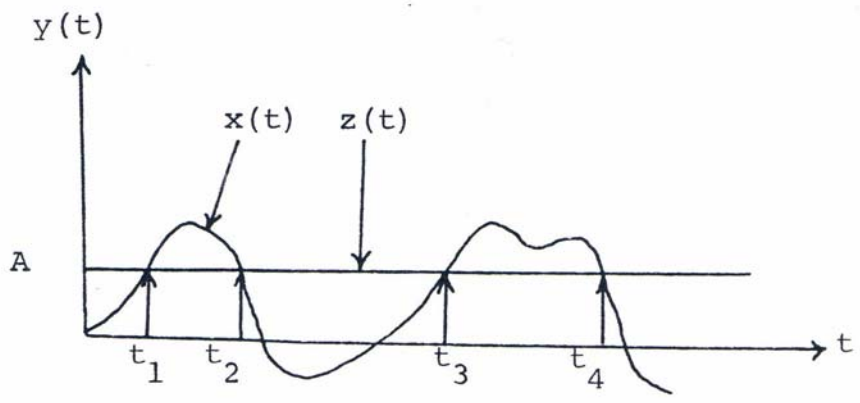

Figure 3-3. Level Crossing Transmission

$$\dot{g}(t) = 1 + a\dot{x}(t) \qquad 3\text{-}20$$

therefore,

$$x_s = (1+a\dot{x}) \sum_{n=-\infty}^{\infty} e^{\frac{jn2\pi}{T}} [t - \tau + a(x-A)] \qquad 3\text{-}21$$

Low pass filtering and integration would have yielded the baseband signal if the Nyquist rate had been satisfied.

2. Intersection with Two or More Levels

It was shown in the previous section that the average number of samples per second are less than or equal to the Nyquist rate. In order to achieve the Nyquist sampling rate, two or more level crossings can be considered. This would naturally increase bits per sample. Other examples should clear this point.

Example 2: From Example 1, the average sampling rate was found to be $\frac{2f_c}{\sqrt{3}}$. If the crossings with a level d are added to the zero crossings, the Nyquist rate can be achieved. The level d, for which the total crossings exactly equal the Nyquist rate, is found as follows:

$$\text{Nyquist rate} = 2f_c = n_o + n_d = n_o + n_o\, e^{\frac{-d^2}{2R(o)}} \qquad 3\text{-}22$$

From Equations 3-4 and 3-22, we can deduce that

$$\frac{2f_c}{\sqrt{3}}\left(1 + e^{\frac{-d^2}{4f_c}}\right) = 2f_c \qquad 3\text{-}23$$

or

$$d = 2\sqrt{f_c}\left[\ln \frac{1}{(\sqrt{3}-1)}\right]^{1/2} = .79\sqrt{2f_c} \qquad 3\text{-}24$$

Hence, the samples at the zero crossings together with the level crossings at d are exactly equal the Nyquist rate.

Example 3: Instead of sampling at the zero crossings and the level crossings as given in the previous example, it is more desirable for the sake of symmetry to sample at the level crossings depicted in Figure 3-1.

To satisfy the Nyquist rate, the new level d may be found as follows:

$$2n_o \, e^{\frac{-d^2}{4f_c}} = 2f_c \qquad 3\text{-}25$$

$$\frac{4f_c}{\sqrt{3}} \, e^{\frac{-d^2}{4f_c}} = 2f_c \qquad 3\text{-}26$$

$$\frac{-d^2}{e4f_c} = \frac{\sqrt{3}}{2} \qquad 3\text{-}27$$

$$\frac{-d^2}{4f_c} = \ln \frac{\sqrt{3}}{2} \Rightarrow d^2 = 4f_c \ln \frac{2}{\sqrt{3}} \qquad 3\text{-}28$$

$$d = \sqrt{4f_c \ln \frac{2}{\sqrt{3}}} = .532\sqrt{2f_c} \qquad 3\text{-}29$$

The above level is smaller than the level derived in the Example 2 (Equation 3-24), which agrees with intuition. If for a particular s(w), n_o is less than 1/2 Nyquist rate = f_c, then there should be more than two quantization levels to satisfy the Nyquist rate.

Our new equation becomes

$$2f_c = n_o + n_o\, e^{-\frac{d_1^2}{2R(o)}} + n_o\, e^{-\frac{d_2^2}{2R(o)}} \qquad 3\text{-}30$$

d_1 and d_2 do not have unique solutions. d_2 can be represented as $2d_1$ to avoid bandwidth constraint.

Another choice is $d_2 = -d_1$. This is the same as choosing d_1 and d_2 for equal probability.

If n_o is less than $\frac{2f_c}{3}$, another quantization level should be added.

In general, if $\frac{2f_c}{n+1} < n_o \leq \frac{2f_c}{n}$, then n levels are needed as well as the zero level. These levels can be chosen equiprobable as follows:

$$\int_0^{d_1} e^{-\frac{x^2}{2\sigma^2}}\, dx = \int_{d_1}^{d_3} e^{-\frac{x^2}{2\sigma^2}}\, dx = \int_{d_3}^{d_5} e^{-\frac{x^2}{2\sigma^2}}\, dx = \ldots$$

and $d_2 = -d_1$, $d_4 = -d_3$ and $d_6 = -d_5$ ... 3-31

Equation 3-31 is substituted in the general equation

$$2f_c = n_o + 2n_o\, e^{-\frac{d_1^2}{2R(o)}} + 2n_o\, e^{-\frac{d_3^2}{2R(o)}} + \ldots \qquad 3\text{-}32$$

The general levels d_1, d_3, ... may then be found.

Equation 3-32 sets a general theory for a Guassian process with known statistical properties. If the Guassian signal was not well defined, i.e., when the mean and the variance are not known or when the signal is not Gaussian or the density is not known, the average number of samples per second cannot be found in general. In Chapter V, some adaptive techniques will be discussed for the general non-Gaussian signals.

To analyze the two level intersection, we refer to Figure 3-1.

The assumption that there is only one sample per interval T yields the following equations.

$$t_m = (m-1)T + \tau \qquad 3\text{-}33$$

$x(t_m) = B$ where B is a binary random variable with the values of d and -d. 3-34

$$g(t) = t - (m-1)\,T - \tau + a(x-B) \qquad 3\text{-}35$$

$$\dot{g}\,(t) = 1 + a\dot{x} \qquad 3\text{-}36$$

$$|a\dot{x}\,(t)| < 1 \qquad 3\text{-}37$$

$$x_s = A \sum_m \delta(t-t_m) = (1+a\dot{x}) \sum_m \delta[t-(m-1)T - \tau + a(x-B)] \quad 3\text{-}38$$

The Fourier series expansion is

$$x_s = (1+a\dot{x}) \sum_{n=-\infty}^{\infty} e^{\frac{jn2\pi}{t}} [t- \tau +a(x-B)] \quad 3\text{-}39$$

The reconstruction of the baseband signal x(t), is achieved by low pass filtering and integration if there is no spectrum overlapping. The random variable, B, is expected to increase the bandwidth of the system. Consequently, the sampling rate has to be higher than the Nyquist rate for this kind of reconstruction, which can be assumed by the methods of this section.

3. Zero crossings of a function of x(t)

If more than two levels are intersected with the random signal, x(t), the bits per sample increase. One way of avoiding this problem is to map the signal x(t) to another function so that the zero crossings increase.[4] Differentiating x(t) will increase the zero crossings since for each zero crossing, x(t) has at least one maximum or minimum. The analysis is similar to the zero crossing analysis, except that x(t) in Equation 3-14 becomes $\dot{x}$ and $\dot{x}$ becomes $\ddot{x}$ while the bandwidth of $\dot{x}$ is still the same as x(t). The Fourier series expansion of the zero crossings is

$$x_s = \frac{1}{T}\,[1+a\ddot{x}(t)] \sum_{n=-\infty}^{\infty} e^{\frac{j2\pi n}{T}\,[t-\tau+a\dot{x}(t)]} \qquad 3\text{-}40$$

T in the above equation is smaller than the T in Equation 3-40 because the average zero crossings of $\dot{x}$ is larger than that of x(t). Thus, there is less spectral overlap to reconstruct $\dot{x}$; the two standard reconstruction schemes are depicted in Figure 3-4 and 3-5.

A different transformation is the absolute value of the random signal, x(t). The average level crossings doubles. The procedure of the encoder and the decoder is as follows.

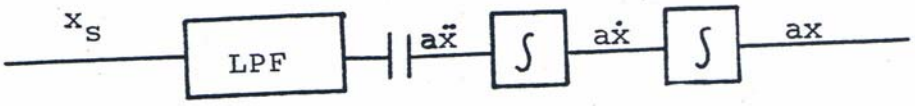

Figure 3-4. Reconstruction of a Signal from the Zero Crossings of its Derivative

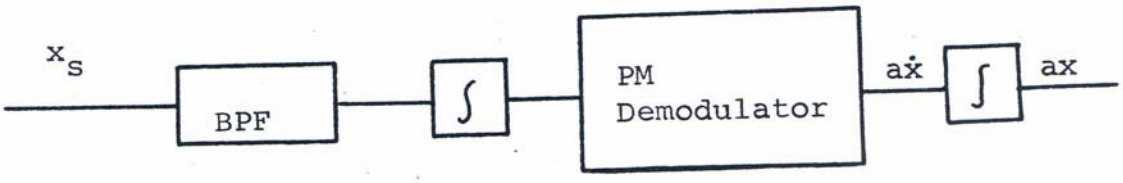

Figure 3-5. Reconstruction of a Signal from the Zero Crossing of its Derivative

The signal x(t) is full wave rectified as shown in Figure 3-6.

The samples are at the zero crossings and level crossings (at A) of the rectified signal. We transmit -1 at the level crossings and +1 at the zero crossings. At the receiver, the samples that are rectified are flipped back again to restore the original signal.

The block diagram of the decoder at the receiver to restore the original samples is represented in Figure 3-7.

The above procedure is valid for any kind of signal. Besides the lower transmission rate, the encoding and decoding of the technique is fairly simple and practical.

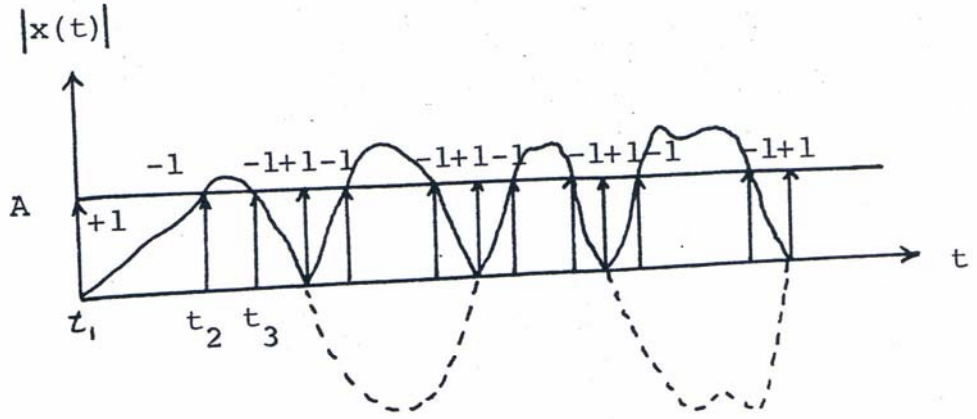

Figure 3-6. Encoder

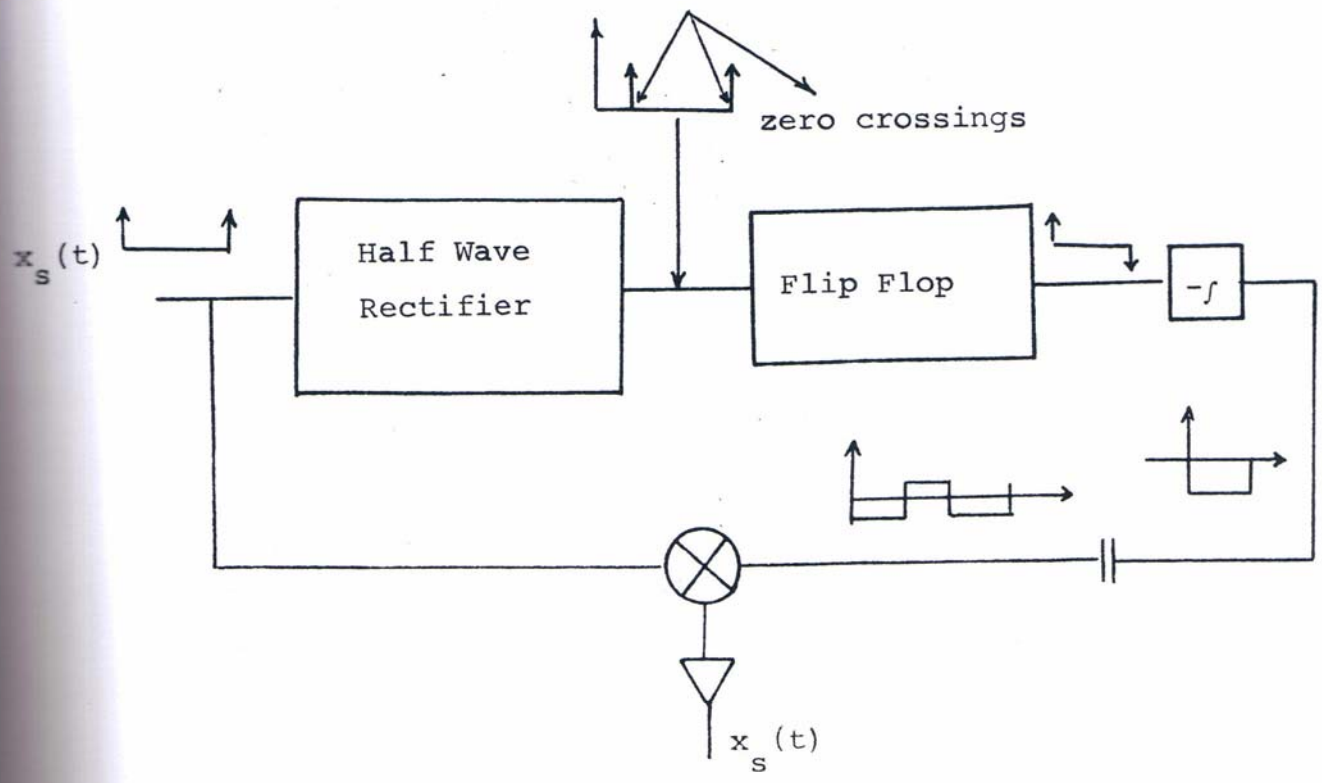

Figure 3-7. Decoder at the Receiver

4. Fixed quantizers

Suppose the signal, x(t), is intersected with n uniform or nonuniform quantization levels. The levels can be set according to the probability density of x(t) or any other optimum way [7,9,10,11,12,13] (Figure 3-8).

To transmit the intersection of the signal x(t) with the quantization levels, $\log_2 n$ bits per sample are needed. However, the samples can be transmitted at a rate of one bit per sample by the following unique and original procedure:

When the slope of x(t) is positive (the amplitude of the present sample is greater than the previous sample), +1 is transmitted at the intersections. Conversely, when the slope of x(t) is negative, -1 is transmitted at the intersections. (See Figure 3-8)

At the receiver, the analog nonuniform samples are reconstructed as follows. When the first +1 pulse is received, the first quantization level is sampled; when the second +1 pulse is received, the second level is sampled and so on until the n^{th} pulse is -1. Then, the lower quantization level [$(n-2)^{th}$] is sampled and the

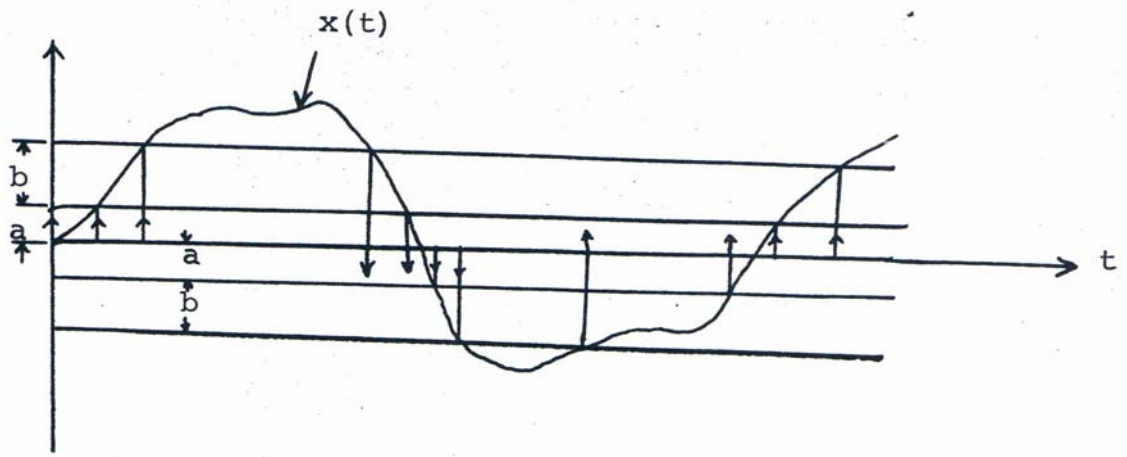

Figure 3-8. Intersection with n Fixed Quantization Level

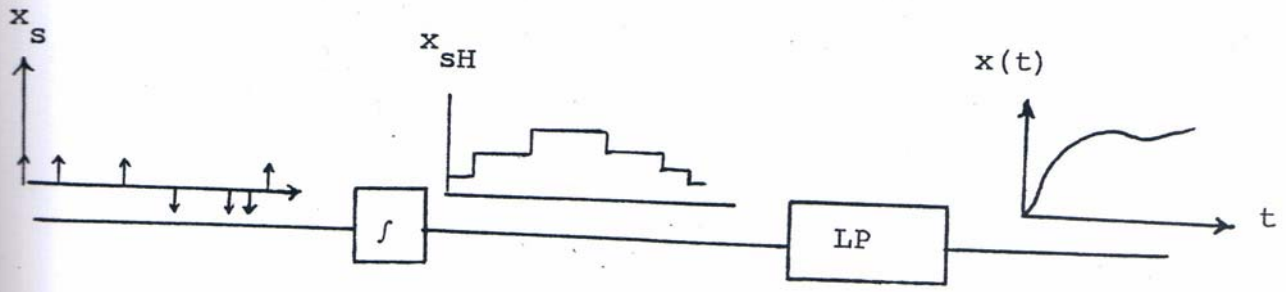

Figure 3-9. Reconstruction for an n Level Uniform Quantizer

procedure continues. The random signal x(t) can be reconstructed from the analog nonuniform samples by any method discussed in Part VIII.

The average number of samples per second produced by n level intersection can be found for a Gaussian signal as illustrated in Example 3 of Section III.

The reconstruction of the random signal, x(t), at the receiver can be much simpler if the quantization levels are uniform. Figure 3-9 shows the reconstruction scheme.

Integration generates the sample and hold version of x(t). An approximation of x(t) is achieved by low pass filtering the sample and hold signal. The higher the quantization levels, the better the approximation (See Section VIII). To analyze the pulses from the intersection point of view, it follows

$$x_s = \sum_{m=1}^{\infty} G(m)\ \delta\ (t-t_m)$$

where G(m) is a binary random variable that has the values +1 and -1 depending on the polarity of the m^{th} pulse. Since G(m) is dependent on m, the analysis of Section II does not hold for the above case. However, the spectrum of x_s

can be guessed by noting that the reconstruction of the general intersection problem. Since the low pass filter in Figure 3-9 is a linear time invariant filter, the position of the integrator and the low pass filter can be exchanged. Hence, low pass filtering the binary pulses x_s results in the derivative of the signal. This fact shows that the spectrum of x_s is approximately like Figure 2-4 , i.e., in the region $-W \leq f \leq W$, the spectrum of x_s is $jWx(f)$ where W is the bandwidth of $x(t)$.

In summary, this chapter has dealt with the zero crossings and the level crossings of a random signal. The above techniques have the following qualities.

1. One bit per sample transmission
2. No amplitude quantization noise at the transmitter
3. Samples are nonuniform and the average samples per second are not known for non-Gaussian signals.
4. The reconstruction of the pulses generated by the uniform n level quantizer is obtained by low pass filtering and integration.

PART IV

PERIODIC WAVEFORMS

1. Intersection with a General Periodic Function

One can choose z(t) to be any periodic function provided that it is continuous within each interval and its inverse function exists. A general periodic function of this sort is represented in Figure 4-1. The analysis is as follows:

Define z(t) in each interval by a function f(t) such that:

$$z(t) = \begin{cases} f(t) & \text{when} \quad o \leq t < T \\ f(t-nT) & \text{when} \quad nT \leq t < (n+1)T \end{cases} \qquad 4\text{-}1$$

where $n = 0,1,\ldots \infty$

$$f(t_1) = x(t_1) \Rightarrow t_1 = f^{-1}[x(t)]$$

$$f(t_2-T) = x(t_2) \Rightarrow t_2 = T + f^{-1}[x(t_2)]$$

$$f[t_m - (m-1)T] = x(t_m) \Rightarrow t_m = (m-1)T + f^{-1}[x(t_m)] \qquad 4\text{-}2$$

It is assumed that $|\dot{f}(t)| > |\dot{x}|$. This assumption assures that there is only one sample in each interval T.

$$g(t) = t - (m-1)T - f^{-1}[x(t)] \qquad 4\text{-}3$$

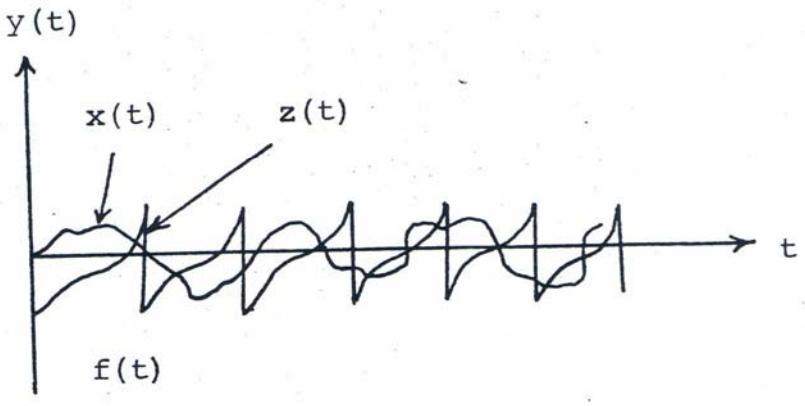

Figure 4-1. A General Periodic Signal (First Category)

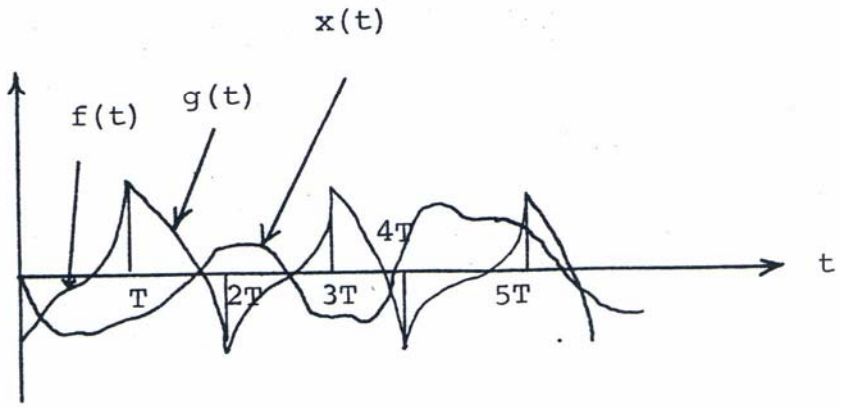

Figure 4-2. A General Periodic Signal (Second Category)

$$\dot{g}(t) = 1 - \frac{\dot{x}(t)}{1} \left\{ \frac{df^{-1}}{dx(t)} [x(t)] \right\} \qquad 4\text{-}4$$

$$x_s = \sum_{m=1}^{\infty} \delta(t-t_m) = \sum_{m=1}^{\infty} |\dot{g}(t_m)| \, \delta[g(t)] =$$

$$= \{1 - \dot{x} \frac{df^{-1}}{dx(t)} [x(t)]\} \sum_{m} \delta\{t - (m-1)T - f^{-1}[x(t)]\} \qquad 4\text{-}5$$

We have assumed in the above that f^{-1} is differentiable and:

$$\left| \dot{x} \frac{df^{-1}}{dx} [x] \right| < 1 \qquad 4\text{-}6$$

Using the equivalent Fourier series, this becomes

$$x_s = \{ 1 - \dot{x} \frac{df^{-1}}{dx} [x(t)] \} \sum_{n=1}^{\infty} \{ 1 + 2 \cos [nwt - nwf^{-1} [x(t)]] \} \qquad 4\text{-}7$$

The two techniques for reconstructing the original signal x(t) were previously discussed and are illustrated in Figure 4-3 and Figure 4-4. A spectral analysis of x_s is given in the next sections for specific periodic functions.

The actual choice of f(t) depends on many factors. Theoretically, f(t) has to be chosen such that the inverse of the function exists. The choice of f(t) also influences the aliasing of the harmonics in Equation 4-7 (see Section 4-1-e) while the spectrum overlap is more severe with a sinusoidal function. (Section 4-1-c). The ease of reconstructing a

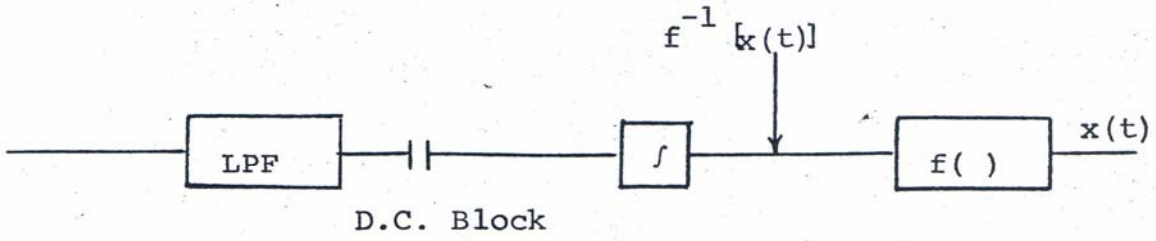

Figure 4-3 Reconstruction of the Signal by Low Pass Filtering

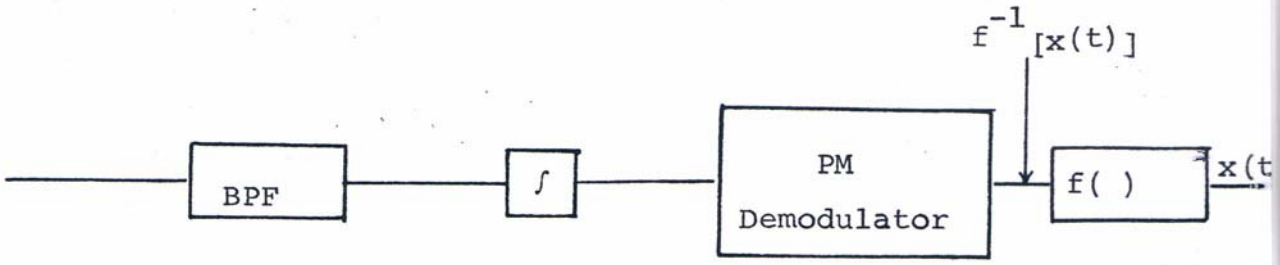

Figure 4-4 Reconstruction of the Signal by Band Pass Filtering

periodic function and the relizability of the block, f( ), in Figure 4-3 and 4-4 are the main factors that should be considered in choosing a particular f(t). A comparison of the periodic waveforms will be discussed in Section IV-2.

The general periodic function in Figure 4-1 can be modified by defining another function g(t) in the next interval after f(t) and repeating it alternatively as depicted in Figure 4-2. The analysis is the same as before and need not be repeated here. A triangular wave is of this form (See Figure 4-6).

a. Sawtooth Waveform

The result of an intersection of the random signal with a sawtooth wave is similar to nonuniform pulse position modulation (PPM) (Figure 4-5-a). The intersection samples are similar to the zero crossings of the difference signal $y(t) = x(t) - z(t)$ where the variables are defined as in Equation 2-1. We can rewrite y(t) as follows:

$$y(t) = x(t) + [-z(t)]$$

z(t) is a sawtooth wave and the inverse of that is also a sawtooth wave with a slope of the opposite sign.

Therefore, the intersection problem reduces to the zero crossings of the sum of the random signal and the sawtooth wave. This is the same as a nonuniform sampling PPM and is discussed in detail in standard textbooks.[7,19]

The analysis is summarized as follows:

$$t_1 = t_o x(t_1)$$

$$t_2 = T + t_o x(t_2)$$

$$\vdots$$

$$t_m = (m-1)T + t_o x(t_m) \qquad 4\text{-}7'$$

The transmitted nonuniform PPM pulses can be represented as:

$$x_s = A \sum_{m=1}^{\infty} \delta(t-t_m) \quad \text{where A is a constant.}$$

Using the analysis of Section II-2, we have:

$$x_s = \sum_{m=1}^{\infty} |\dot{g}(t_m)| \, \delta[g(t)]$$

where $g(t) = t - (m-1)T + t_o x(t)$, $g(t_m) = o$, $g(t \neq t_m) \neq o$

$$\dot{g}(t) = 1 + t_o \dot{x}(t), \quad \dot{g}(t_m) \neq o$$

The Fourier series expansion of the above equation is

$$x_s = [1 + t_o \dot{x}(t)] \sum_{n=-\infty}^{\infty} e^{jnw_c[t + t_o x(t)]}$$

where it is assumed that $[1 + t_o \dot{x}(t)] > o$. This assumption implies that $\dot{x} > -\frac{1}{t_o}$. The original signal from the PPM pulses can be reconstructed by two different methods depicted in Figures 4-5-b and 4-5-c. Figure 4-5-b is the reconstruction of the original signal by low pass filtering and integration. Figure 4-5-c is the reconstruction of the original signal by low pass filtering and integration. Figure 4-5-c is the reconstruction of the original signal by band pass filtering, integration and PM demodulation. The effect of aliasing and a comparison of the two reconstruction techniques will be discussed in the next section.

b. Triangular Wave

A triangular wave intersected with a random wave is shown in Figure 4-6. The first harmonic of the periodic signal occurs at twice the highest frequency content of the random bandlimited signal. The number of samples per interval T satisfies the Nyquist rate provided that the amplitude of the triangular wave is large enough and the frequency of the periodic wave is larger or equal to the Nyquist rate. Thus, there will be one sample per each half cycle of the triangular wave. The purpose of the following analysis is to show, by

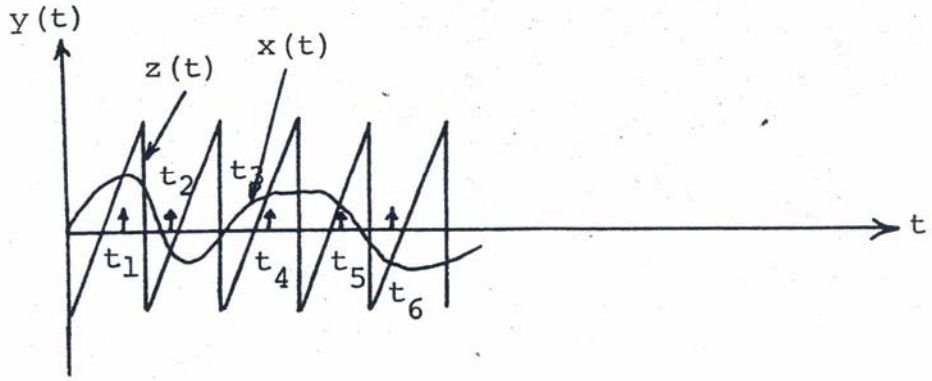

a. Intersection with a Sawtooth Wave

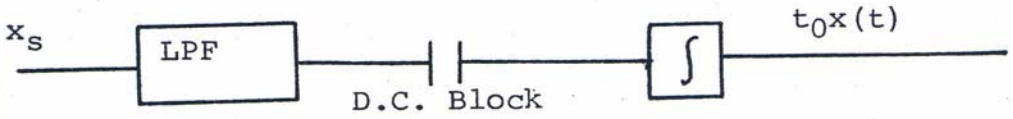

b. Reconstruction of the Baseband Signal from the PPM Pulses

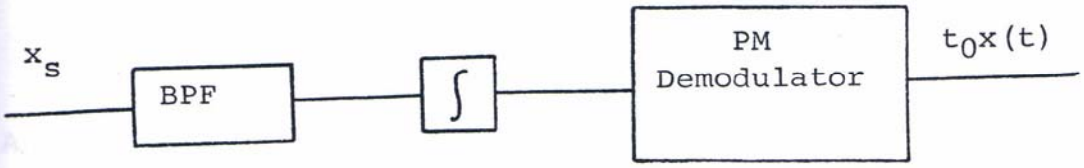

c. Reconstruction of the Baseband Signal by Band Pass Filtering

Figure 4-5. Non-Uniform PPM

analytical tools, a simple reconstruction method of the random signal from its nonuniform samples.

Assume t_o is the inverse of the slope of the triangular wave. Since the signal information is coded in the time interval between nonuniform pulses, one can relate the sampling time intervals to the amplitude of the samples such that:

$$t_1 = t_o x(t_1)$$

$$t_2 = \frac{T}{2} - t_o x(t_2)$$

$$t_3 = T + t_o x(t_3)$$

$$t_m = \frac{(m-1)}{2} T + (-1)^{m-1} t_o x(t_m) \qquad 4\text{-}8$$

where the t_m's are depicted in Figure 4-6. The transmitter transmits impulses of fixed areas at these times. The samples can be represented as:

$$x_s = A \sum_{m=1}^{\infty} \delta(t-t_m) \quad \text{where A is a constant} \qquad 4\text{-}9$$

An impulse can be represented by:

$$\delta(t-t_m) = |\dot{g}(t_m)|\ \delta[g(t)] \qquad 4\text{-}10$$

where $g(t_m) = o$, $g(t \neq t_m) \neq o$ and $\dot{g}(t_m) \neq o$ $\qquad 4\text{-}11$

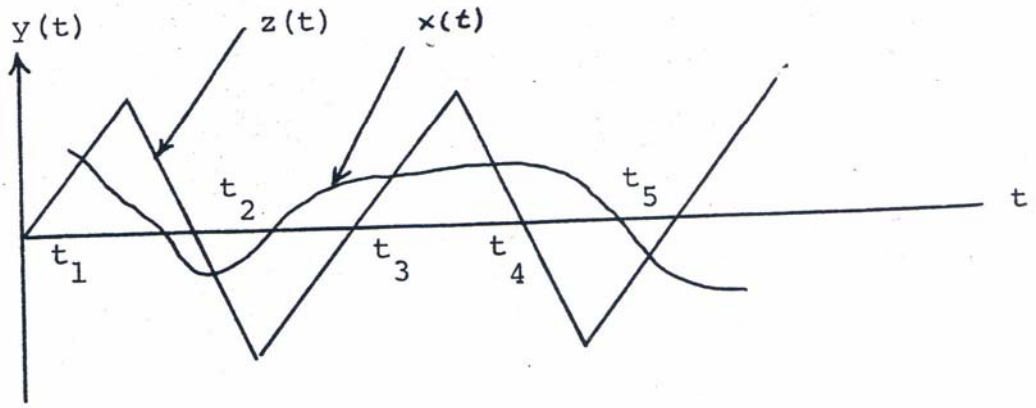

Figure 4-6 Intersection with a Triangular Wave

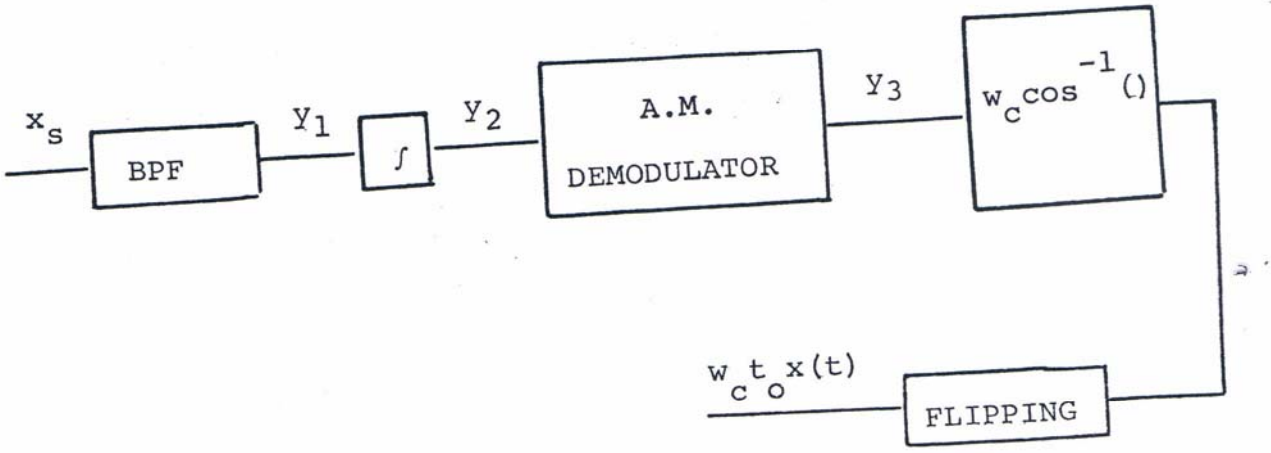

Figure 4-7 The Reconstruction of the Baseband Signal from the Unipolar Pulses generated by a Triangular Wave.

$g(t)$ can be any function satisfying the preceding conditions.

Therefore, we choose:

$$g(t) = t - \frac{(m-1)}{2} T - (-1)^{m-1} t_o x(t) \qquad 4\text{-}12$$

This function satisfies the preceding conditions because:

$$g(t_m) = o, \; g(t_q) \neq o \text{ when } q \neq m \qquad 4\text{-}13$$

$$\dot{g}(t_m) = 1 - (-1)^{m-1} t_o \dot{x}(t_m) \qquad 4\text{-}14$$

$\dot{g}(t_m) \neq o$ if we assume:

$$t_o \dot{x}(t_m) < 1 \qquad 4\text{-}15$$

Substituting Equations 4-10 and 4-12 in Equation 4-9, we get:

$$x_s = A \sum_{m=1}^{\infty} |1 - (-1)^{m-1} t_o \dot{x}(t_m)| \; \delta[t - \frac{(m-1)}{2} T - (-1)^{m-1} t_o x(t)] \qquad 4\text{-}16$$

x_s can be rewritten in terms of odd and even:

$$x_s = A \sum_{m=odd} |1 - t_o \dot{x}(t_m)| \; \delta[t - \frac{m-1}{2} T - t_o x(t)] + A \sum_{m=even} |1 + t_o \dot{x}(t_m)| \; \delta[t - \frac{m-1}{2} T + t_o x(t)] \qquad 4\text{-}17$$

or

$$x_s = A\,|1 - t_o\dot{x}(t)| \sum_{m=odd} \delta\,[t - \frac{m-1}{2}\,T - t_o x(t)] + \qquad 4\text{-}18$$

$$+ A\,|1 + t_o\dot{x}(t)| \sum_{m=even} \delta\,[t - \frac{m-1}{2}\,T + t_o x(t)]$$

Using the following substitution, we get:

$$p = t - t_o x(t), \quad q = t + t_o x(t) \qquad 4\text{-}19$$

$$x_s = A\,|1 - t_o\dot{x}(t)| \sum_{m=odd} \delta\,[p - \frac{m-1}{2}\,T] + \qquad 4\text{-}20$$

$$+ A\,|1 + t_o\dot{x}(t)| \sum_{m=even} \delta\,[q - \frac{m-1}{2}\,T]$$

The sum of periodic impulses can be expanded in Fourier series:

$$x_s = \frac{w_c A}{2\pi}\,|1 - t_o\dot{x}(t)| \sum_{n=-\infty}^{\infty} e^{jnw_c p} + \qquad 4\text{-}21$$

$$+ \frac{w_c A}{2\pi}\,|1 + t_o\dot{x}(t)| \sum_{n=-\infty}^{\infty} e^{jnw_c q}$$

Substituting the values of p and q (Equation 4-19) in the

preceding equation:

$$x_s = A\frac{w_c}{2\pi}|1 - t_o\dot{x}(t)|\sum_{n=-\infty}^{\infty} e^{jnw_c[t - t_o x(t)]} + \qquad 4\text{-}22$$

$$+ A\frac{w_c}{2}|1 + t_o\dot{x}(t)|\sum_{n=-\infty}^{\infty} e^{jnw_c[t + t_o x(t)]}$$

or

$$x_s = \frac{w_c}{2\pi}A|1 - t_o\dot{x}(t)|\{1 + 2\sum_{n=1}^{\infty}\cos[nw_c t - nw_c t_o x(t)] + \qquad 4\text{-}23$$

$$+ \frac{w_c}{2\pi}A|1 + t_o\dot{x}(t)|\{1 + 2\sum_{n=1}^{\infty}\cos[nw_c t + nw_c t_o x(t)]\}$$

From the condition $t_o\dot{x}(t) < 1$, we have

$$x_s = \frac{w_c}{2\pi}A[1 - t_o\dot{x}(t)]\{1 + 2\sum_{n=1}^{\infty}\cos[nw_c t - nw_c t_o x(t)]\} + \qquad 4\text{-}24$$

$$+ \frac{w_c}{2\pi}A[1 + t_o\dot{x}(t)]\{1 + 2\sum_{n=1}^{\infty}\cos[nw_c t + nw_c t_o x(t)]\}$$

In order to reconstruct the signal, $x(t)$, from the set of impulses, x_s, we use a bandpass filter centered around w_c, which results in the following equation, assuming there is no spectrum overlap.

$$y_1 = [1 - t_o\dot{x}(t)] \cos [w_c t - w_c t_o x(t)] +$$

$$+ [1 + t_o\dot{x}(t)] \cos [w_c t + w_c t_o x(t)] \qquad 4\text{-}25$$

Integrating the above equation yields:

$$y_2 = \frac{1}{w_c} \sin [w_c t - w_c t_o x(t)] +$$

$$\frac{1}{w_c} \sin [w_c t + w_c t_o x(t)] = \qquad 4\text{-}26$$

$$\frac{2}{w_c} (\sin w_c t) \cos [w_c t_o x(t)]$$

The above signal is an A.M. modulated signal. After A.M. demodulation we arrive at:

$$y_3 = \frac{1}{w_c} \cos [w_c t_o x(t)] \qquad 4\text{-}27$$

The baseband signal x(t) is extracted from the above signal by finding the inverse cosine of the Equation 4-27. The cosine function absorbs the sign of x. Hence, the reconstructed signal is full wave rectified. In order to get the original signal, the full wave rectified signal is

flipped alternatively. Thus, the baseband signal is reconstructed. This procedure is depicted in Figure 4-7.

To be more rigorous, we will elaborate further on the assumption that there is no aliasing after bandpass filtering and demodulation. Equation 4-24 is a summation of phase modulated signals. w_c is the frequency that is twice the bandwidth of the baseband signal x(t). Since the equivalent of the PM signal given in Equation 4-24 is about twice the bandwidth of the baseband signal,[7] the aliasing is negligible after bandpass filtering. The same reasoning holds for the low pass filter of the demodulator.

The demodulator and the inverse cosine circuits are complicated. The flipping process at the end also adds to the complexity of the system. Besides the sampling rate is twice the Nyquist rate.

A slight modification will greatly simplify the circuitry. We shall show that the original signal may be reconstructed using nonuniform pulses by low pass filtering and integration. The key to this simplification is to transmit negative impulses when the slope of the triangular wave is negative. This

adds one more bit, which is the penalty for a simpler implementation. The analysis is as follows:

$$x_s = A \sum_{m=odd} \delta(t-t_m) - A \sum_{m=even} \delta(t-t_m) \qquad 4\text{-}28$$

Substituting Equations 4-10 and 4-12 in the above, we have:

$$x_s = A \sum_{m=odd} |1 - t_o\dot{x}(t_m)| \, \delta[t - \frac{m-1}{2} T - t_o x(t)] - \qquad 4\text{-}29$$

$$- A \sum_{m=even} |1 + t_o\dot{x}(t_m)| \, \delta[t - \frac{m-1}{2} T + t_o x(t)]$$

Using the Fourier series for a train of periodic impulses, we get:

$$x = Af_c |1 - t_o\dot{x}(t)| \sum_{n=-\infty}^{\infty} e^{jnw_c[t - t_o x(t)]} - \qquad 4\text{-}30$$

$$- Af_c |1 + t_o\dot{x}(t)| \sum_{n=-\infty}^{\infty} e^{jnw_c[t + t_o x(t)]}$$

if

$$t_o\dot{x}(t) < 1 \qquad 4\text{-}31$$

$$x_s = Af_c [1 - t_o\dot{x}(t)] \{ 1 + 2 \sum_{n=1}^{\infty} \cos[nw_c t - nw_c t_o x(t)] \} - \qquad 4\text{-}32$$

$$- Af_c [1 + t_o\dot{x}(t)] \{ 1 + 2 \sum_{n=1}^{\infty} \cos[nw_c t + nw_c t_o x(t)] \}$$

Low pass filtering to extract the D.C. value, provided that there is no spectrum overlap, we derive:

$$y_1 = -2Af_c t_o \dot{x}(t) \qquad 4\text{-}33$$

The baseband signal can thus be derived from a simple integration. The block diagram for the reconstruction of nonuniform impulses is given in Figure 4-8. It would have been just as correct to use a bandpass filter instead of a low pass filter. The circuitry involved is still much more simplified than that of Figure 4-8. The result is:

$$y_2 = [1 - t_o\dot{x}(t)] \cos [w_c t - w_c t_o x(t)] - [1 + t_o\dot{x}(t)] \cos [w_c t + w_c t_o x(t)] \qquad 4\text{-}34$$

After integration we have:

$$y_3 = \frac{1}{w_c} \sin [w_c t - w_c t_o x(t)] - \frac{1}{w_c} \sin [w_c t + w_c t_o x(t)] = \frac{-2}{w_c} \cos w_c t \sin w_c t_o x(t) \qquad 4\text{-}35$$

Figure 4-8. The Reconstruction of the Base Band Signal from the Train of Bipolar Impulses

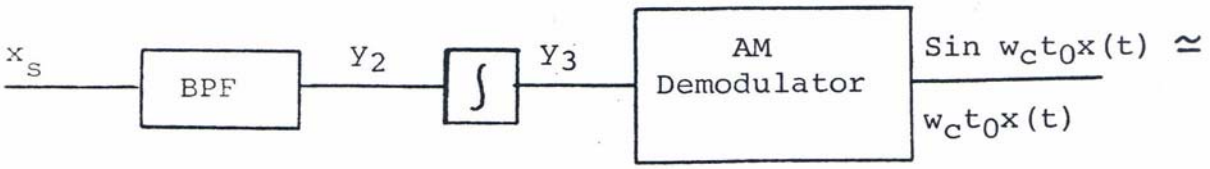

Figure 4-9. The Reconstruction of the Base Band Signal by Band Pass Filtering

After demodulating the above A.M. signal, the baseband signal could be retrieved if:

$$w_c t_o x(t) << \frac{\pi}{2} \qquad 4\text{-}36$$

i.e.,

$$\sin w_c t_o x(t) \simeq w_c t_o x(t) \qquad 4\text{-}37$$

This is illustrated in Figure 4-9.

Note that Figure 4-8 is demodulating the baseband part of the train of impulses while Figure 4-9 suggests that the P.M. portion of the set of impulses is being demodulated. Naturally, the second method takes advantage of noise immunity of P.M. signals and hence, is superior to the first method even though the reconstruction procedure is more involved. (See Section II-4)

To be mathematically rigorous, we cannot talk about the equality of a train of delta functions to a Fourier series. We can only talk about functional identities of delta functions. Hence, instead of using Equation 4-32, we should write the functional identity:

$$\int x_s dt = -2Af_c t_o x(t) + \frac{A}{\pi} \sum_{n=1}^{\infty} \sin [w_c t - w_c t_o x(t)] - \qquad 4\text{-}38$$

$$- \frac{A}{\pi} \sum_{n=1}^{\infty} \sin [nw_c t + nw_c t_o x(t)]$$

where the right hand side is the integral of Equation 4-32 and the left hand side is the integral of impulses which is a random squarewave depicted in Figure 4-10. Equation 4-38 can now be low pass filtered to extract the baseband signal. In other words, the integrator and the low pass filter in Figure 4-8 are switched, which is admissible for a linear time invariant system.

c. Sine Waves

The intersection of a sinusoidal wave and a random signal is illustrated in Figure 4-11. As before, negative pulses are transmitted for negative slopes. Assuming there is only one pulse per interval T/2 which is true for a sinusoidal wave with sufficiently high amplitude, we relate the time information to the amplitude of the random signal as follows:

$$A \sin w_c t_1 = x(t_1) \qquad 4\text{-}39$$

or

$$\sin w_c t_1 = \frac{1}{A} x(t_1) \Rightarrow w_c t_1 = \sin^{-1}\left[\frac{1}{A} x(t_1)\right] \qquad 4\text{-}40$$

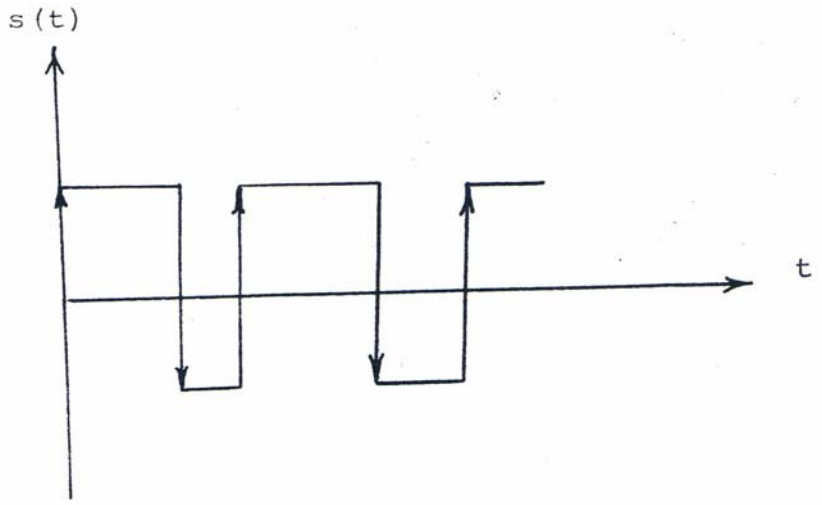

Figure 4-10. The Integral of Bipolar Impulses

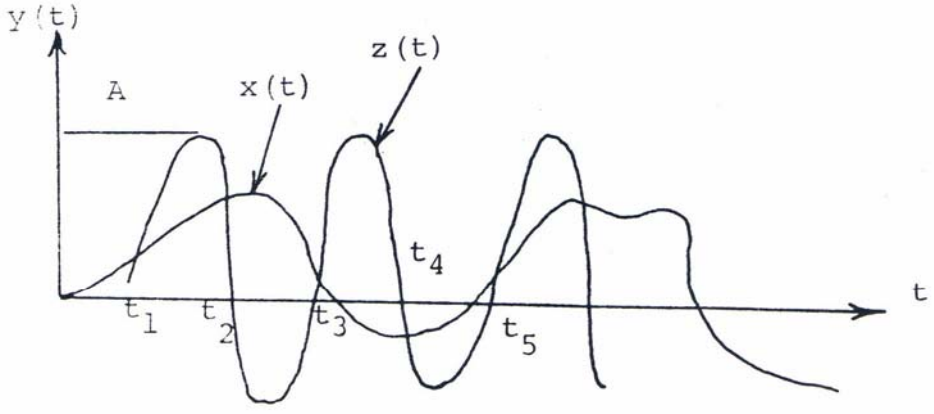

Figure 4-11. Intersection with a Sine Wave

Hence,

$$t_1 = \frac{1}{w_c} \sin^{-1}\left[\frac{1}{A} x(t_1)\right] \qquad 4\text{-}41$$

where $\sin^{-1}$ is the principle sine inverse and $w_c = \frac{2\pi}{T}$.

Likewise,

$$t_2 = T/2 - \frac{T}{2\pi} \sin^{-1}\left[\frac{x(t_2)}{A}\right]$$

$$t_3 = T + \frac{T}{2\pi} \sin^{-1}\left[\frac{x(t_3)}{A}\right]$$

$$t_4 = \frac{3T}{2} - \frac{T}{2\pi} \sin^{-1}\left[\frac{x(t_4)}{A}\right]$$

$$t_m = \frac{(m-1)T}{2} + (-1)^{m-1} \frac{T}{2\pi} \sin^{-1}\left[\frac{x(t_m)}{A}\right] \qquad 4\text{-}42$$

The train of impulses is:

$$x_s = A \sum_{m=odd} \delta(t-t_m) - A \sum_{m=even} \delta(t-t_m) \qquad 4\text{-}43$$

Using the functional identity discussed before:

$$\delta(t-t_m) \equiv |\dot{g}(t_m)| \delta[g(t)] \qquad 4\text{-}44$$

g(t) is chosen such that:

$$g(t) = t - \frac{m-1}{2} T - (-1)^{m-1} \frac{T}{2\pi} \sin^{-1}\left[\frac{x(t)}{A}\right] \qquad 4\text{-}45$$

$$g(t_m) = o, \; g(t_n) \neq o \; m \neq n \qquad 4\text{-}46$$

$$\dot{g}(t) = 1 - (-1)^{m-1} \frac{T}{2\pi} \frac{\dot{x}/A}{\sqrt{1-x^2/A^2}} = \qquad 4\text{-}47$$

$$= 1 - (-1)^{m-1} \frac{T}{2\pi} \frac{\dot{x}}{\sqrt{A^2 - x^2}}$$

$$\dot{g}(t_m) \neq o \text{ in general} \qquad 4\text{-}48$$

Hence,

$$x_s = A \sum_{m=odd} \left| 1 - \frac{\dot{x}T/2\pi}{\sqrt{A^2 - x^2}} \right| \delta\left[t - \frac{m-1}{2} T - \frac{T}{2\pi} \sin^{-1} \frac{x(t)}{A} \right] \qquad 4\text{-}49$$

$$- A \sum_{m=even} \left| 1 + \frac{\dot{x}T/2\pi}{\sqrt{A^2 - x^2}} \right| \delta\left[t - \frac{m-1}{2} T + \frac{T}{2\pi} \sin^{-1} \frac{x(t)}{A} \right]$$

Using the following substitution, we get:

$$u = t - \frac{T}{2\pi} \sin^{-1} \frac{x(t)}{A} \quad , \quad v = t + \frac{T}{2\pi} \sin^{-1} \frac{x(t)}{A} \qquad 4\text{-}50$$

Hence,

$$x_s = A \left| 1 - \frac{\dot{x}T/2\pi}{\sqrt{A^2 - x^2}} \right| \sum_{m=odd} \delta\left[u - \frac{m-1}{2} T \right] - \qquad 4\text{-}51$$

$$- A \left| 1 + \frac{\dot{x}T/2\pi}{\sqrt{A^2 - x^2}} \right| \sum_{m=even} \delta\left[v - \frac{m-1}{2} T \right]$$

This is equivalent to:

$$x_s = \frac{w_c A}{2\pi}\left|1 - \frac{\dot{x}T/2\pi}{\sqrt{A^2 - x^2}}\right| \sum_{n=-\infty}^{\infty} e^{jnw_c u} - \frac{w_c A}{2\pi}\left|1 + \frac{\dot{x}T/2\pi}{\sqrt{A^2 - x^2}}\right| \sum_{n=-\infty}^{\infty} e^{jnw_c u} \qquad 4\text{-}52$$

Substituting the equivalents of u and v and expanding the Fourier series we reach:

$$x_s = \frac{Aw_c}{2\pi}\left|1 - \frac{\dot{x}T/2\pi}{\sqrt{A^2 - x^2}}\right|\{1 + 2\sum_{n=1}^{\infty} \cos[nw_c t - n \sin^{-1}\frac{x(t)}{A}]\}$$

$$- \frac{Aw_c}{2\pi}\left|1 + \frac{\dot{x}T/2\pi}{\sqrt{A^2 - x^2}}\right|\{1 + 2\sum_{n=1}^{\infty} \cos[nw_c t + n \sin^{-1}\frac{x(t)}{A}]\} \qquad 4\text{-}53$$

By demodulating the D.C. part of x_s as described before, the baseband signal is retrieved, and it is depicted in Figure 4-12. We assume:

$$\frac{\dot{x}T/2\pi}{\sqrt{A^2 - x^2}} \leq 1 \text{ and } f_c = 2W \qquad 4\text{-}54$$

where W is the bandwidth of $\sin^{-1}\frac{x(t)}{A}$.

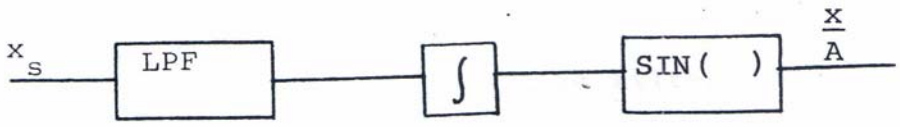

Figure 4-12. Retrieval of the Signal from the Train of Impulses by Low Pass Filtering

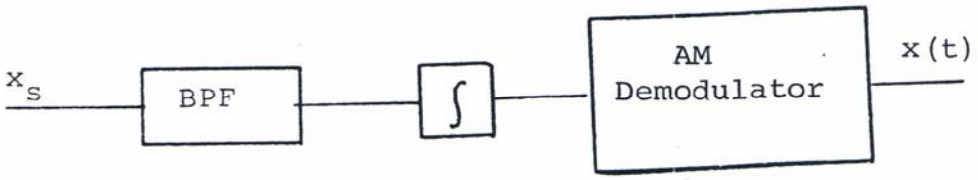

Figure 4-13. Retrieval of the Signal from the Train of Impulses by Band Pass Filtering

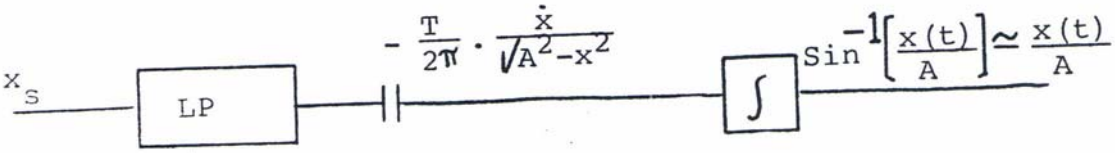

Figure 4-14. Reconstruction of the Signal from the Positive Impulses Only

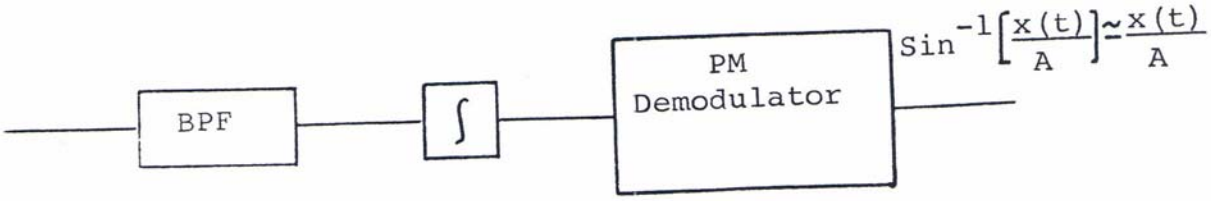

Figure 4-15. Retrieval of the Signal from the Train of Impulses

For the P.M. part, we bandpass filter around the principle frequency of the cosine function. Assuming no spectrum overlap, as usual, we have:

$$y_1 = \frac{2Aw_c}{2\pi}\left[1 - \frac{\dot{x}T/2\pi}{\sqrt{A^2 - x^2}}\right]\cos\left[w_c t - \sin^{-1}\frac{x(t)}{A}\right] -$$

$$- \frac{2Aw_c}{2\pi}\left[1 + \frac{\dot{x}T/2\pi}{\sqrt{A^2 - x^2}}\right]\cos\left[w_c t + \sin^{-1}\frac{x(t)}{A}\right] \qquad 4\text{-}55$$

After integrating y_1 in the above equation, we have:

$$y_2 = \frac{2A}{2\pi}\sin\left[w_c t - \sin^{-1}\frac{x(t)}{A}\right] -$$

$$- \frac{2A}{2\pi}\sin\left[w_c t + \sin^{-1}\frac{x(t)}{A}\right] = \qquad 4\text{-}56$$

$$= -\frac{4A}{2\pi}\cos w_c t\left[\frac{x(t)}{A}\right]$$

Suprisingly, after bandpass filtering, the integrated signal is a simple A.M. modulated signal that can be easily demodulated to yield the baseband signal. The reconstruction procedure is shown in Figure 4-13. This reconstruction method has two major advantages over the previous one. First, it

takes advantage of the P.M. noise reduction property (Section II-4); and secondly, it is an exact reproduction of the baseband signal unlike the first technique that uses the small angle approximation of

$$\sin^{-1} \frac{x}{A} \simeq \frac{x}{A}$$

For this reason it also has an advantage over the triangular wave given in Figure 4-9. Although the reconstruction block diagram is the same in both cases.

In comparison to a sawtooth generator, we could have suppressed the negative impulses totally and have transmitted only positive impulses. This suppression decreases the transmission rate by a half and as will be seen, it will simplify the reconstruction scheme. Equation 4-53 becomes:

$$x_s = \frac{Aw_c}{2} \left[1 - \frac{\dot{x}T/2\pi}{\sqrt{A^2 - x^2}}\right] \left\{1 + 2 \sum_{n=1}^{\infty} \cos \left[nw_c t - n \sin^{-1} \frac{x(t)}{A}\right]\right\} \qquad 4\text{-}57$$

Low pass filtering and blocking the D.C. value results in the derivative of:

$$\sin^{-1} \frac{x}{A}$$

This case is shown in Figure 4-14.

The baseband signal could also be retrieved from the P.M. part of the signal. Figure 4-15 shows the procedure by bandpass filtering and P.M. demodulation. The equations are as follows:

$$y_1 = \frac{Aw_c}{2\pi} \left[1 - \frac{\dot{x}T/2\pi}{\sqrt{A^2 - x^2}} \right] \cos \left[w_c t - \sin^{-1} \frac{x(t)}{A} \right] \qquad 4\text{-}58$$

After integration, we have:

$$y_2 = \frac{A}{2\pi} \sin \left[w_c t - \sin^{-1} \frac{x(t)}{A} \right] \qquad 4\text{-}59$$

After P.M. demodulation, we can deduce:

$$y_3 = \sin^{-1} \frac{x(t)}{A} \qquad 4\text{-}60$$

It should be mentioned that we could still have extracted the baseband signal from the sinusoidal signal if all the pulses, unlike Figure 4-11, had been positive. But the reconstruction technique would have been as complicated as the case discussed in Figure 4-7 for the triangular wave.

d. Exponential Waves

It is natural to extend the intersection problem to other periodic signals such as exponential waves (Figure 4-16). The corresponding analysis is now given.

$$x(t_1) = Ae^{at_1} - B \Rightarrow e^{at_1} = \frac{x(t_1) + B}{A} \qquad 4\text{-}61$$

Taking the logarithm of both sides, we have:

$$at_1 = \ln\left[\frac{x(t_1) + B}{A}\right] \Rightarrow t_1 = \frac{1}{a} \ln\left[\frac{x(t_1) + B}{A}\right] \qquad 4\text{-}62$$

As before

$$t_2 = T + \frac{1}{a} \ln\left[\frac{x(t_2) + B}{A}\right] \qquad 4\text{-}63$$

$$\vdots$$

$$t_m = (m-1)\,T + \frac{1}{a} \ln\left[\frac{x(t_m) + B}{A}\right] \qquad 4\text{-}64$$

$$x_s = \sum_m \delta(t - t_m) = \sum_m |\dot{g}(t_m)| \; \delta[g(t)] \qquad 4\text{-}65$$

where $g(t)$ is defined as:

$$g(t) = t - (m-1)\,T - \frac{1}{a} \ln\left[\frac{x(t) + B}{A}\right] \qquad 4\text{-}66$$

$$\dot{g}(t) = 1 - \frac{\dot{x}(t)}{a[x(t) + B]} \qquad 4\text{-}67$$

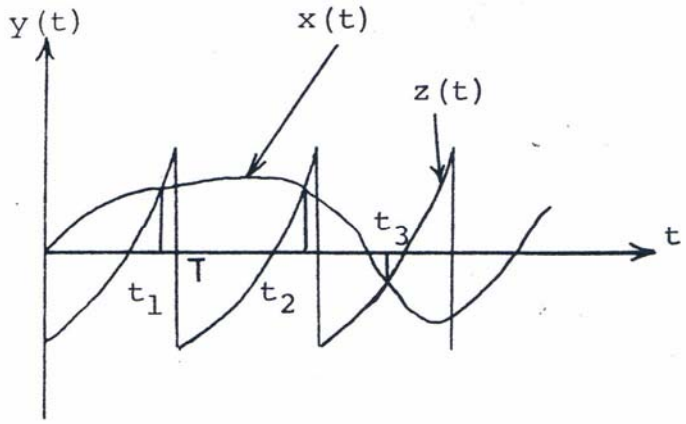

Figure 4-16. Intersection of a Random Wave with a Triangular Wave

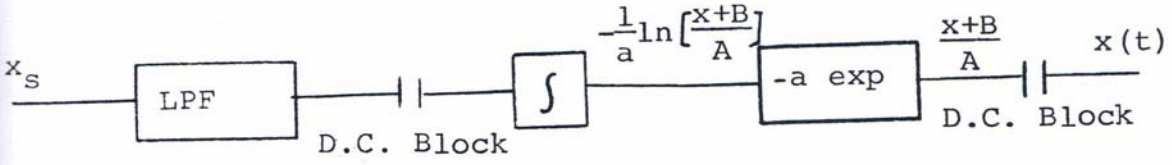

Figure 4-17. The Baseband Reconstruction of Equation 4-69

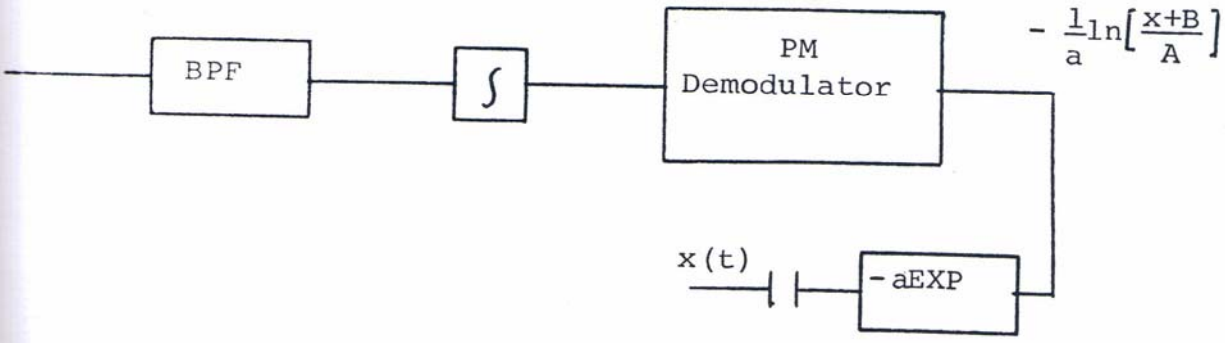

Figure 4-18. The Reconstruction of the Baseband Signal from the PM Part of Equation 4-69

Substituting the above equations in Equation 4-65 we arrive at:

$$x_s = \left|1 - \frac{\dot{x}}{a[x(t) + B]}\right| \sum_m \delta\{t - (m-1)\ T - \frac{1}{a} \ln[\frac{x(t) + B}{A}]\} \qquad 4\text{-}68$$

Using the familiar Fourier series expansion

$$x_s = [1 - \frac{\dot{x}}{a(x + B)}] \sum_{n=-\infty}^{\infty} e^{jnw\{t - \frac{1}{a} \ln[\frac{x + B}{A}]\}} \qquad 4\text{-}69$$

Assuming that $\left|\frac{\dot{x}}{a(x + B)}\right| < 1$ and $x \neq -B$, i.e., $x > -B$

A and $B > o$ 4-70

As before, there are two ways to reconstruct the baseband signal, x(t). The baseband demodulation is depicted in Figure 4-17 and the P.M. demodulation in Figure 4-18.

The assumption that there is no aliasing has to be investigated further. The bandwidth of the signal represented as the phase of the P.M. signal has to be less than half of the sampling rate. This requirement was discussed in Section IV-1-b. When the periodic signal is exponential, the phase of the Equation 4-69 is logarithmic, the bandwidth of which has to be found.

The analysis of an exponential function of the second category (Figure 4-19) is as follows:

$$t_1 = \frac{1}{a} \ln \left[\frac{x(t_1) + B}{A}\right]$$

$$t_2 = T - \frac{1}{a} \ln \left[\frac{x(t_2) + B}{A}\right]$$

$$\vdots \qquad \vdots$$

$$t_m = (m-1)T + (-1)^{m-1} \frac{1}{a} \ln \left[\frac{x(t_m) + B}{A}\right] \qquad 4\text{-}71$$

$$x_s = \sum_{m=odd} A\, \delta(t-t_m) - \sum_{m=even} A\, \delta(t-t_m) \qquad 4\text{-}72$$

$$\delta(t-t_m) = \dot{g}(t_m)\, \delta[g(t)] \qquad 4\text{-}73$$

$$g(t) = t - (m-1)T - (-1)^{m-1} \frac{1}{a} \ln\left[\frac{x(t) + B}{A}\right] \qquad 4\text{-}74$$

$$\dot{g}(t) = 1 - (-1)^{m-1} \frac{1}{a} \frac{\dot{x}(t)}{[x(t) + B]} \qquad 4\text{-}75$$

Hence,

$$x_s = \sum_{m=odd} \left|1 - \frac{1}{a} \frac{\dot{x}}{[x(t) + B]}\right| \delta \left\{t - (m-1)T - \frac{1}{a} \ln\left[\frac{x(t) + B}{A}\right]\right\} -$$

$$- \sum_{m=even} \left|1 + \frac{1}{a} \frac{\dot{x}}{[x(t) + B]}\right| \delta \left\{t - (m-1)T + \frac{1}{a} \ln\left[\frac{x(t) + B}{A}\right]\right\}$$

4-76

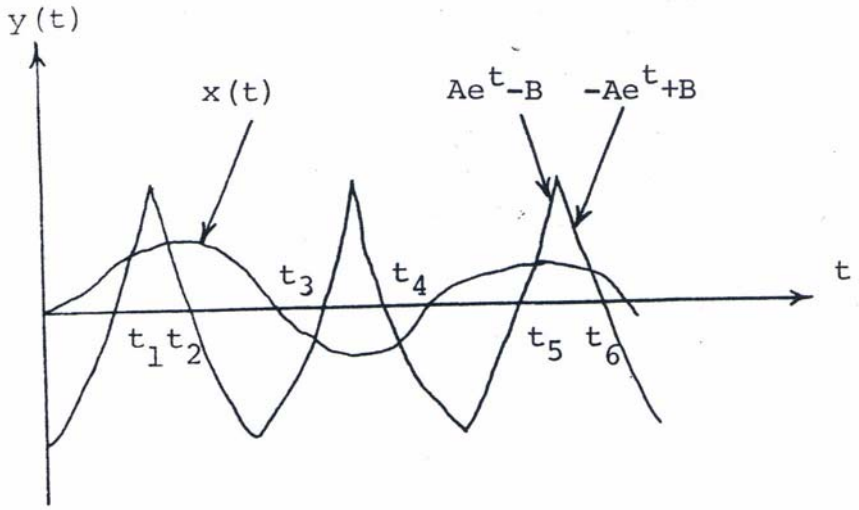

Figure 4-19.

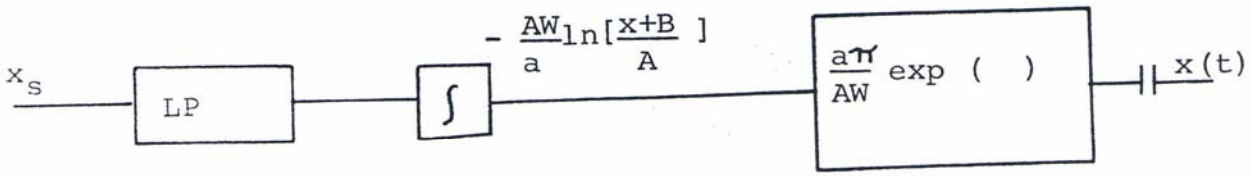

Figure 4-20. Reconstruction by Low Pass Filtering

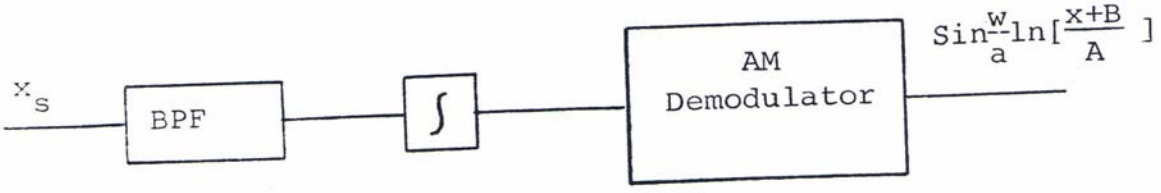

Figure 4-21. Reconstruction by Band Pass Filtering

Using the Fourier series, we can deduce that:

$$x_s = \frac{Aw_c}{2\pi}\left[1 - \frac{\dot{x}}{a(x+B)}\right]$$

$$\left\{1 + 2\sum_{n=1}^{\infty}\cos\left[nw_c t - \frac{nw_c}{a}\ln\left(\frac{x+B}{A}\right)\right]\right\} -$$

$$-\frac{Aw_c}{2\pi}\left[1 + \frac{\dot{x}}{a(x+B)}\right]$$

$$\left\{1 + 2\sum_{n=1}^{\infty}\cos\left[nw_c t + \frac{nw_c}{a}\ln\left(\frac{x+B}{A}\right)\right]\right\} \qquad 4\text{-}77$$

where

$$\left|\frac{\dot{x}}{a(x+B)}\right| < 1 \qquad 4\text{-}78$$

The two ways of reconstructing the baseband signal are illustrated in Figure 4-20 and Figure 4-21.

If the exponential function is almost linear, then Figure 4-21 resembles Figure 4-9 for the triangular wave, which is in practice usually generated as an exponential with a long time constant, i.e., $\ln\frac{x+B}{A}$ becomes equivalent to $x(t)$ and $\frac{1}{a}$ is the same as t_o.

If B is equal to zero, the inequality condition (Equation 4-78) is not satisfied, i.e., $\left|\frac{\dot{x}}{ax}\right|$ is not always less than one. Thus, the analysis fails for a non-negative exponential periodic function where $B = o$.

e. Parabolic Waves

Consider the intersection of the random signal with a parabolic function of the type $b + at^2$ illustrated in Figure 4-22.

Tha analysis is similar to the previous ones and is now discussed briefly.

$$b + at_1^2 = x(t_1) \Rightarrow t_1 = \sqrt{\frac{x(t_1) - b}{a}} \qquad \text{where } b<o \text{ and } a>o \text{ and } x(t)-b>o$$

$$t_2 = T + \sqrt{\frac{x(t_2) - b}{a}}$$

$$\vdots \qquad \vdots$$

$$t_m = (m-1)T + \sqrt{\frac{x(t_m) - b}{a}} \qquad 4\text{-}79$$

$$g(t) = t - (m-1)T - \sqrt{\frac{x(t) - b}{a}} \qquad 4\text{-}80$$

$$\dot{g}(t) = 1 - \frac{\dot{x}}{2a\sqrt{\frac{x-b}{a}}}$$

$$\text{where } g(t_m) = o,\ g(t \neq t_m) \neq o \text{ and } \dot{g}(t_m) \neq o \qquad 4\text{-}81$$

$$x_s = \sum_{m=1}^{\infty} \delta(t-t_m) = \left(1 - \frac{\dot{x}}{2a\sqrt{\frac{x-b}{a}}}\right) \sum_{m=1}^{\infty} \delta\left[t - (m-1)T - \sqrt{\frac{x-b}{a}}\right] \qquad 4\text{-}82$$

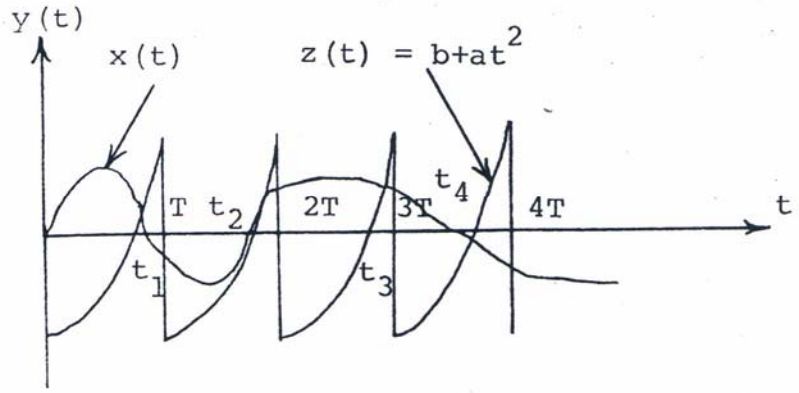

Figure 4-22. Intersection with a parabolic Function

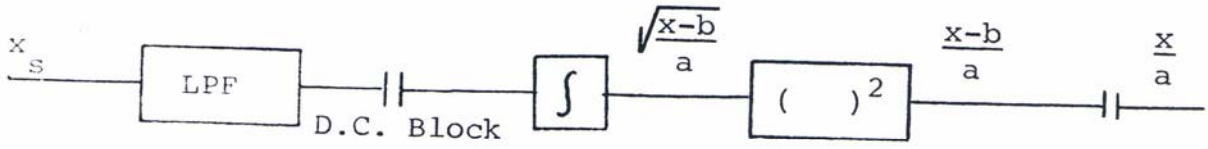

Figure 4-23. Reconstruction of the Baseband Signal by Low Pass Filtering

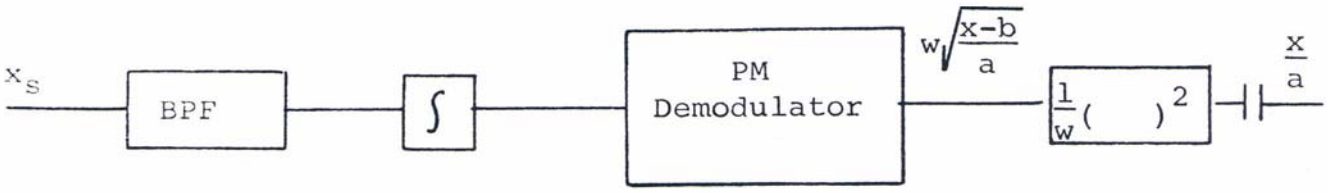

Figure 4-24. Reconstruction of the Signal by Bandpass Filtering

where $1 > \frac{\dot{x}}{2a\sqrt{\frac{x-b}{a}}}$

$$x_s = f_c\left(1 - \frac{\dot{x}}{2a\sqrt{\frac{x-b}{a}}}\right) \sum_{n=1}^{\infty} \left\{1 + 2\cos\left[nw_c t - nw_c\sqrt{\frac{x-b}{a}}\right]\right\} \quad 4\text{-}83$$

The two ways of reconstructing the original signal are depicted in Figure 4-23 and 4-24.

From the theoretical point of view, the square root of a signal has half the bandwidth of the original signal.[7] Therefore, the bandwidth of the P.M. signal is reduced by half. The frequency of the periodic signal z(t) in Figure 4-22 can thus be T/2.

e. Square Waves

A square wave cannot be in the category of the general periodic functions discussed before because the inverse of the function does not exist. There are several ways to solve this problem. One way is to approximate a square wave as has been illustrated in Figure 4-25.

The approximated square wave in Figure 4-25 is then solved as a special case of the general periodic function discussed in Section IV-1. A different approach would be

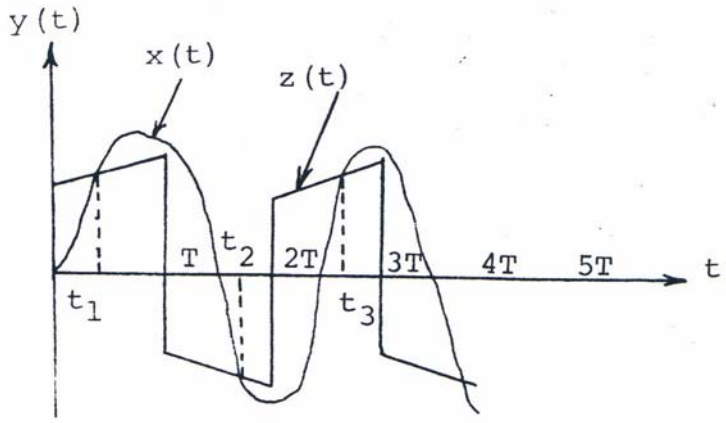

Figure 4-25. Intersection with an Approximately Square Wave

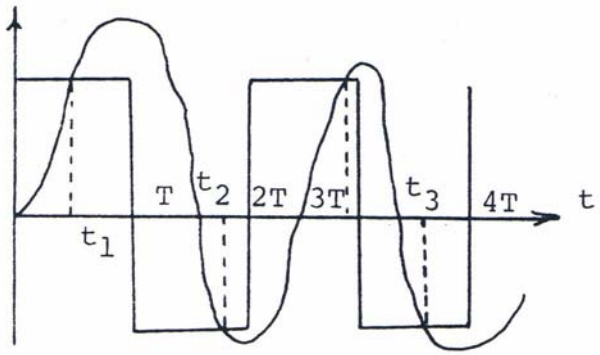

Figure 4-26. Intersection with a Square Wave

to use the original square wave depicted in Figure 4-26 and analyze the train of impulses in a different way.

$$x(t_1) = A,\ x(t_2) = -A,\ \ldots\ x(t_m) = (-1)^{m-1}A \qquad 4\text{-}84$$

With the assumption that there is only one sample per interval T, it can be written:

$$t_m = (m-1)T + t_m' \qquad 4\text{-}85$$

where t_m' is a random variable that lies in the region:

$$o < t_m' < T \qquad 4\text{-}86$$

$$x_s = A \sum_{m=odd} \delta(t-t_m) + A \sum_{m=even} \delta(t-t_m) \qquad 4\text{-}87$$

$$g(t) = t - (m-1)T - t_m' + \alpha(x-B) \qquad 4\text{-}88$$

$$\dot{g}(t) = 1 + \alpha \dot{x}(t)$$

$g(t)$ is a valid equation because:

$$g(t_m) = o$$

$$g(t) \neq o \text{ for } t \neq t_m$$

$$\dot{g}(t_m) \neq o \qquad 4\text{-}89$$

Figure 4-27. Reconstruction of the Baseband Signal by Low Pass Filtering

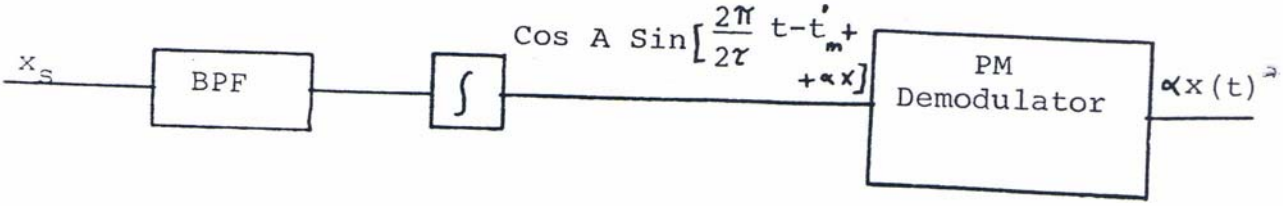

Figure 4-28. Reconstruction of the Baseband Signal by Band Pass Filtering

therefore,

$$x_s = A\,|\,1 + \dot{x}(t)\,|\sum_{m=odd} \delta[\,t - (m-1)T - t_m' + \alpha\,(x-A)\,] + \qquad 4\text{-}90$$

$$+ A\,|\,1\ \alpha\,\dot{x}(t)\,|\sum_{m=even} \delta[\,t - (m-1)T - t_m' + \alpha\,(x+A)\,]$$

Using the equivalent Fourier series, we can deduce the following:

$$x_s = A\,[\,1 + \alpha\dot{x}(t)\,]\{\,1 + 2\cos[\,\frac{2\pi}{2T}\,t - t_m' + \alpha\,(x-A)]\,\} \qquad 4\text{-}91$$

$$A\,[\,1 + \alpha\dot{x}(t)\,]\{\,1 + 2\cos[\,\frac{2\pi}{2T}\,t - t_m' + \alpha\,(x+A)]\,\}$$

The two standard techniques for reconstructing the baseband signal are illustrated in Figure 4-27 and 4-28.

α is an arbitrary constant in the Equation 4-88. It should not affect the equation when x = B. But in Figure 4-27 and 4-28, it is observed that the reconstruction technique deperds on α. This interesting paradox can be answered as follows: The bandwidth of the P.M. signal is approximately given by the following formula:[7]

$$B_T \simeq 2(\,\phi_d + 1)\,W \qquad 4\text{-}92$$

where W is the bandwidth of the baseband signal and $\Phi_d = \alpha$ in our case.

For $\alpha = 1$, $B_T \simeq 4W$ and for $\alpha << 1$ (Narrowband P.M.), $B_T = 2W$. Hence, the bandwidth of the P.M. signal is directly proportional to α . Therefore, if the pass band of the low pass filter in Figure 4-27 is 2W, α is equal to zero. On the other hand, if the pass band is 4W, α is equal to 1. Thus, the pass band of the low pass filter in Figure 4-27 and the band pass filter in Figure 4-28 determine the value of α. i.e., from Equation 4-92, we derive:

$$\alpha \simeq \frac{B_T}{2W} - 1 \qquad 4\text{-}93$$

where B_T is the pass band of the filters in Figure 4-27 and 4-28.

The principle frequency of the square wave has to be chosen such that there is no spectrum overlapping. Hence, we infer:

$$\frac{1}{2T} \geq 2(\alpha + 1)W \qquad 4\text{-}94$$

The basic flaw in the foregoing analysis is the assumption that there is only one sample in each interval T

for a square wave. This assumption may not be true. Consequently, the analysis is hypothetical for the aforementioned specific assumption.

2. Comparison of the Periodic Waveforms

In order to compare the effects of the different periodic waveforms intersected with a random signal, the following performance indices should be considered.

1. Transmission rate (bits/second)
2. Bandwidth requirement
3. The ease of reconstructing the periodic signal at the transmitter.
4. The ease of reconstructing the random signal at the receiver.
5. Sensitivity of the reconstructed signal to channel noise

The first criterion (bits/second) also depends on the method of reconstruction from the nonuniform pulses (x_s), e.g., for a triangular wave, the transmission rate is at the Nyquist rate if the reconstruction is done by the nonuniform sampling theorem and is twice the Nyquist rate if the reconstruction is done by low pass filtering and integration as described in Section IV-1-b. For the general reconstruction by the intersection technique, the periodic functions that fall in the category of Figure 4-1, e.g., a sawtooth wave, the transmission rate is at the Nyquist rate with one bit

per sample. The periodic functions that fall in the second category Figure 4-2, e.g., a sine wave, the transmission rate is at twice the Nyquist rate with one or two bits per sample, depending on the reconstruction scheme (Section IV-1-c). Any periodic waveform in the second category can be modified to become a member of the first category. For instance, a sine wave falls into the first category by suppressing the negative pulses (Section IV-1-c).

The bandwidth of transmission depends both on the transmission rate and the position of the pulses. The position of the pulses is governed by the random signal, $x(t)$, and the periodic waveform. The train of impulses is a summation of P.M. signals (Equation 4-6). Each P.M. signal, $\cos \{nw_c t + nw_c f^{-1} [x(t)]\}$, has a bandwidth proportional to the bandwidth of $f^{-1}[x(t)]$, where $f^{-1}[\ ]$ is the inverse periodic function. Hence, depending on the periodic wave, the bandwidth of the harmonic terms in Equation 4-6 changes. This fact is important for the reconstruction method where it is assumed in Equation 4-6 that there is no aliasing effect.

From a practical point of view, some periodic waveform generators are more common than other ones. For example, a sine wave generator is more common than a periodic parabolic generator. The availability of a signal generator of a certain type is therefore a factor in favor of that waveform than others.

The most important consideration of all is the ease of reconstruction method. If the reconstruction technique is done by the general nonuniform sampling techniques (Part VIII), there is no preference in selecting a particular periodic signal as long as the Nyquist criterion (Appendix A) is satisfied. If the reconstruction technique is achieved by the general intersection methods (Figure 4-3 and Figure 4-4), the choice of the periodic signal is contingent upon the ease to implement the block f [ ] in Figure 4-3 and Figure 4-4. For example, the block sin( ) in Figure 4-12 is not as easy to realize than the block $(\ )^2$ in Figure 4-23. However, for small angles, the block sin( ) can be totally eliminated, the same as a triangular wave where the block f( ) is only a gain factor (Figure 4-8). In general, the periodic functions that are in the first category (Section IV-1), the choice of

the periodic signal depends on the block f( ) in Figure 4-3 and Figure 4-4.

The periodic waveforms in the second category, fall into three distinct cases. If all the pulses are positive, the reconstruction is quite complex and not feasible relative to the other cases. If the pulses have positive and negative polarity according to the slope of the periodic waveform, there are two distinct cases. If the reconstruction of x(t) is achieved by low pass filtering and integration, the triangular waveform is the simplest (Figure 4-8) as opposed to other periodic functions in this category (e.g., Figure 4-12). This point is also verified experimentally as explained in Section IX-1. If the reconstruction of x(t) is done by bandpass filtering, the sine wave is the best as described and proved in Section IV-1-C and Figure 4-13.

Finally, the choice of the periodic function is dependent on the noise immunity at the receiver. The dependence of the periodic functions on noise is analyzed in Section II-4.

PART V-

ADAPTIVE INTERSECTING WAVEFORMS

1. Introduction

Extensions of previous methods may be obtained by considering adding the features of adaptivity. Various adaptive procedures have been suggested [14,15,16,17] to exploit the redundancy in the signal samples and hence to reduce the number of transmitter bits per sample. It was stated in Part III that zero crossings and level crossings of a signal x(t) can be transmitted at one bit per sample. At the receiver, x(t) is reconstructed provided that the Nyquist rate is satisfied. Unfortunately, the number of levels and their positions can only be calculated for a well defined Gaussian signal, x(t); for a Gaussian signal added to a sinusoidal waveform.[18] In the case of a Gaussian process with unknown parameters or a non-Gaussian signal like a voice signal, the average number of zero crossings is not known. In order to satisfy the Nyquist rate hence to optimize the transmission rate, the intersecting levels have to be determined adaptively. So far most of the adaptive techniques have been based on adapting the quantization levels for uniform samples to reduce bits per sample or to reduce the quantization

noise at transmission rates comparable to P.C.M.[14,15] To the best of the author's knowledge, adaptive intersecting levels with random signals have never been considered. Its advantage to the conventional adaptive techniques and P.C.M. is that an optimum transmission rate at one or two bits per sample can be attained with no quantization noise at the instants of transmission. The main difference in the samples is that the pulses are nonuniform. Further comments on the above points are discussed in detail in this section.

2. General Adaptive Technique (Adaptive Quantizer)

a. General Description

A novel adaptive technique will be developed. This method, unlike conventional P.C.M., quantizes first and then samples. Instead of setting the quantizing levels to cover the whole amplitude range of the signal, only a portion of the signal is quantized with fewer quantization intersection levels (two levels q_1 and q_2). The range of the quantization is chosen arbitrarily. q_1 and q_2 can both intersect the signal and the first intersection of the signal, and threshold determines the point in time to be sampled. Next, the levels q_1 and q_2 are adapted according to a variety of algorithms to be studied. The general approach is to adapt the levels upward if the higher level intersects first, then vice versa, Figure 5-1. This procedure of sampling is repeated for each iteration. If the number of samples in T seconds are less than the average Nyquist rate, the distance between the two levels is decreased in order to get more samples and vice versa. Hence, the average Nyquist criterion can also be achieved.

A comparison of the new method and the other methods reveal that our method is appealing from the transmission's

point of view. For example, for telephone channels, it is required to use 8 bits/ sample for P.C.M. transmissions.

By using the adaptive quantizers developed recently,[3,15] the bits per sample can be reduced by less than a half (2 - 5 bits for a given data). Our adaptive scheme uses 2 levels, i.e., 1 bit per sample. By varying the quantization level adaptively, the Nyquist rate (samples per second) can be achieved. This implies that the transmission rate is optimized i.e.,

bits/sample X samples/sec. = bits/sec.

1 bit/sample X N/sec = N/sec = Nyquist rate

In the Adaptive Quantizer developed by Golding[3], the quantization noise increases at the Nyquist rate. Our method does not produce any quantization noise because the samples are chosen exactly when the quantization level intersects the signal. Also, in Golding's method there are clipping errors due to wrong predictions of the future samples. Our technique does not depend on predictions of future samples as such.

Because of quantizing first, the inactive regions of the signal, which are highly correlated, are sampled less often than the other regions. Thus the average samples per second

are decreased. In other words, the method transmits the samples with maximum information content and discards the least informative ones. If the signal was sampled first, we could not have achieved the aforementioned results, and a complicated method would be needed to get the same results[17,20,21,22]

Occasional test signal for the synchronization of the transmitter and receiver is not a serious problem as it is in Golding's method. At the receiver of our method, the intersection (quantization) levels are already known. As the quantization levels are adapted at the transmitter the levels at the receiver are adapted likewise. The amplitude of the samples are the same as the quantization levels, and if there is channel noise, a threshold device can choose which quantization level is the amplitude of the coming sample. The probability that the amplitude is corrected by the threshold device is greater than 1/2. Hence, the channel noise is also suppressed most of the time (Section II-4). In Golding's method, the receiver adapts its levels from the quantized samples rather than the actual samples.

The transmission rate of the new method is much better than the transmission rates of P.C.M. and a delta modulator. It has

the same drawback as a delta modulator in the sense that the error at the receiver is propagated. This error is due to the fact that the quantization levels at the receiver are adapted according to the received sample. If due to channel noise, there is an error in a sample, the quantization levels are adapted incorrectly and all the future samples are in error. Our method, like the delta modulator and any nonuniform sampling transmissions, depends on the time intervals of the nonuniform samples, i.e., these time intervals carry information. In case of channel distortion in phase, there might be a time delay or intersymbol interference. This error can be reduced by using phase channel equalizers. In case the samples are too close, the bandwidth of the signal increases. To avoid this problem, the future uniform sample has to be predicted (Section II-2-1); then one must adapt the quantization levels according to the predicted value. This adaptation would make the nonuniform samples as close to uniform samples as possible. Also this adaptation would reduce the bandwidth requirement as well as simplify the reconstruction of samples (Part VIII).

An example of the technique for a sinusoidal signal, x(t), is given in page . It shows that by varying the length

of the quantization level, one can achieve the Nyquist rate. After this example, the next two sections (V-2-6 and V-2-c) consist of the prediction of the future samples and the analysis of the technique respectively. The new technique has been simulated on the computer (Section IX-1) and built in the laboratory sucessfully (Section IX-3). The results are promising. The analysis of our Adaptive Quantizer is given in Section V-2-c.

In comparison to other methods like Δ.M., P.C.M., our method has the following advantages:

1. The quantization error of samples is zero.

2. The transmission rate is optimum (one bit per sample).

Comparing our system to other adaptive techniques, we can state that our system is still better in terms of the quantization error and transmission rate. Also the problems of predicting the future samples and then adapting the intersection levels do not exist. In addition, due to the nonexistence of samples in the inactive low frequency regions of a signal, the pulses can be coded in time using run length coding[30] or the recently developed coding for asynchronous pulses called "CODEST"[31]

This kind of coding reduces the transmission time. For example in facsimile transmission, run length coding reduces the transmission time almost by a factor of five.

Example 1: Figure 5-1 demonstrates graphically the application of the Adaptive Quantizer on a random signal, x(t), in detail. It depicts the variables which determine the number of samples per second. The quantization distance "a" and the guardband "l" are the determining variables. Figure 5-2 shows the samples obtained by using the new method on a sine signal. Figures 5-3 through 5-8 are the plots of the sampling rate "R" versus the distance of the quantization level "l". The sampling rate is in terms of the ratio of the number of samples per second over the Nyquist rate "R".

The range of "a" is chosen to be between 1/4 and 5/4 of the maximum amplitude of the sine signal. Figures 5-3 through 5-8 show interesting results. "R" in general, is increasing with increasing "l". This increase is continuous except where the maximum amplitude of the signal is a multiple integer of "a" (e.g. when a = 1/4, 1/2 and 1). For this special case "R" is constant when $o < l < \frac{a}{2}$ and then it jumps discontinuously

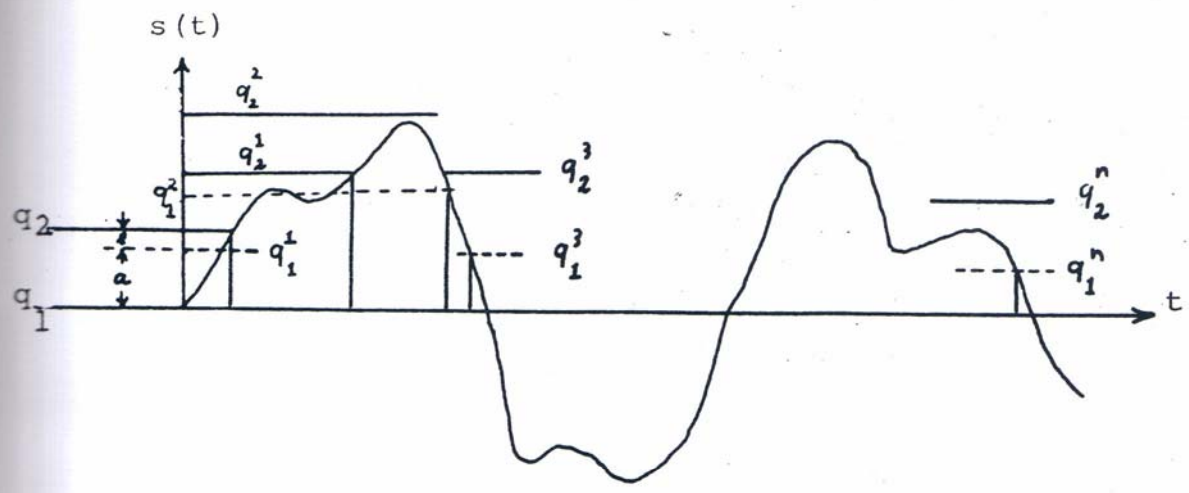

Figure 5-1. The Adaptive Quantize

where $s(t)$ = Any Signal

$h_o = q_1$ = Lower Level of the First Step

$h_1 = q_2$ = Higher Level of the First Step

$h_o' = q_1^1$ = Lower Level of the Second Step

$h_1' = q_2^1$ = Higher Level of the Second Step

.

.

.

$h_o^n = q_1^n$ = Lower Level of the $(n+1)^{th}$ Step

$h_1^n = q_2^n$ = Higher Level of the $(n+1)^{th}$ step

$t_n = n^{th}$ Non-Uniform Sample

to a higher value. One must consider that this special case holds true only for deterministic signals that are periodic. For a random signal like voice, there is no discontinuous jump in these special cases. Figure 5-6 is the only exception that behaves slightly differently in the range $0 < l < \frac{a}{2}$. In Figure 5-7 and 5-8 we observe that the sampling rate approaches zero. For Figure 5-3, the sampling rate is 3/2 of the Nyquist rate (R = 1.5) when $l = 0$. Therefore, the sampling rate depends on "a" and "l" simultaneously. If the performance index is the difference between the sampling rate and the Nyquist rate, the levels are adapted to a = 1, 5/4 or 1/2 and l = 0 to achieve the Nyquist rate. If "a" is fixed, "l" has to be decreased to zero and if "l" is fixed, "a" has to be adapted so that "R" is minimized. The sine signal in Figure 5-8, a = 5/4 yields the lowest "R" for a given "l". We note that an adaptive technique is only required when the signal is random or unknown. Therefore, if we don't know that a sine signal is being transmitted at the receiver, we have to use the adaptive method.

b. Uniformizing Samples by Prediction

We have seen that the new method has the disadvantage of nonuniform sampling. This might not be desirable for bandwidth

constraints. Also nonuniform sampling is more difficult to be reconstructed. Therefore, it is more desirable to work with uniform sampling.

Using the correlation of adjacent samples, one can predict the future sample.[23,24] This can be done by using a linear predictor based on the last few samples. By finding the future sample, one can adapt the quantization level to that predicted value. This technique results in uniform samples with jitter noise. The equations describing the linear predictor are as follows.[23]

Suppose the future sample x_{n+1} is estimated by a linear combination of the past n samples so that the mean square error is minimized, i.e.,

$$e = E\{ [x_n - (a_1 x_1 \ldots\ldots + a_n x_n)]^2 \} \qquad 5\text{-}1$$

Using the orthogonality principle, we find the parameters, $a_1 \ldots a_n$, to be the solution to the following equations:

$$\begin{aligned} &R_{11} a_1 + \ldots\ldots\ldots\ldots\ldots + R_{1n} a_n = R_{o1} \\ &\vdots \\ &R_{n1} a_1 + \ldots\ldots\ldots\ldots\ldots + R_{nn} a_n = R_{on} \end{aligned} \qquad 5\text{-}2$$

Choosing these values for a's, we would get the least mean square estimate for the future sample.

To uniformize nonuniform samples, we propose another method. Ideally, uniform samples can be calculated if all the past and future nonuniform samples are known. We have to reconstruct the signal from the nonuniform samples first and then sample uniformly to get the uniform samples. The problem of nonuniform sampling reconstruction will be discussed in depth in Part VIII. The reconstruction formula for nonuniform samples is (Appendix A):

$$s(t) = \sum_{p=1}^{N} s(\tau_p)\, \Psi_p(t) \qquad 5\text{-}3$$

where

$$\Psi_p(t) = \sum_{q=1}^{N} a_{qp} \frac{\sin 2\pi W(t - \tau_q)}{2\pi (t - \tau_q)} \qquad 5\text{-}4$$

The coefficients a_{qp} are the coefficients of the inverse matrix of a matrix whose elements are:

$$\frac{\sin 2\pi W(\tau_p - \tau_q)}{2\pi W(\tau_p - \tau_q)} \qquad p,q = 1,2,\ldots,N \qquad 5\text{-}5$$

If we try to approximate the signal by the past M samples, we have

$$s(t) = \sum_{p=1}^{M} s(\tau_p)\,\psi\, p(t) \quad \text{(See Figure 5-9)} \qquad 5\text{-}6$$

This approximation is the least mean square estimate of the signal since p(t) is an orthogonal function.[26] To estimate the next uniform sample, we proceed as follows:

Only the right hand side of the scanning functions for nonuniform samples is needed (Figure 5-10). We add the scanning functions and sample the resultant at $t = \tau_{M+1}$ where the future uniform sample is. The amplitude sampled at $t = \tau_{M+1}$ is the predicted uniform sample. The actual implementation of this scheme will be discussed in Part VIII.

Returning to our original adaptive technique, we adapt our level to the predicted amplitude. At the intersection a sample is generated. The future sample is again predicted from the last M samples, and the whole procedure is repeated. We note that this method of uniformizing the samples is much more complicated than the linear prediction scheme. But as a trade off, we expect a more accurate result. The purpose of uniformizing the samples as mentioned before are threefold:

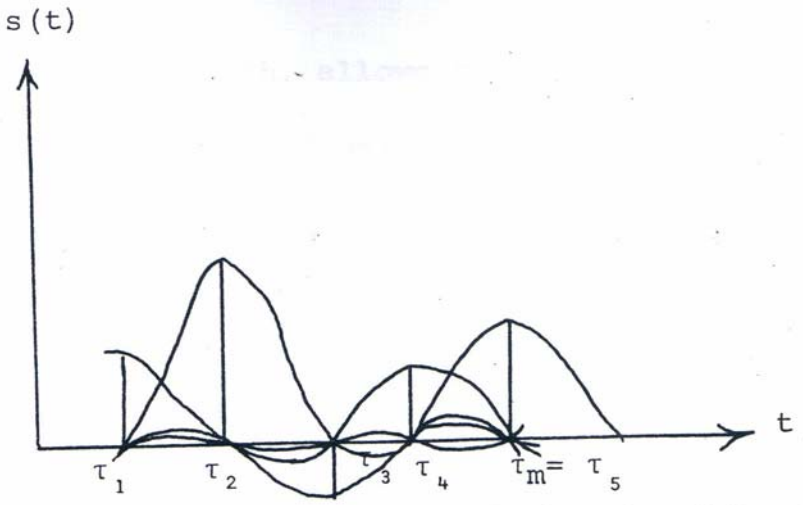

Figure 5-9: Approximation of the Signal by the Past M Samples

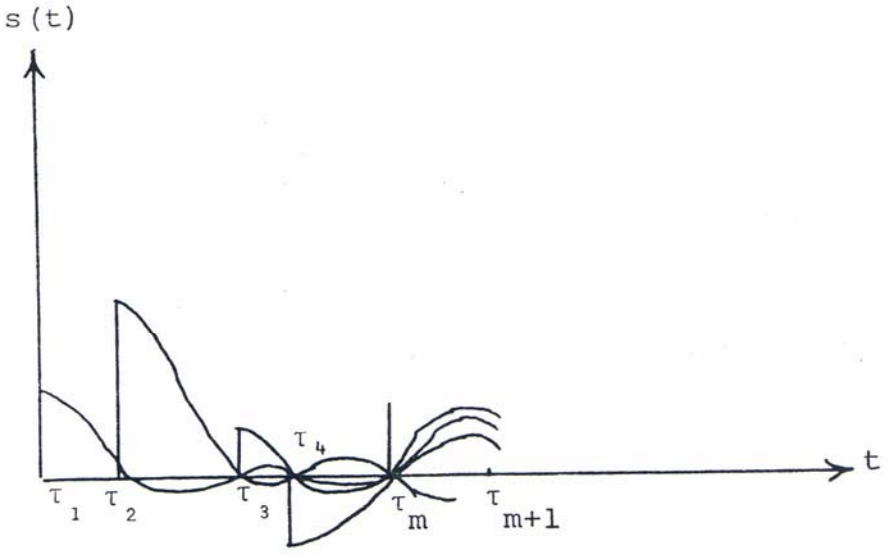

Figure 5-10: Predicting the Future Uniform Sample from the Past M Samples

uniformizing saves bandwidth, allows for a better reconstruction scheme, and also allows time domain multiplexing.

c. Mathematical Analysis of the Adaptive Technique

It is the purpose of this section to analytically formulate a relationship between the sampling rate and the parameters of the adaptive technique based on the statistics of the signal. We must first try to solve the problem by assuming a signal with a Gaussian distribution function and then by trying to generalize to any signal with known statistics, the Adaptive Quantizer is also analyzed from the intersection point of view.

i - Gaussian Signal:

For practical signals, the amplitude is limited within a region. Hence, we assume that the probability density function of the signal is negligible beyond the 3σ level where σ is the standard deviation of the random signal. Assume the h_o level in Figure 5-1 is at zero and the h_1 at the level "a". Level h_1 intersects the signal with the average level crossing.[5]

$$n_{h_1} = N_o \, e^{\frac{-a}{2R(o)}} \qquad 5\text{-}7$$

where N_o is the average zero crossing per second and R(o) is the autocorrelation of the signal at $\tau = o$.

The average time interval between the level crossings at h_1 is:[5]

$$T_{h_1} = \frac{1}{n_{h_1}} = \frac{1}{N_o} e^{\frac{a}{2R(o)}} \qquad 5\text{-}8$$

At this time the two levels h_o and h_1 are adapted to the new values h_o' and h_1' as shown in Figure 5-1. According to our method the level that intersects the signal first is chosen as the next sample. Since it cannot be predicted which level intersects the signal due to the randomness of the signal, a statistical time average has to be taken into consideration for the next sample. Level h_o' intersects the signal on the average in time intervals

$$T_{h_o'} = \frac{1}{n_{h_o'}} = \frac{1}{N_o} e^{\frac{a-1}{2R(o)}} \qquad 5\text{-}9$$

We are interested to find out when h_o' intersects the signal relative to the previous sample, which is at $t_1 = T_{h_1}$ seconds from the origin. In order to evaluate this we must observe

that T_{h_o}' is smaller than T_{h_1}', which is obvious from Equations 5-8 and 5-9. First, we find out how many T_{h_o}' intervals are contained in the interval T_{h_1}

$$\frac{T_{h_1}}{T_{h_o}'} = \frac{1/No\ e^{\frac{a}{2R(o)}}}{1/No\ e^{\frac{a-1}{2R(o)}}} = e^{\frac{1}{2R(o)}} \qquad 5\text{-}10$$

Since the ratio has to be an integer, we truncate the ratio and get:

$$M_{h_o}' = INT\left[\frac{T_{h_1}}{T_{h_o}'} + 1\right] = INT\left[e^{\frac{1}{2R(o)}} + 1\right] \qquad 5\text{-}11$$

Hence, level h_o' intersects the signal at $M_{h_o}'\ T_{h_o}'$. Likewise, level h_i' crosses the signal at $M_{h_1}'\ T_{h_1}'$ where M_{h_1}' is defined as

$$M_{h_1}' = INT\left[\frac{T_{h_1}}{T_{h_1}'} + 1\right] = INT\left[\frac{1/N_o\ e^{\frac{a}{2R(o)}}}{1/N_o\ e^{\frac{2a-1}{2R(o)}}} + 1\right] = \qquad 5\text{-}12$$

$$= INT\left[e^{\frac{1-a}{2R(o)}} + 1\right]$$

For the special case shown in the preceding equation, Equation 5-12 is equal to 1 because $1 < a$ and $0 < e^{1-a} < 1$. According to our hypothesis, we select the level that has a shorter time interval. But since we do not know which level intersects the signal first, we must take a statistical time average between M_{h_o} ' T_{h_o} ' and M_{h_1} ' T_{h_1} '. However, each time interval has to be weighed differently. This depends on two factors. The closer a level is to zero, the higher the probability that it intersects the signal because the signal is Gaussian distributed. The second factor depends on the amplitude of the previous sample (at t_1), and the slope of the signal at that point. The problem of finding the probability of which level crosses the signal first is tremendously difficult, if not impossible for the general random signal. But we can approximate this probability considering the following observations:

a. If there is no extremum point between the two levels and the slope is positive, the upper level will cross the signal first.

b. On the contrary, if there is no extremum point between the two lines and the slope is negative, then the lower level will cross the signal first. In any case, the

intersection of the upper level is always at the positive slope of the signal and vice versa.

c. If there is no extremum point, we have the following inequality deduced from Figure 5-11.

$$t_1 < t_2 < t_3 \qquad 5\text{-}13$$

where t_1 is the second sample at h_1' , t_2 and t_3 are the level crossings at h_1 and h_o' respectively.

d. If there is an extremum point between the two intersecting levels, level h_1 would be intersected before the other two levels h_o' and h_1'. The rare case depicted in Figure 5-12 is an exception.

ii - Analysis by a Random Walk Method

A different approach to the problem is the same as a simple random walk problem.[27] Suppose X_i denotes the time interval at the i^{th} adaptive step for the quantization levels. By this time interval, we mean the time difference between the i^{th} sample and the previous one. The time required after n steps is given by the random variable

$$X = X_1 + X_2 + \ldots . X_i \ldots . + X_n = \sum_{i-1}^{n} X_i \qquad 5\text{-}14$$

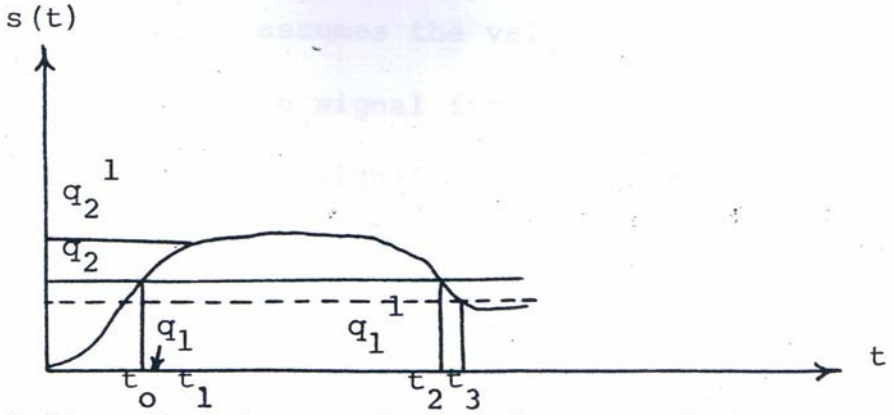

Figure 5-11: The First and Second Steps of the Adaptive Quantizer where there is no Extremum Point Between q_1^1 and q_2^1 where

$q_1 = h_o$

$q_2 = h_1$

$q_1^1 = h_o'$

$q_2^1 = h_1'$

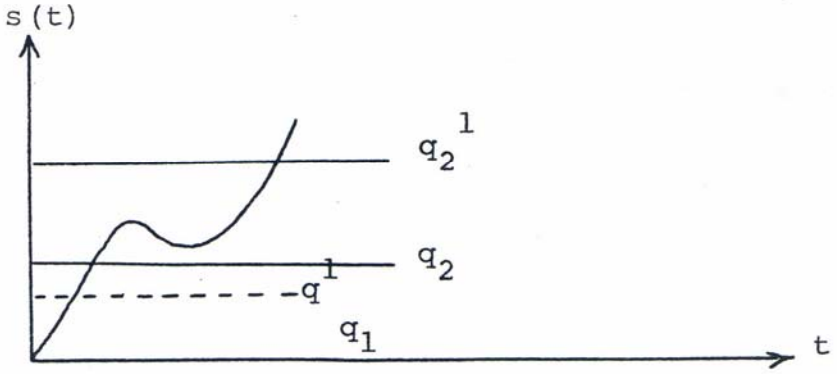

Figure 5-12

Each random variable X_i assumes the value T_{Ui} if the upper level intersects the signal first and T_{Li} if the lower level intersects the signal first. Therefore,

$$EX_i = P_{Ui}\, T_{Ui} + (1-P_{Ui})\, T_{Li} \quad \text{for each } i \text{ where } P_{Ui} \text{ is} \qquad 5\text{-}15$$

the probability that the upper level is intersected first.

$$EX_i^2 = P_{Ui} T_{Ui}^2 + (1 - P_{Ui})\, T_{Li}^2 \quad \text{for each } i$$

$$\text{Var } X_i = EX_i^2 - (EX_i)^2 = P_{Ui} T_{Ui}^2 (1 - P_{Ui}) + T_{Li}^2 (P_{Ui})(1-P_{Ui}) -$$

$$- 2\, P_{Ui} T_{Ui} (1 - P_{Ui})\, T_{Li} \quad \text{for each } i \qquad 5\text{-}16$$

$$EX = \sum_{i=1}^{n} EX_i, \quad \text{Var } X = \sum_{i=1}^{n} \text{Var } X_i \qquad 5\text{-}17$$

The distribution of the variable, $X_o = \dfrac{X-EX}{\sqrt{\text{Var } X}}$, approaches a standard normal curve as n goes to infinity. This is the result of the central limit theorem if the X_i's are independent.

$$EX_o = 0 \text{ and } \sigma = 1$$

EX is the average time taken for n nonuniform samples to be transmitted. If EX is less than the Nyquist time T_n for n uniform samples, then each EX_i has to be increased. This implies that T_{Li} and T_{Ui} have to be increased. T_{Li} and T_{Ui} are dependent on the quantization levels, which have to be adjusted accordingly. The probability that X is less than T_N after n steps is given by:

$$P(X<T_n) \simeq P(X_o < \frac{T_n - EX}{\sqrt{Var\ X}}) = \frac{1}{\sqrt{2\pi}} \int_{-\infty}^{\frac{T_n - EX}{\sqrt{Var\ X}}} e^{-u^2/2}\, du \qquad 5\text{-}18$$

For small n, the exact distribution of X is a binomial type. The probability of obtaining one ensemble of X is (an outcome is the upper level or the lower level)

$X^r = \underbrace{(ULLUU...L)}_{n}$ is one ensemble (It has r upper levels)

$$PX^r = P_{U1}\, P_{L2}\, P_{L3}\, P_{U4}\, P_{U5} \cdots P_{Ln} \qquad 5\text{-}19$$

Consider a random variable Y_i associated with the i^{th} step. If the upper level is intersected, we assign the value of 1 to Y_i, otherwise we assign the value of zero.

The average and variance of Y_i are as follows:

$$E Y_i = 1 \times P_{Ui} + 0 \times P_{Li} = P_{Ui} \qquad 5\text{-}20$$

$$E Y_i^2 = 1^2 \times P_{Ui} + 0^2 \times P_{Li} = P_{Ui}$$

$$\text{Var } Y_i = P_{Ui} - P_{Ui}^2 = P_{Ui}(1 - P_{Ui}) = P_{Ui} P_{Li} \qquad 5\text{-}21$$

$$\text{Define, } Y = \sum_{i=1}^{n} Y_i \text{ where } E\ Y = \sum_{i=1}^{n} P_{Ui}, \text{ Var } Y = \sum_{i=1}^{n} P_{Ui} P_{Li} \qquad 5\text{-}22$$

$$\text{Define, } Y_o = \frac{Y - \sum_{i=1}^{n} P_{Ui}}{\left(\sum_{i=1}^{n} P_{Ui} P_{Li} \right)^{\frac{1}{2}}} \qquad 5\text{-}23$$

According to the central limit theorem, if Y_is are independent, the distribution of Y_o approaches a normal distribution. Y represents the number of times the upper quantization level is intersected first. The probability that the number of times the upper level intersects the signal between $a < y < b$ is a binomial distribution approximated by:

$$P(a< <b) \quad \frac{1}{\sqrt{2\pi}} \int_{\frac{a - \sum_{i=1}^{n} P_{Ui}}{\left(\sum_{i=1}^{n} P_{Ui} P_{Li}\right)^{1/2}}}^{\frac{b - \sum_{i=1}^{n} P_{Ui}}{\left(\sum_{i=1}^{n} P_{Ui} P_{Li}\right)^{1/2}}} e^{-w^2/2} \, dw \qquad 5\text{-}24$$

where $b \leq n$. Therefore, $P(a< y <b) \simeq \sum_{a<r<b} X^r$ where X^r is defined in the Equation 5-19. Hence, we expect E Y, which is the number of upper levels, to be n/2 for large n, i.e.

$$Ey = \sum_{i=1}^{n} P_{Ui} = \frac{n}{2} \text{ for large } n \qquad 5\text{-}25$$

We should note that X_i's and Y_i's are actually not independent due to the correlation of the adjacent samples and hence X and Y are not Gaussian.

iii - Analysis from the Intersection Point of View

The samples derived from the adaptive technique are the same samples derived at the intersection of a random signal and a multilevel signal dependent on x(t) depicted in Figure 5-13.

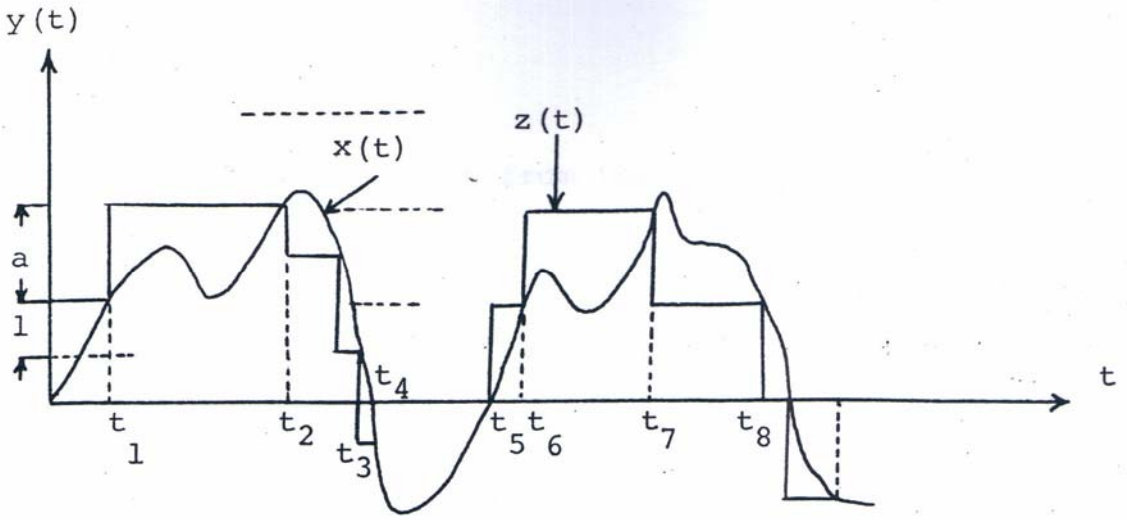

Figure 5-13: Adaptive Technique viewed as an Intersection of Two Signals

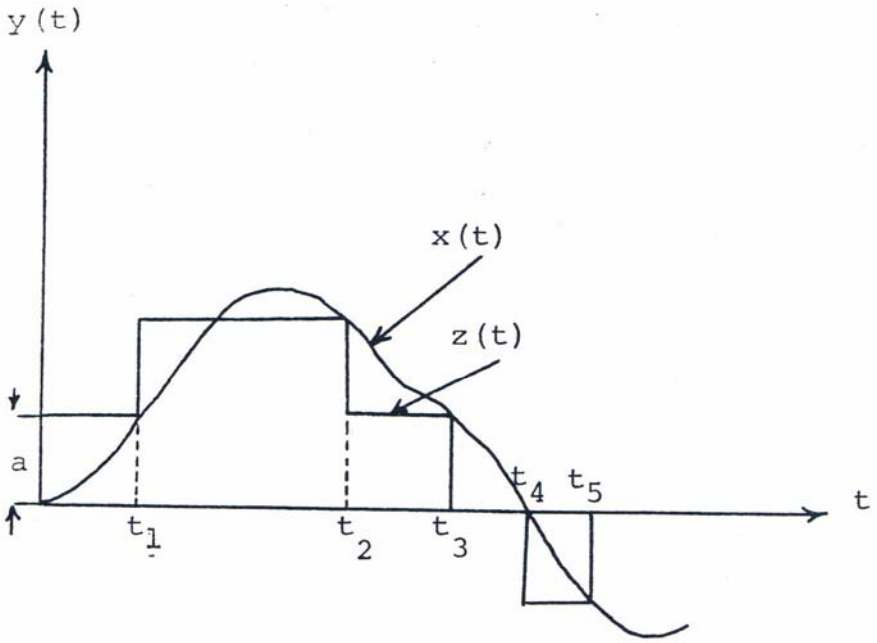

Figure 5-14: The Adaptive Quantizer in Figure 5-13 when "l" = 0. It is the Same as the Fixed Quantizer in Figure 3-8

We will try now to analyze it from the general theory of intersections. For the sake of analysis we shall consider the Adaptive Quantizer in Figure 5-13 when "1" = 0. The procedure is repeated in Figure 5-14. The samples at t_1 , t_2 ... t_m are derived by intersecting the information signal, x(t), with the signal,z(t). It is assumed that there is only one sample per interval T, where T is at least at the Nyquist rate. Consequently it follows:

$$t_m = (m-1)\ T + \tau \qquad 5\text{-}26$$

where τ is a random variable of which its value is within the range

$$0 \leq \tau < T \qquad 5\text{-}27$$

We define the function g(t) in the following equations:

$$g(t) = t - t_m + \alpha\ [x(t) - z(t)\ ]= \qquad 5\text{-}28$$

$$= t - (m-1)\ T - \tau + \alpha(x_t - z_t)$$

$$g(t_m)= o,\ g(t) \neq o \text{ if } t \neq t_m \qquad 5\text{-}29$$

$$\dot{g}\ (t) = 1 + \alpha[\dot{x}\ (t) - \dot{z}\ (t)\ ] \qquad 5\text{-}30$$

$$x_s = A \sum_m \delta(t-t_m) = A \sum_m |\dot{g}(t_m)| \delta[g(t)] \qquad 5\text{-}31$$

Hence from the above equations, we deduce

$$x_s = A\{1 \pm \alpha[\dot{x}(t)-\dot{z}(t)]\} \sum_m \delta\{t-(m-1)T-\tau+\alpha[x(t)-z(t)]\} \qquad 5\text{-}32$$

The Fourier series equivalent is:

$$x_s = A\{1+\alpha[x'(t)-z'(t)]\} \sum_m e^{jwn\{t-\tau+\alpha[x(t)-z(t)]\}} \qquad 5\text{-}33$$

If there is no spectrum overlapping, the baseband signal can be reconstructed as depicted in Figure 5-15.

The value α is determined by the bandwidth of the low pass filter. Due to the random variable τ and $z(t)$, the bandwidth of the harmonic functions increases.[28,29] To avoid aliasing, the sampling rate has to be higher than the Nyquist rate. This fact is undesirable because the purpose of the adaptive quantizers is to optimize the transmission rate. But if we reconstruct the nonuniform samples using the techniques discussed in Part VIII, the samples will be reconstructed at less than or equal to the Nyquist rate.

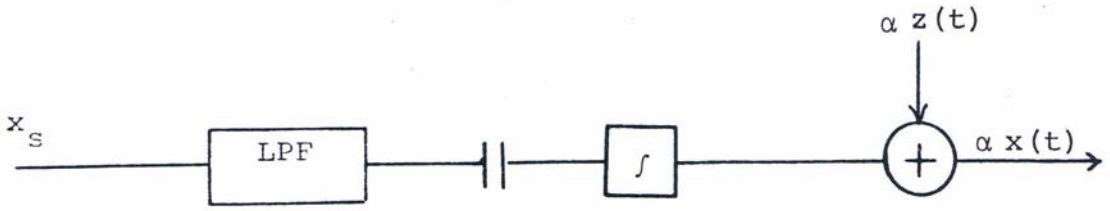

Figure 5-15 - Reconstruction of Baseband Signal by Low Pass Filtering

V.B.4

The advantage of the Adaptive Quantizer above some periodic intersection modulations is that the inaccuracy of its samples in time does not produce inaccuracy in the amplitude of the samples as it is for a sharp slope sawtooth intersected with a random signal x(t). In other words, unlike the other zero crossing modulations, time jitter is not a serious problem.

A technique was discussed in Section V-2-6 that would uniformize the nonuniform samples of the Adaptive Quantizer. An algorithm of uniformization that can be analyzed by the analytical tools of the general intersection technique is discussed in the following.

The quantization level is proportionally adapted to the time difference of the last two samples. If the interval of the last two samples is less than the Nyquist rate, the quantization level should be adapted to a much higher value provided that the slope is positive as shown in Figure 5-16 Conversely if the time interval of the previous two samples is larger than T, the quantization level should be adapted downward proportional to the time interval. For the Adaptive Quantizer discussed in Section V-2, both the upper and lower

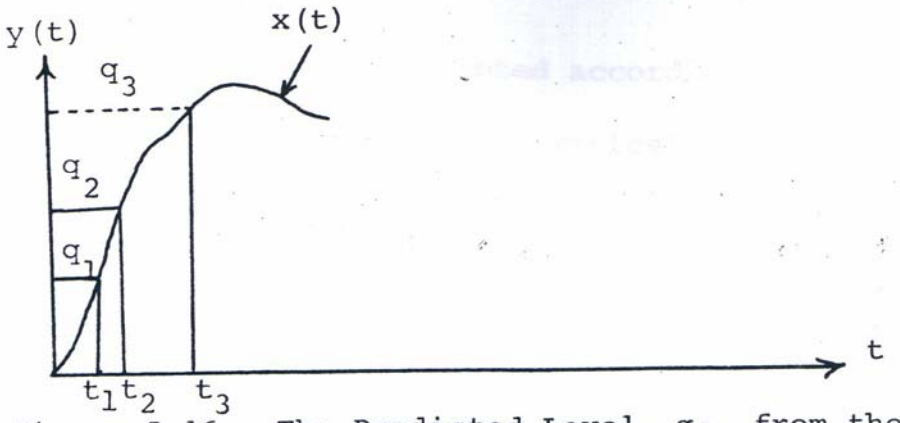

Figure 5-16: The Predicted Level, q_3, from the Time Interval of the Past Two Samples

$$\dot{g}(t)\,[q(t_2) + \alpha_1(t_2-t_1) + \cdots] + [q(t_1)^2 - q(t_2) - \alpha_1(t_2-t_1)]\,\text{sinq}\; w(t-t_1)$$

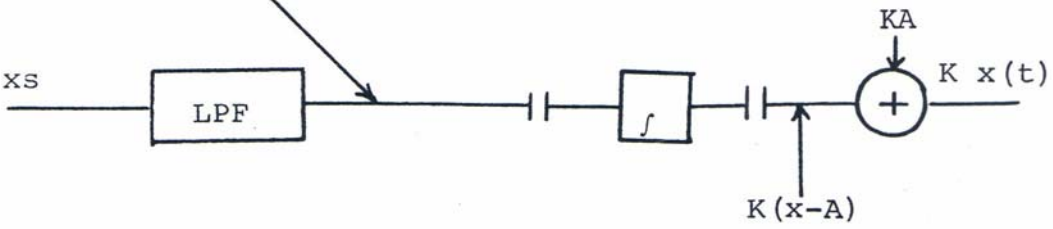

Figure 5-17: Reconstruction of the Uniformized Adaptive Quantizer

quantization levels are adapted according to the time intervals of the previous samples. Mathematically, the aforementioned algorithm is represented as:

$$X_s = q(t_1)\ \delta(t-t_1) + q(t_2)\ \delta(t-t_2) + [q(t_2) + \alpha_1(t_2-t_1)]\ x$$
$$x\ \ \delta(t-t_3) + [q(t_2) + \alpha_1(t_2-t_1)] + \alpha_2(t_3-t_2)]\ \delta(t-t_4) + \ldots \qquad 5\text{-}34$$

The above equation can be rewritten as:

$$x_s = q(t_1)\ \delta(t-t_1) + q(t_2) \sum_{m>1} \delta(t-t_m) + \alpha_1(t_2-t_1)\ x \qquad 5\text{-}35$$
$$x \sum_{m>2} \delta(t-t_m) + \alpha_2(t_3-t_2) \sum_{m>3} \delta(t-t_m) + \ldots$$

$$t = (m-1)T + t'_m \qquad 5\text{-}36$$

$$g(t) = t - (m-1)T + t'_m + P[x(t) - A(t)]$$

$$g'(t) = 1 + P[\dot{x}(t) - \dot{A}(t)] \qquad 5\text{-}37$$

where

$$A(t) = q(t_2)U_{-1}(t-t_2) - \alpha_1(t_2-t_1)U_{-1}(t-t_3) - \qquad 5\text{-}38$$
$$- \alpha_2(t_3-t_2)U_{-1}(t-t_4)\ldots$$

Hence,

$$x_s = [q(t_1) - q(t_2) - \alpha_1(t_2-t_1)\ldots]\delta(t-t_2) +$$

$$+ \{[q(t_2) + \alpha_1(t_2-t_1)\ldots]\dot{g}(t)\} \sum_{n=-\infty}^{\infty} e^{\frac{j2\pi n}{T}\{t+P[x(t)-A(t)]\}}$$

By low pass filtering the above equation, one would get the result demonstrated in Figure 5-17.

K in Figure 5-17 is dependent on P, $A(t_2)$, α_1, $\alpha_2\ldots$ and t_1, $t_2\ldots$, A is the adaptive signal generated at the receiver as the samples are being received. Since A has a higher bandwidth than x(t), the sampling rate has to be higher than the Nyquist rate. This fact makes the reconstruction scheme unattractive relative to the other schemes discussed in Part VIII.

3. Analysis of a Modified Asynchronous Delta Modulator

The modified delta modulation is represented in Figure 5-18, which is viewed as the intersection of a random signal, x(t), with an adaptive signal, z(t). The difference between Figure 5-18 and a standard asynchronous delta modulation is that the samples in Figure 5-18 are exactly at the intersection of the baseband signal, x(t), and the set of ramp functions, z(t). After each sample, the ramp function continues for δ units and then its slope is reversed. The modification has two main advantages. Firstly, the quantization noise is zero, and secondly, the analysis is simpler.

It is assumed for the analysis that there is only one sample per interval T. This interval may be equal or higher than the Nyquist rate. Figure 5-19 shows the relationship among δ, t_o, a and h.

$$h = \frac{\delta}{\sqrt{1 + t_o^2}} \qquad 5\text{-}39$$

$$a = \frac{t_o \delta}{\sqrt{1 + t_o^2}} \qquad 5\text{-}40$$

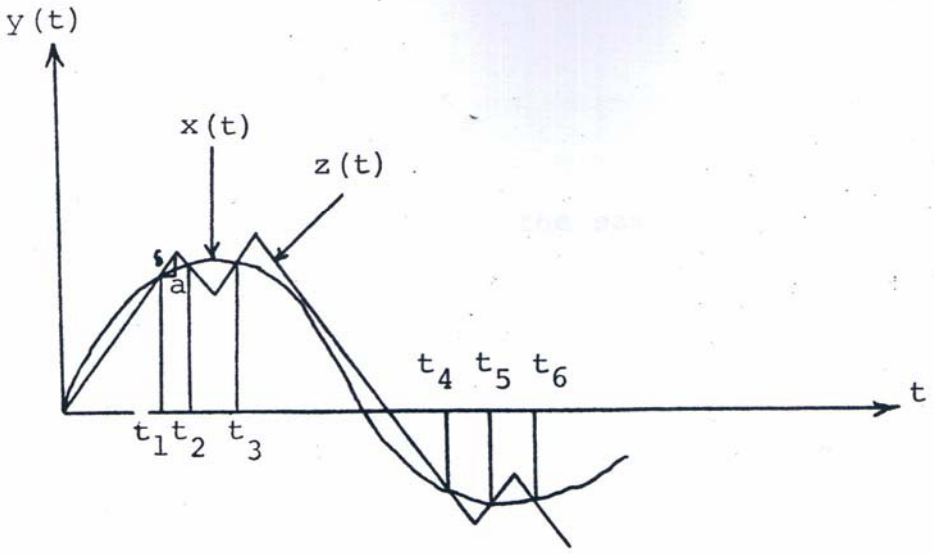

Figure 5-18: A Modified Asynchronous Delta Modulation

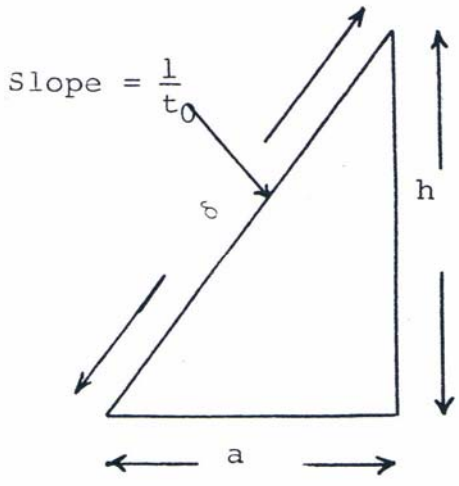

Figure 5-19

Thus, $a = ht_o$ 5-41

We relate the time instants of the samples to the amplitudes in the following:

$t_1 = t_o x(t_1)$ where t_o is inverse of the slope

$t_2 = t_1 + a + t_o x(t_1) + t_o h - t_o x(t_2)$

$t_3 = t_2 + a - t_o x(t_2) + ht_o + t_o x(t_3) = t_1 + 2(a+ht_o) + t_o x(t_1) -$

$- 2t_o x(t_2) + t_o x(t_3)$

$t_4 = t_3 + a + t_o x(t_3) + ht_o - t_o x(t_4) = t_1 + 3(a+ht_o) + t_o x(t_1) -$

$- 2\, t_o x(t_2) + 2t_o x(t_3) - t_o x(t_4)$

. .
. .
. .

$t_m = t_1 + (m-1)(a+ht_o) + [t_o x(t_1) - 2t_o x(t_2) + 2t_o x(t_3) \ldots] +$

$+ (-1)^{m-1} t_o x(t_m)$ 5-42

$$g(t)=t-t_m=t-\{t_1+(m-1)(a+ht_o)+[t_o x(t_1)-2t_o x(t_2)+2t_o x(t_3)+\ldots]$$

$$+2(-1)^m t_o x(t_m-1)+(-1)^{m-1} t_o x(t)\} \qquad 5\text{-}43$$

$$\dot{g}(t) = 1-(-1)^{m-1} t_o \dot{x}(t) \qquad 5\text{-}44$$

$$x_s = \sum_m (-1)^{m-1}\, \delta(t-t_m) = \sum_m (-1)^{m-1} |\dot{g}(t_m)|\,[g(t)] \qquad 5\text{-}45$$

Substituting equations 5-43 and 5-44 in the above equation, we get:

$$x_s = \sum_{m=odd} |1+t_o x(t)|\,\delta\{t-t_1-(m-1)2a-[t_o x(t_1)-2t_o x(t_2) +$$

$$+ 2t_o x(t_3)\ldots -2t_o x(t_{m-1})] - t_o x(t)\} -$$

$$- \sum_{m=even} |1-t_o x(t)|\,\delta\{t-t_1-(m-1)2a-[t_o x(t_1)-\ldots+2t_o x(t_{m-1})]$$

$$- t_o x(t)\} \qquad 5\text{-}46$$

Applying the Fourier series, we can deduce:

$$x_s = [1+t_o \dot{x}(t)] \sum_{n=\infty}^{\infty} e^{\frac{j2\pi}{4a} n [t-t_1-t_o Y_{m-1} + t_o x(t)]} -$$

$$- [1-t_o \dot{x}(t)] \sum_{n=-\infty}^{\infty} e^{\frac{j2\pi}{4a} n [t-t_1-t_o Y_{m-1} - t_o x(t)]} \qquad 5\text{-}47$$

where

$$Y_{m-1} = x(t_1) - 2x(t_2) + 2x(t_3) \ldots + 2(-1)^m x(t_{m-1}) \qquad 5\text{-}48$$

and

$$| t_o \dot{x}(t) | < 1 \qquad 5\text{-}49$$

Y_{m-1} is a random variable. If the samples had been independent, Y_{m-1} would have approached a normal distribution with increasing m. The standard deviation would also have approached infinity. However, the samples are actually dependent and the standard deviation is given by:

$$\begin{aligned} EY^2 &= Ex^2(t_1) + 4Ex^2(t_2) + 4Ex^2(t_3) + \ldots \\ &+ 4Ex^2(t_{m-1}) - 2Ex(t_1)x(t_2) - \ldots \\ &- 2Ex(t_1)x(t_{m-1}) - 4Ex(t_2)x(t_3) \ldots \end{aligned} \qquad 5\text{-}50$$

In practice the random variable Y_{m-1} is bounded because after each n samples, the delta modulator is reset and a test signal is transmitted. Therefore Y_{m-1} can be treated as a random variable such that its absolute value is bounded. The bound is determined by the maximum amplitude of the signal, x(t), and the parameter, n.

If it is assumed that there is no spectrum overlapping, the reconstruction of the baseband signal is as stated previously and represented in Figure 5-20.

Due to the random phase Y_{m-1} in the equation it is difficult to retrieve the information by band pass filtering. This random phase Y_{m-1} also increases the equivalent bandwidth of the principle component of the Fourier series in Equation 5-47. Hence, low pass filtering may not give the result shown in Figure 5-20 unless the sampling rate is high enough. In practice the samples are integrated twice and then low pass filtered to yield the baseband signal. The reconstruction technique for a conventional delta modulator is illustrated in Figure 5-21. A conventional delta modulator samples the baseband signal at $t_m + a$, introducing quantization error. The reconstruction technique for a modified delta modulator (Figure 5-20) seems to be simpler than that of a conventional delta modulator (Figure 5-21). The reconstruction of the modified delta modulation can be also achieved by the same method that the samples are derived at the transmitter (Figure 5-18). Since asynchronous delta modulation is rarely discussed or analyzed in literature, the preceding analysis is a unique approach toward this problem.

Figure 5-20: Reconstruction by Low Pass Filtering

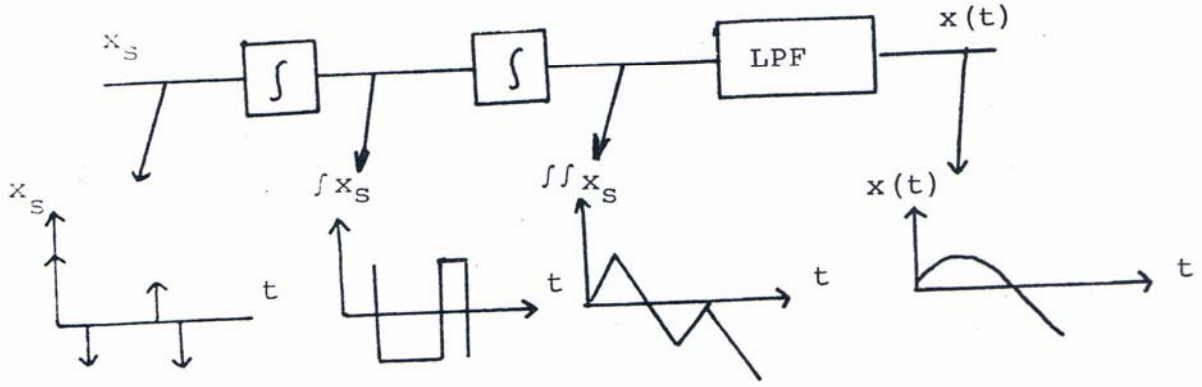

Figure 5-21: Reconstruction of a Delta Modulated Signal

PART VI

OTHER METHODS OF NONUNIFORM PULSE TRANSMISSION

This section is provided to show the applicability of the general formulation of the transmission problem as an intersection problem. A variety of existing as well as newly formulated methods are devised in this Section in terms of an intersection problem.

1. The Transmission of the Zero Crossings of the Signal and its Derivatives

Suppose the transmitted samples are at the extremum points of the information signal. These samples are equivalent to the zero crossings of the derivative of the signal. In order to satisfy the Nyquist rate, both the zero crossings of the signal and the derivative of the signal are transmitted (Figure 6-1). The analysis is as follows:

$$x_s = \sum_m \delta(t-t_m) \qquad 6\text{-}1$$

It is again assumed that there is only one sample per interval, T. Thus, we have:

$$t_m = (m-1)T + \tau, \qquad o \leq \tau < T \qquad 6\text{-}2$$

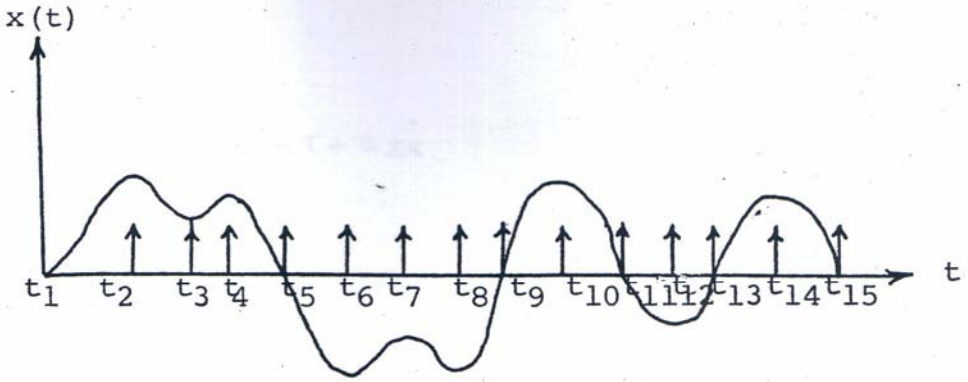

Figure 6-1: The Zero Crossings of the Signal and the Derivative of the Signal

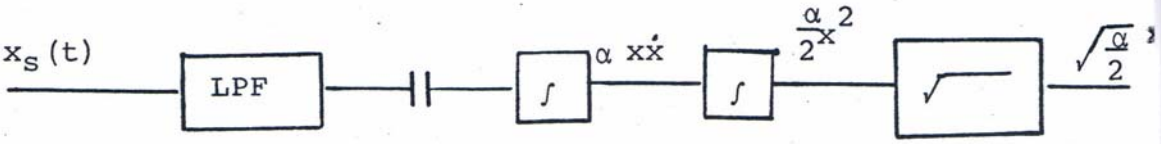

Figure 6-2: Reconstruction of Samples at the Zero Crossings of the Signal and the Derivative of the Signal

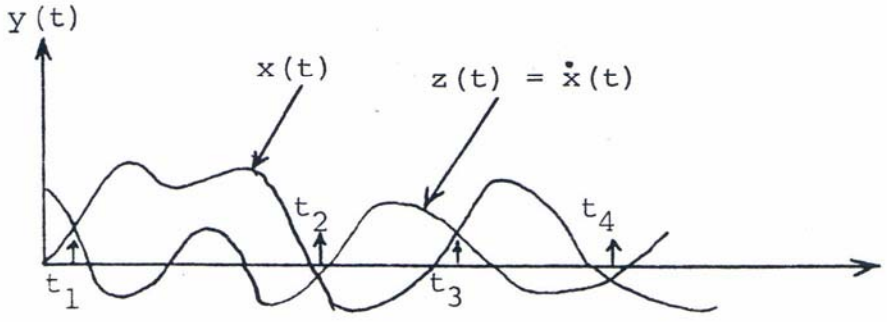

Figure 6-3: Intersection of the Signal with its Derivative

$$g(t) = t - (m-1)T - \tau + \alpha x\dot{x} \qquad 6\text{-}3$$

where α is a constant

$$g(t_m) = 0 \qquad 6\text{-}4$$

$$g(t \neq t_m) \neq 0 \Rightarrow t - (m-1)T - \tau \neq -\alpha x\dot{x} \qquad 6\text{-}5$$

$$g(t) = 1 + (x\dot{x} + x^2) \text{ where } g(t_m) \neq 0 \qquad 6\text{-}6$$

$$x_s = A \sum_m \delta(t-t_m) = A[1+\alpha(x\dot{x}+\dot{x}^2)] \sum_{n=-\infty}^{\infty} e^{\frac{jn2\pi}{T}[t-\tau+x\dot{x}]} \qquad 6\text{-}7$$

The reconstruction scheme is demonstrated in Figure 6-2. The phase in the exponential function in the Equation 6-7 determines the bandwidth of the signal. The bandwidth of $x\dot{x}$ is twice that of the bandwidth of x because the bandwidth of $\dot{x}$ is the same as the bandwidth of x if it is strictly bandlimited, and multipication doubles the frequency. The sampling rate has to be twice the improved bandwidth. The zero crossings of $\dot{x}(t)$ are greater or equal the zero crossings of x(t). Hence, the samples are more than doubled but are still less than the Nyquist rate.

2. The Intersection of Random Functions

The intersection of a random signal, $x(t)$, with a function of $x(t)$ is given below:

a. The Intersection of a Signal with its Derivative

Instead of sampling at the zero crossings of $x(t)$ and $\dot{x}(t)$, the samples at the intersection of $x(t)$ and $\dot{x}(t)$ can be transmitted (Figure 6-3).

The main difference in this case is that the intersection is between a signal and a function of the signal that are both random functions. The analysis is as follows:

$$t_m = (m-1)T + \tau \ , \qquad x_s = A \sum_m (t-t_m) \tag{6-8}$$

where it is assumed that there is only one sample per interval, T, and is a random variable defined in the region $0 \leq \tau < T$. $g(t)$ is defined as:

$$g(t) = t - (m-1)T - \tau + \alpha (x-\dot{x}) \tag{6-9}$$

where α is a constant and

$$g(t_m) = 0, \quad g(t \neq t_m) \neq 0$$

$$\dot{g}(t) = 1 + \alpha (\dot{x} - \ddot{x}) \tag{6-10}$$

Hence,

$$x_s = [1 + \alpha(\dot{x} - \ddot{x})] \sum_{n=-\infty}^{\infty} e^{\frac{j2\pi n}{T}[t - \tau + \alpha(x - \dot{x})]} \qquad 6\text{-}11$$

where it is assumed

$$|\alpha(\dot{x} - \ddot{x})| < 1 \qquad 6\text{-}12$$

Low pass filtering would result in the following:

$$x_{slp} = 1 + \alpha(\dot{x} - \ddot{x}) \qquad 6\text{-}13$$

where α is determined by the bandpass of the low pass filter.

After D.C. blocking and integration, we can deduce the following:

$$\alpha(x - \dot{x}) = f(t) \qquad 6\text{-}14$$

The above equation is rewritten as:

$$e^{-t}x - e^{-t}\dot{x} = \frac{1}{\alpha} e^{-t} f(t) \qquad 6\text{-}15$$

Integrating both sides yields:

$$x(o) - xe^{-t} = \int_o^t dh \, \frac{1}{\alpha} e^{-h} f(h) \qquad 6\text{-}16$$

or

$$x = -e^{t} \int_o^t dh \, \frac{1}{\alpha} e^{-h} f(h) \qquad 6\text{-}17$$

since

$$x(o) = o \qquad 6\text{-}18$$

Hence, the reconstruction method is depicted in Figure 6-4. In order to make the reconstruction technique practically realizable, the Equation 6-17 is rearranged as follows:

$$x = -\frac{1}{\alpha}\int_{o}^{t} dh e^{t-h} f(h) = -\frac{e^{t}}{\alpha} * f(t)$$

The convolution is illustrated in Figure 6-5. The impulse response of the system is unstable, but realizable and the output of the system is stable.

b. The Intersection of a Signal with its Delayed Form

The intersection of a signal with its delayed form is represented in Figure 6-6. If the delay time (τ) is small, the number of samples will be equal to the number of extremum points. The impulses at $t_1, t_2, \ldots t_m$ approach the zero crossings of $\dot{x}(t)$ if τ approaches zero. Therefore, the sampling rate cannot be higher than the Nyquist rate. The time information of the impulses and the bandwidth of the signal, together with the assumption that there is only one impulse per interval T, lead to the following analysis:

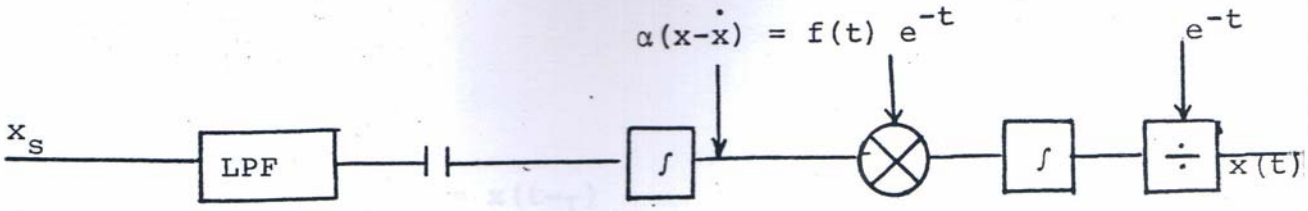

Figure 6-4: The Block Diagram for Reconstructing the Baseband Signal from the Intersection of the Signal and its Derivative

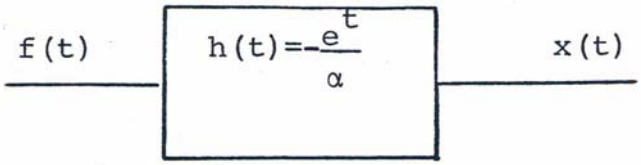

a.

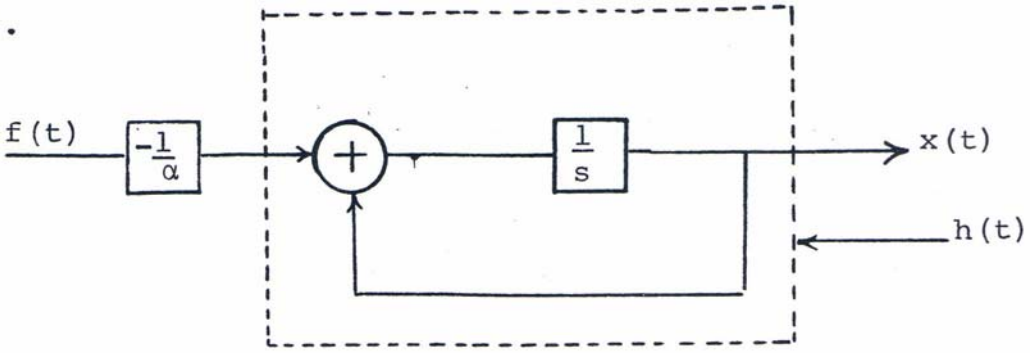

Figure 6-5: Reconstruction of the Baseband Signal by Convolution

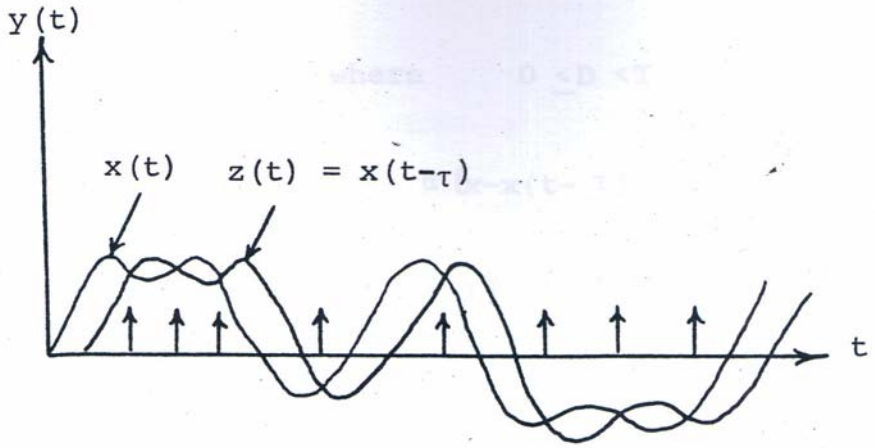

Figure 6-6: Intersection of x(t) and x(t-τ)

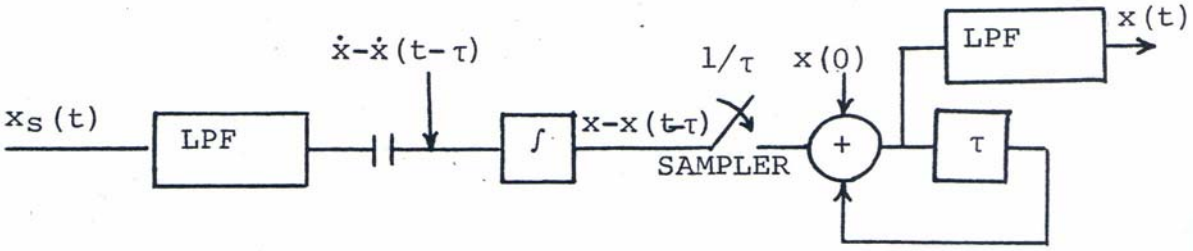

Figure 6-7: The Reconstruction of the Signal from the Intersection of the Signal and its Delayed Form

$$t_m = (m-1)T + D, \quad \text{where} \quad 0 \leq D < T \tag{6-19}$$

$$g(t) = t - (m-1)T + D + \alpha [x - x(t-\tau)] \tag{6-20}$$

$$\dot{g}(t) = 1 + \alpha [\dot{x} - \dot{x}(t-\tau)] \tag{6-21}$$

thus,

$$x_s = A \sum_m (t-t_m) = \{1 + \alpha [\dot{x} - \dot{x}(t-\tau)]\} \; x \sum_{n=-\infty}^{\infty} e^{\frac{j2\pi n}{T}[t + D + \alpha [x - x(t-\tau)]]} \tag{6-22}$$

If we ignore the spectrum overlapping, the low pass filtered and integrated x_s will yield:

$$f(t) = x(t) - x(t-\tau) \tag{6-23}$$

The function f(t) is known. In order to find x(t) from the Equation 6-23, f(t) is sampled at every τ seconds.

$$x(o) = o$$

$$x(\tau) = x(o) + f(\tau)$$

$$x(2\tau) - x(\tau) + f(2\tau) = x(o) + f(\tau) + f(2\tau)$$

$$\vdots$$

$$x(n\tau) - x[(n-1)\tau] + f(n\tau) = x(o) + f(\tau) + f(2\tau) \ldots + f(n\tau) \tag{6-24}$$

If the samples of x(t) are known at t = n , n = 0,1,2,...,x(t) can be reconstructed by low pass filtering the samples. This fact is true provided that τ is less than the Nyquist interval. The block diagram for the reconstruction procedure is shown in Figure 6-7. The intersection of the two signals could have been generalized in the form, $y = x(t) - cx(t-\tau)$. The analysis is the same as above.

Other functions of x(t) besides $\dot{x}$ and $x(t-\tau)$ can be used. $\int x$, lnx, cosx are some examples. In the next section, the properties of the zero crossings of some functions of x(t) will be examined.

3. Inverting Uniform Samples and the Transmission of Zero Crossings

A different approach to the transmission of uniform samples is illustrated in Figure 6-8. The original uniform samples can be reconstructed from the zero crossings of the waveform (Figure 6-8-c). This kind of transmission is another example of the transformation of the amplitude of samples into time. This transformation is similar to PPM, where only one bit per sample is transmitted. In PPM, the zero crossings of a sawtooth waveform is transmitted, (Figure 6-9). The main difference between PPM and the flipping technique is that in the latter case the reconstructed samples depend on the previous samples. Therefore, the flipping technique is vulnerable to propagation of error. To avoid this problem, a new method is discussed below, which is similar to pulse frequency modulation. The technique is depicted in Figure 6-10. Each point on level A is connected to the next sample. The zero crossings are then sampled and transmitted at one bit per sample. This method would not propagate errors in the reconstruction of samples. In the flipping technique the polarity of the pulses contains the information concerning the flipped samples. The impulses in Figure 6-8-d are derived from the

a. Uniform Samples

b. Flipped Samples

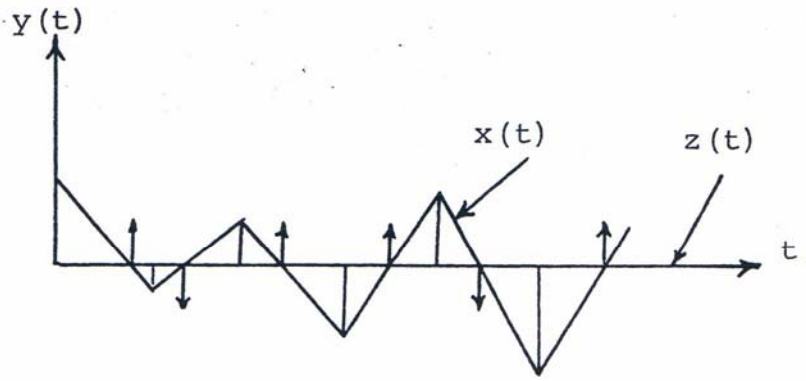

c. Forming a Waveform by Connecting the Flipped Samples and Transmission of the Zero Crossings

Figure 6-8

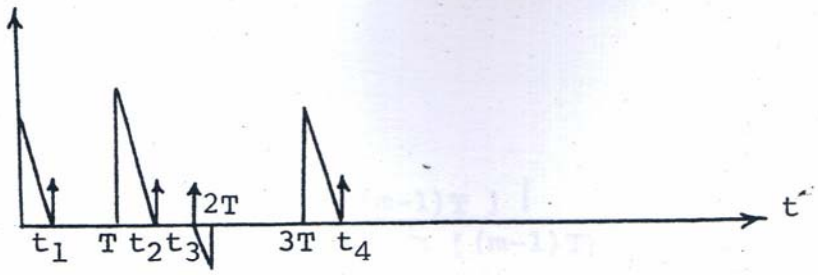

Figure 6-9: Generation of Uniform PPM Samples

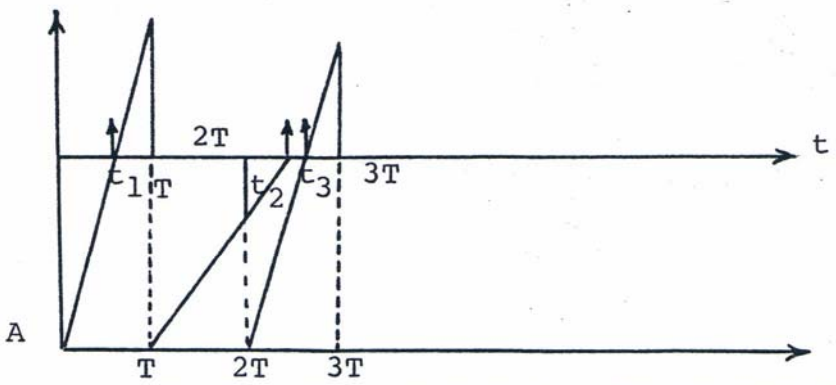

Figure 6-10: A new Modulation Technique for Uniform Samples

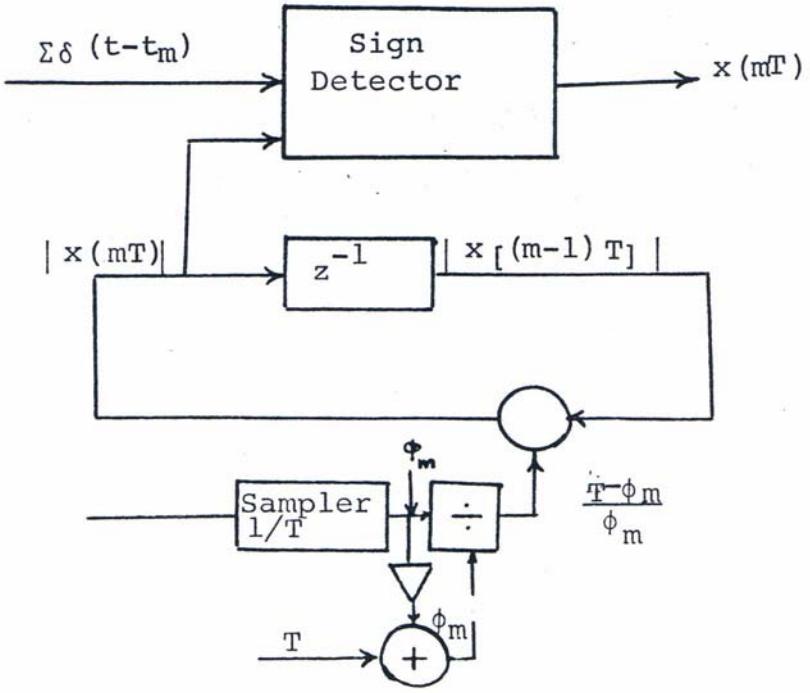

Figure 6-11: Reconstruction of the Flipped Samples

following equation:

$$t_m - (m-1)T = \frac{T\,|x\,[(m-1)T\,]\,|}{|x(m)| + |x\,[(m-1)T]|} = \phi_m$$

or

$$x(mT) = \frac{(T - \phi_m)}{\phi_m}\; x\,[(m-1)T\,] \qquad 6\text{-}25$$

The block diagram of the reconstructed samples from the impulses in Figure 6-8-c is demonstrated in Figure 6-11. The impulses in Figure 6-10 are derived as follows:

$$t_m - (m-1)T = \frac{Tx(mT)}{A-x(mT)} = \phi_m = x(mT) = \frac{A\;\phi_m}{T + \phi_m} \qquad 6\text{-}26$$

The reconstruction scheme at the receiver is similar to the transmitter. Its block diagram is shown in Figure 6-12. The above scheme can also be analyzed by the tools developed in Section II-2. The basic assumption is that $x(mT) \simeq x(t_m)$. The same assumption has also been done for uniform pulse duration modulation. The analysis is as follows:

$$x_s = \sum_m (t-t_m) \qquad 6\text{-}27$$

$$g(t) = t-(m-1)\;T - \frac{Tx(t)}{A-x(t)} \qquad 6\text{-}28$$

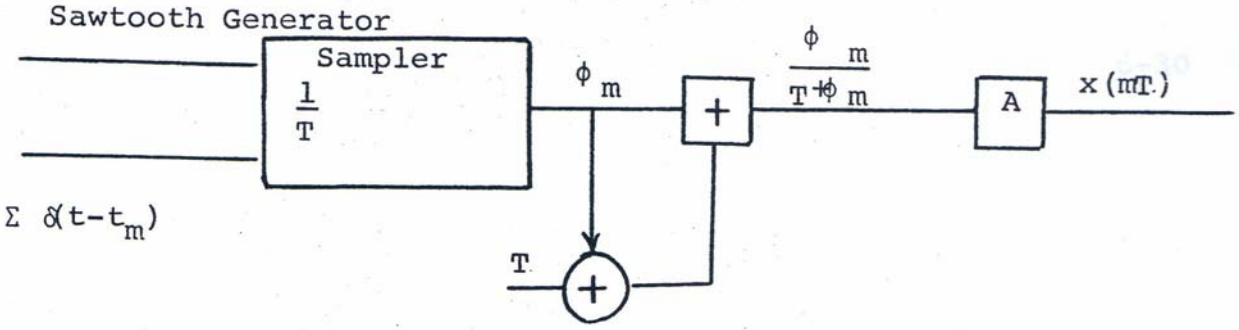

Figure 6-12: Reconstruction of the Uniform Samples from the Impulses Generated in Figure 6-10

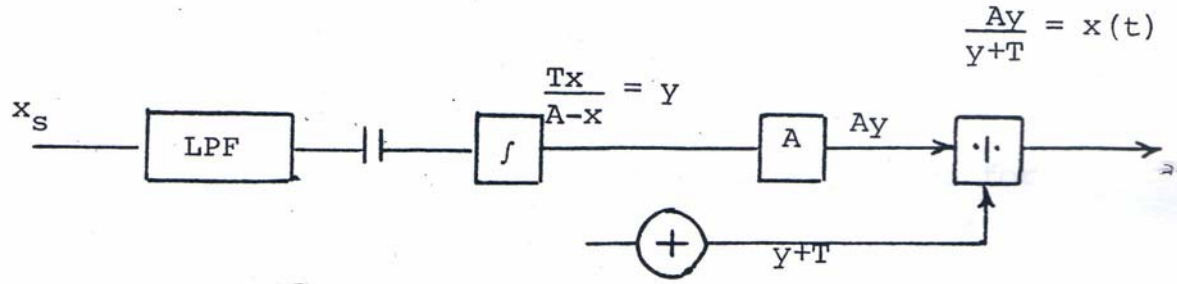

Figure 6-13: Reconstruction of Figure 6-10 Using the Intersection Technique

where

$$g(t_m) = o,\ g(t \neq t_m) \neq o \text{ and } A \neq x(t) \qquad 6\text{-}29$$

$$\dot{g}(t) = 1 - T\left(\frac{x(t)}{A-x(t)}\right)', \quad g(t_m) \neq o \qquad 6\text{-}30$$

thus,

$$x_s = \sum_m \left|1 - T\left(\frac{x}{A-x}\right)'\right| \delta\left[t-(m-1)T - \frac{Tx(t)}{A-x(t)}\right] \qquad 6\text{-}31$$

If $\left[1-T\left(\frac{x}{A-x}\right)'\right] > o$, i.e., $1 > \frac{TA\dot{x}}{(A-x)^2}$, which is true for large A, we have:

$$x_s = \left[1-T\left(\frac{x}{A-x}\right)'\right] \sum_{n=-\infty}^{\infty} e^{\frac{j2\pi n}{T}\left[t - \frac{Tx(t)}{A-x(t)}\right]} \qquad 6\text{-}32$$

If $\frac{x}{A-x}$ is bandlimited and there is no spectrum overlapping, the reconstruction technique is depicted in Figure 6-13. It is difficult to use the same kind of analysis for the flipping technique. An analysis for the reconstruction and noise for a similar technique is discussed in Fawe's dissertation.[4]

4. Analysis of Uniform Pulse Position Modulation (PPM) by Intersection Technique

PPM pulses are usually derived from pulse duration modulation (PDM) by differentiating the PDM pulses. PDM pulses, in turn, are derived from nonuniform slicing circuit, which approximates uniform samples.[7] Using the intersection technique, we propose a different analysis for the generation and demodulation of uniform PPM. So far the intersection analysis has been for nonuniform samples including nonuniform PPM. It can be imagined that uniform PPM is the intersection of a sawtooth wave z(t) with the output $x_{SH(t)}$ of a sample and hold circuit as illustrated in Figure 6-14 and 6-15. The analysis for the reconstruction is as follows:

It is assumed that a D.C. voltage is added to $x_{SH(t)}$ so that there is no negative samples. This assumption, plus restricting the slope of the sawtooth wave assures one pulse per uniform sample. Denoting the PPM impulses by u(t), we have:

$$u = A \sum_{m} (t-t_m) \qquad 6\text{-}33$$

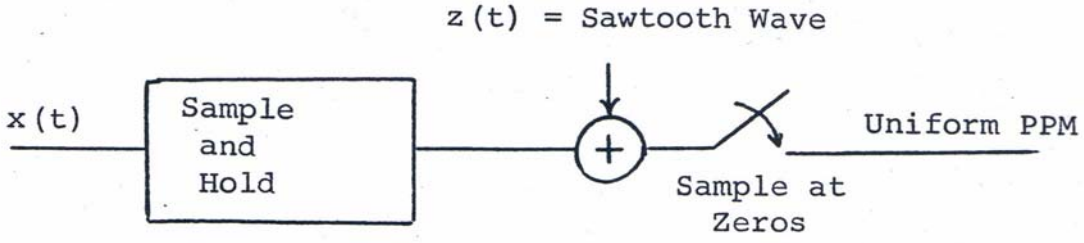

Figure 6-14: Generation of Uniform PPM by the Intersection of Two Waves

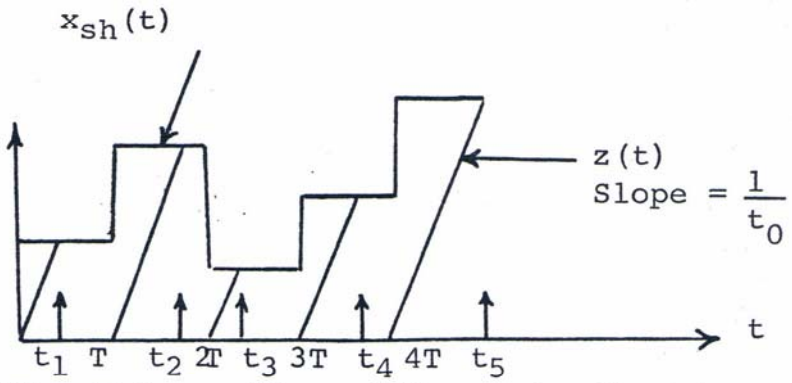

Figure 6-15: Intersection of the Sawtooth and Sample and Hold Signals

where

$$t_m = (m-1)T + t_o x_{SH}(t_m) \qquad 6\text{-}34$$

$$g(t) = t-(m-1)T + t_o s(t) \qquad 6\text{-}35$$

where $s(t)$ is a bandlimited curve passing through the nonuniform samples $x_{SH}(t_m) = s(t_m)$. According to the theorems in Appendix A, the curve with the lowest bandwidth that fits the nonuniform samples $x_{SH}(t_m)$ has a bandwidth of $\frac{1}{2T}$. Therefore, it is assumed that $s(t)$ has a bandwidth $\frac{1}{2T}$. Equation 6-36 has the following property:

$$g(t_m) = o, \quad g(t \neq t_m) \neq o \qquad 6\text{-}36$$

$$\dot{g}(t) = 1 + t_o \dot{s}(t) \qquad 6\text{-}37$$

$$\dot{g}(t_m) \neq o \qquad 6\text{-}38$$

Equation 6-33 can thus be written as:

$$u = A \sum_m |1 + t_o \dot{s}(t)| \, \delta [t+(m-1)T + t_o s(t)] \qquad 6\text{-}39$$

Assuming $|t_o \dot{s}(t)| < 1$, we have

$$u = A [1 + t_o \dot{s}(t)] \sum_{n=-\infty}^{\infty} e^{\frac{2\pi n}{T}[t + t_o s(t)]} \qquad 6\text{-}40$$

The reconstruction of s(t) from the PPM pulses, u(t), is depicted in Figure 6-16. The reconstruction of the original signal from s(t) is depicted in the same Figure. s(t) is sampled at t_m and then is hold. If this signal is sampled uniformly at the rate $\frac{1}{T}$, the origianl uniform samples are reproduced. Thus, low pass filtering would yield the original signal.

There are other ways to generate uniform PPM. These techniques are shown in Figure 6-17. The initial condition of the sawtooth is at the amplitude of the previous sample. If the positive going slope hits the signal,a positive pulse is generated, otherwise a negative pulse is generated. This is a combination of delta modulation and PPM. This kind of adaptive PPM reduces the bandwidth somewhat but like the delta modulation, propagates the error.

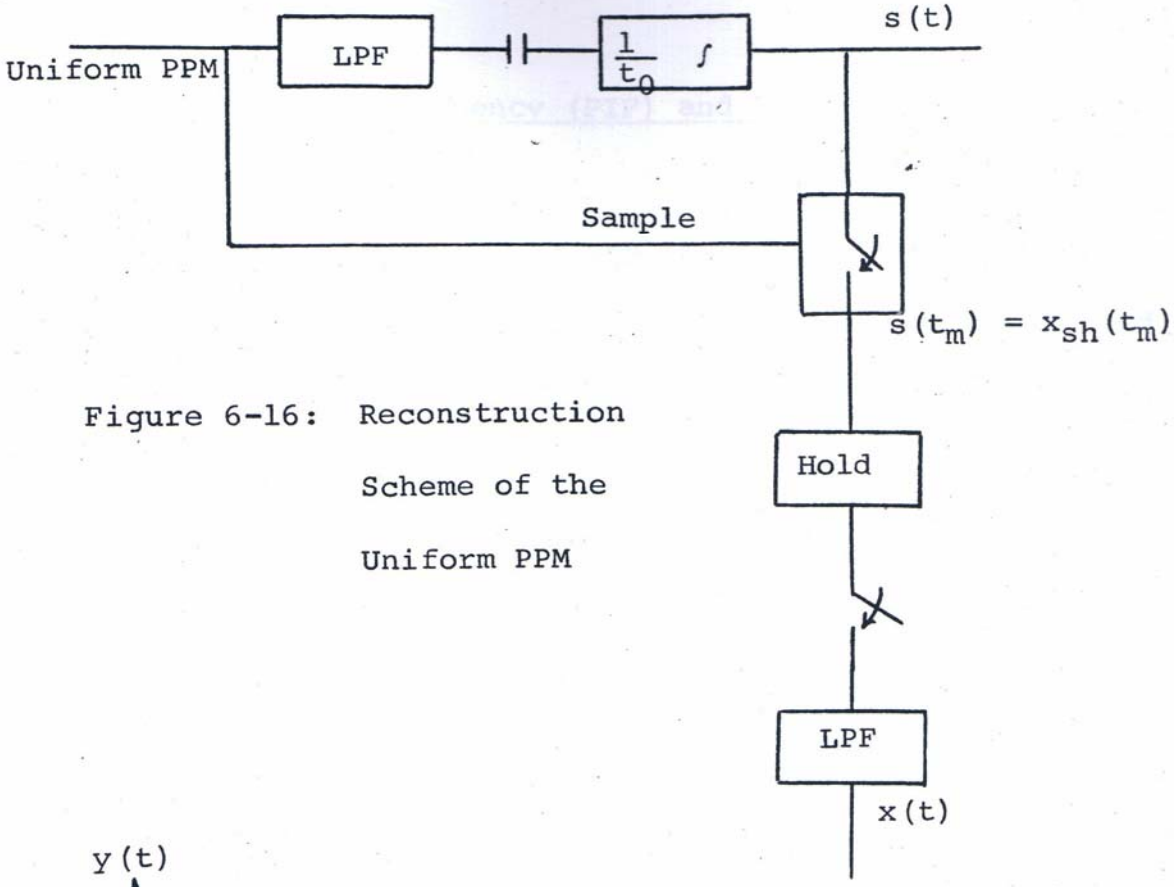

Figure 6-16: Reconstruction Scheme of the Uniform PPM

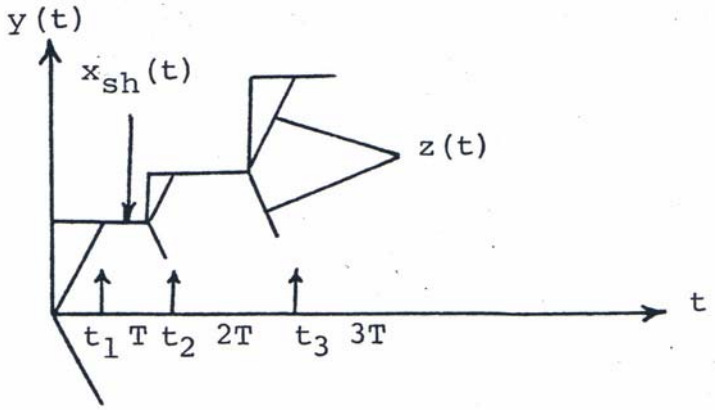

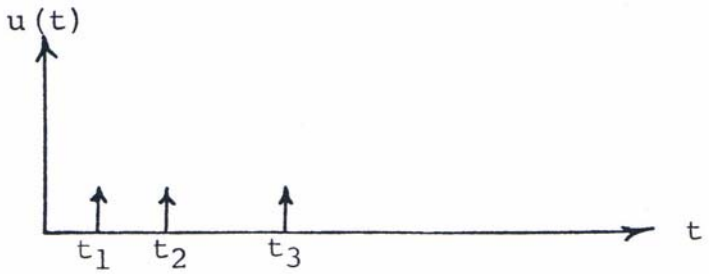

Figure 6-17: A Different Way of Generating Uniform PPM

5. Pulse Integral Frequency (PIF) and Pulse Frequency Modulations (PFM)

In biomedical engineering applications, the behaviour of neurons is simulated by pulse integral modulation (PIM)[32] and pulse frequency modulation (PFM)[33], which are known as syncoders. In control systems, PIM and PFM are used for their phase locking feedback loop characteristics.[34] These modulation techniques have not been really explored in the field of digital communication. Rock[33] has briefly discussed the application of PIM and PFM in digital communication systems[35,36,37] but he has pended this kind of application for future work. Also, he states that the problem of finding a practical demodulation scheme remains to be solved. It is the purpose of this section to explore the application of PIM and PFM in the field of digital communication and to analyze these modulation schemes from the intersection point of view. We shall show that PIM and PFM are nothing but the intersection of a random signal and a deterministic or an adaptive signal.

Definition:

"PIM is a signal-dependent sampling device which: (1) generates an output pulse every time a decaying threshold

intersects its analog input signal, (2) resets the threshold to its initial value during each pulse, so that (3) the threshold decays towards the signal along with a fixed trajectory between pulses."[38] An example of PIM is depicted in Figure 6-18.

Definition:

"PFM is a signal dependent sampling device which: (1) generates an output pulse every time a growing encoding function intersects the non-increasing threshold, (2) resets the encoding function to zero and resets the threshold to its initial value during each pulse, so that (3) the encoding function grows towards the threshold between pulses. The slope of encoding function depends upon the input signal, and the threshold may be fixed or may decay toward the encoding function."[38] An example of PFM is given in Figure 6-19.

The single-signed integral pulse frequency modulation[39] (S-S LPFM) is a special class of PFM where $\frac{dz(t)}{dt} = -s(t)$ and $x(t) = -B$ (See Figure 6-19). In other words the pulses are generated when the integral of the signal (S(t)) reaches a fixed level and the integral is reset. If the sign of the

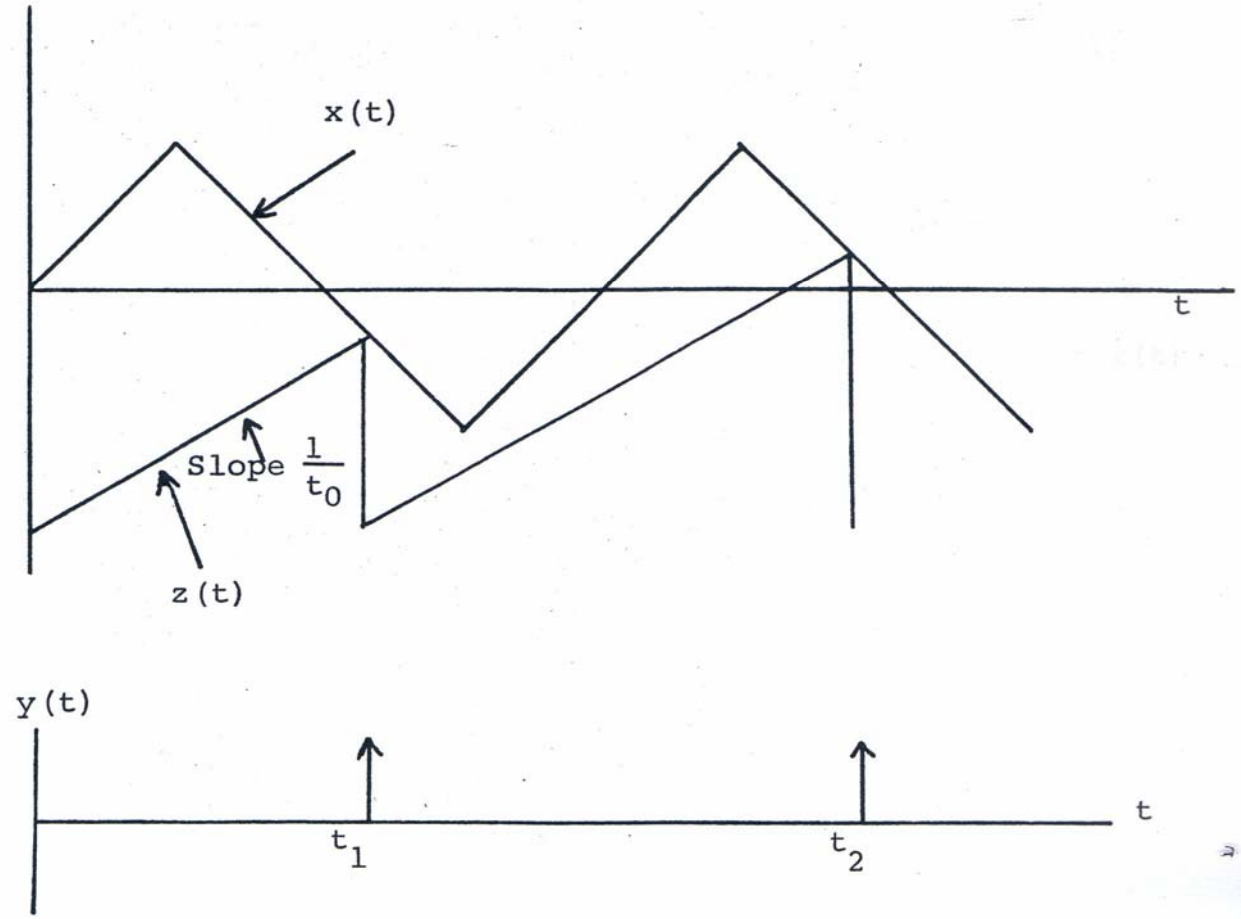

Figure 6-18: Pulse Integral Modulation

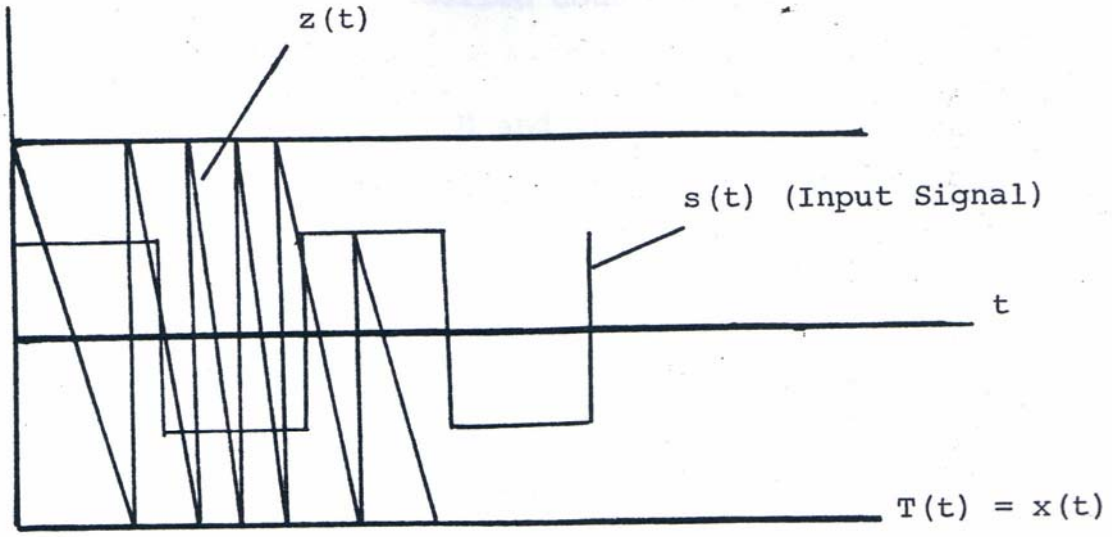

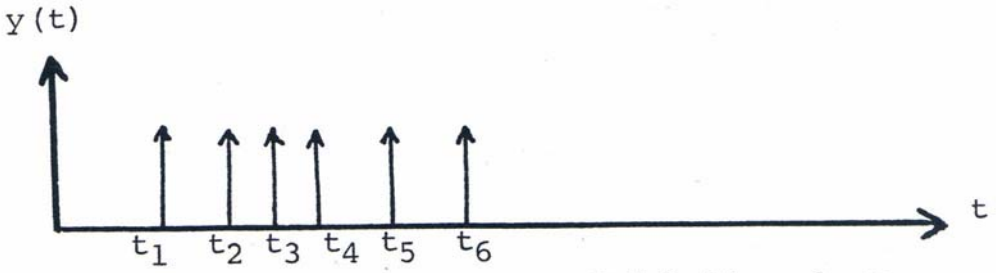

Figure 6-19: Pulse Frequency Modulation where

$$\frac{dz(t)}{dt} = f[A(t)] + g[z(t)]$$

integral is also considered in the polarity of the pulses, the modulation technique is called double-signed integral pulse modulation (D-S-1 PFM).

It is observed that PIM,PFM and IPFM can all be viewed as the intersection of the random signal with a signal that is either adaptive (PIM) or is a function of the random signal (PFM). The samples in PFM, unlike PIM, are independent from the previous samples. Hence, PIM cannot be analyzed by the intersection method. The reason is as follows:

From Figure 6-18

$$x(t_1) = -B + \frac{t_1}{t_o} \Rightarrow t_1 = t_o x(t_1) + Bt_o$$

$$t_2 = t_o x(t_2) + Bt_o + t_1$$

$$t_m = t_o x(t_m) + Bt_o + t_o t_{m-1}$$

Hence, the train of PIM pulses cannot be expanded in terms of Fourier series. PIM pulses, however, are demodulated by a ramp generator, sample and hold and a low pass filter. Besides the complexity of the demodulator, it was found that for a good demodulation, it is necessary to sample at four times the Nyquist rate, [40] which is typical of any sample and hold reconstruction of nonuniform samples. PIM modulator is claimed[41] to reduce the transmission bits per second if the derivative of the signal is encoded with a PIM encoder. This

reduction is true because the concentration of transmitted pulses is around the high frequency content of the signal.

The Adaptive Quantizer discussed in Section V-2 is superior to PIM in this aspect, which only samples at the active (high frequency) regions. The reduction of bits per second in the above cases is the direct consequence of the concept of instantaneous bandwidth.[42]

PFM, on the other hand is simpler to demodulate, both theoretically and practically. Figure 6-19 shows the generation of PFM by the intersection of functions. S-S IPFM and D-S IPFM can be regarded as the intersection of the integral of the signal with some fixed quantization levels (Figure 6-20 and 6-21).

PFM analysis is then reduced to the problem of the intersection of a signal with quantization levels. For S-S IPFM, the analysis is as follows:

$$x_s = A \sum_m \delta(t-t_m)$$

$$t_m = (m-1)\ T + \tau + [x(t) - mA]$$

where τ is a random variable confined in the region $o \leq \tau < T$ and T is dependent on A.

$$g(t) = t - (m-1)T - \tau - [x(t)-mA] = t-m(T+A) + T - \tau - x$$

$$g(t_m) = o \text{ and } g(t \neq t_m) \neq o$$

$$\dot{g}\ (t) = 1 - \dot{x}\ (t), \quad \dot{g}\ (t_m) \neq o \text{ and } \dot{x}\ (t) < 1$$

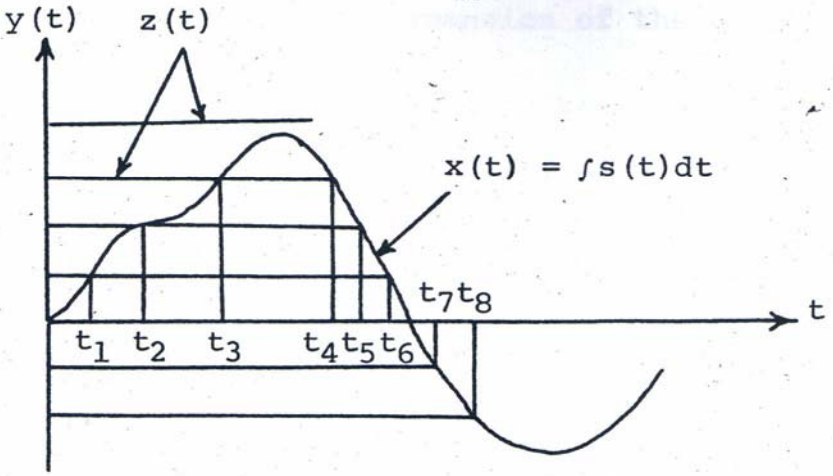

Figure 6-20: Double Signed Integral Pulse Frequency Modulation Depicted as the Intersection of Two Signals

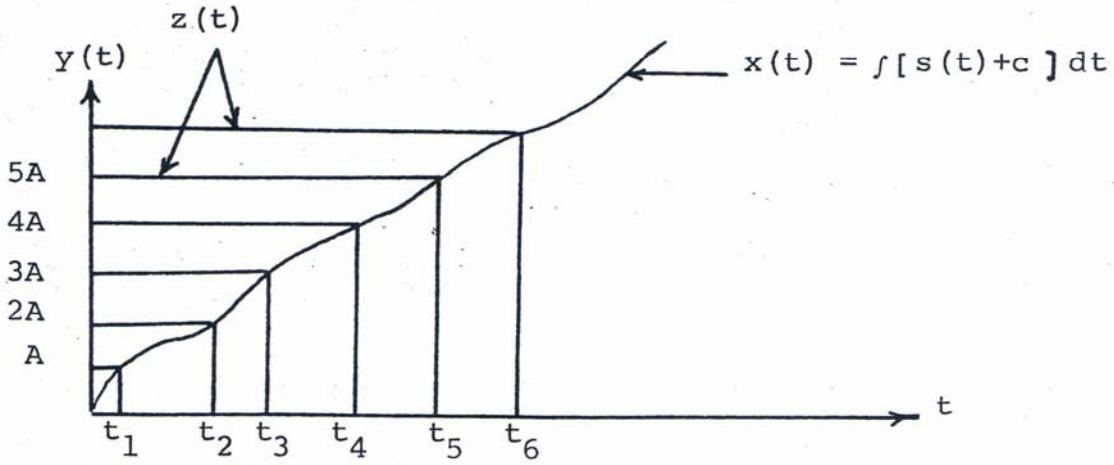

Figure 6-21: Single Signed Integral Pulse Frequency Modulation Depicted as the Intersection of Two Signals

Thus, the Fourier series expansion of the above Equation is:

$$x_s = A\,[1-\dot{x}\,(t)] \sum_m \delta\,[t-m(T+A) + T - \tau - x(t)] =$$

$$= A\,[1-\dot{x}\,(t)] \sum_{n=-\infty}^{\infty} e^{\left(\frac{j2\pi n}{T+A}\right)[t + T - \tau - x(t)]} \qquad 6\text{-}41$$

thus, if the principle frequency in the above equation is high (A and T are small), low pass filtering will result in $A(1-\dot{x})$, which is equal to $s(t) + c_1$. for D-S IPFM, the analysis is as follows:

$$x_s = A \sum_m (-1)^{f(m)}\, \delta(t-t_m)$$

$$t_m = (m-1)T + \tau$$

where τ is a random variable confined in the region

$$o \leq \tau < T$$

$$g(t) = t-(m-1)T - \tau + [x(t)-x(t_m)$$

$$g(t_m) = o, \quad g(t \neq t_m) \neq o$$

$$\dot{g}\,(t) = 1 + \dot{x}\,(t)$$

thus, $x_s = A \sum_m (-1)^{f(m)} |1 + \dot{x}\,(t)|\, \delta\,\{t-(m-1)T-\tau+[x(t)-x(t_m)]\}$

Hence, the intersection analysis fails to show that D-S IPFM can be demodulated by a simple low pass filtering. Intuitively, the reconstruction of PFM can be imagined [43] by integrating the PFM pulses as shown in Figure 6-22. This sample and hold signal after low pass filtering yields the integral of the original signal. Therefore, differentiation after low pass filtering results in the baseband signal (Figure 6-23). If the system is linear and time invariant the integrator and the differentiator can be removed without changing the system output. The above result verifies that the frequency spectrum of both S-S IPFM and D-S IPFM resembles the spectrum shown in Figure 6-24. The Fourier series analysis (Equation 6-41) yields the same result for S-S IPFM. This fact is not so obvious for D-S IPFM.

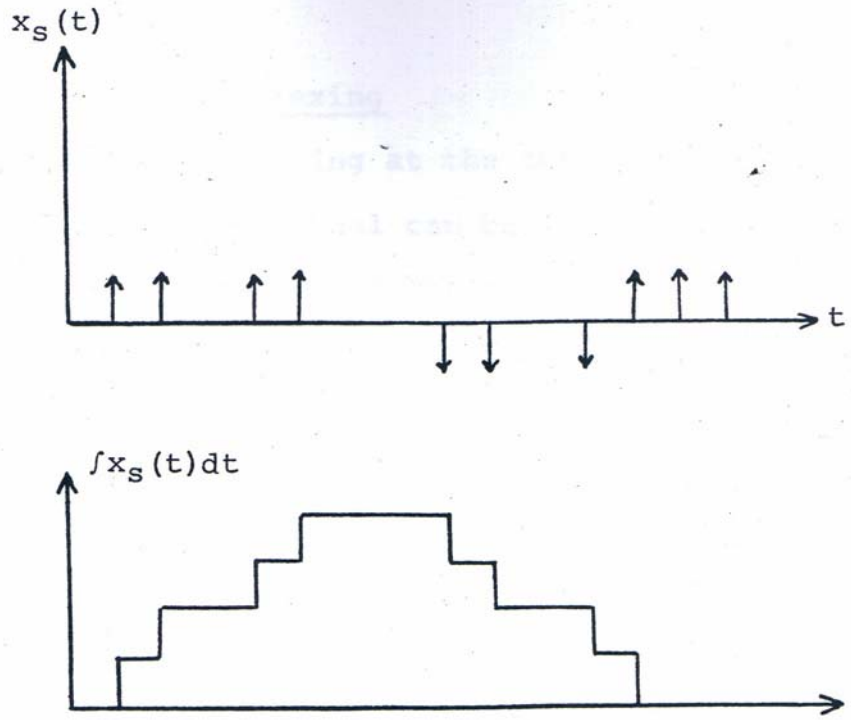

Figure 6-22: Integrating the PFM Pulses

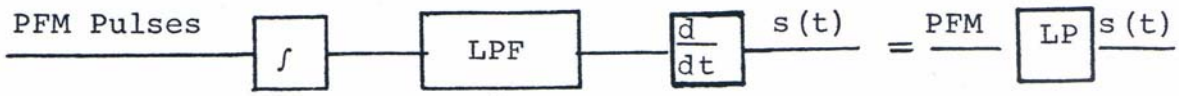

Figure 6-23: Demodulation of PFM Pulses

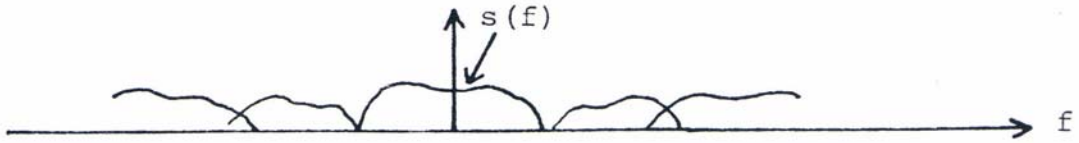

Figure 6-24: The Frequency Spectrum of PFM Pulses

6. Time Domain Multiplexing

The concept of sampling at the intersection of a random signal and a periodic signal can be extended to time domain multiplexing. The period of the sawtooth wave is n times that of the maximum Nyquist rate of the n baseband signals. Each half a period is allocated for only one of the n signals, i.e., in each half a period, the intersection of the periodic signal and one of the n random signals is sampled. Time domain multiplexing for uniform PPM has been discussed in Literature.[45] Other periodic signals like Sine, Triangular and etc. could have been used. Indeed one of the main advantages of pulse time modulations is its time domain multiplexing capability.[46] The intersection with periodic signals are good examples. However, the adaptive techniques are only easily multiplexed in time after some kind of run length coding. [31] A method for time domain multiplexing of the Adaptive Quantizer without run length coding is described below.

If the prediction discussed in Section V-6 can uniformize the samples, then the Adaptive Quantizer can be used for time domain multiplexing. In the case of nonuniform samples, the following method can be used. Divide each signal in time slots T. Each time slot is allocated for one signal alternatively. During the interval for s_1, the quantization levels for s_2 are inactive. The sampling rate should be twice the Nyquist rate so that

the overall sampling rate is the Nyquist rate. At each time slot, the quantization levels are adjusted to a fixed value. This would avoid the propagation of errors at the input. But this is not necessary, and the levels can be changed according to our adaptive scheme.

PART VII

The Zero Crossings of Exponential Modulated Signals

1. Introduction

The zero crossings of an angle modulated signal can be interpreted to represent various kinds of pulse time modulations. In particular, the zero crossings of $\cos\{w_c t+F[x(t)]\}=0$ are the intersection of the random signal, $x(t)$, and the deterministic signal, $F^{-1}(t)$. For example a PPM signal is the zero crossings of $\cos[w_c t + t_o x(t)] = 0$, which is proved in Section IV-1-a. If $F[x(t)] = \sin^{-1}[x(t)]$, the zero crossings in the above equation become the intersection of a sine wave with $x(t)$.

The intersection of the random signal, $x(t)$, with a periodic function, $z(t) = F^{-1}(t)$, can be represented as the intersection of a sawtooth wave with $z^{-1}[x(t)]$ if the periodic function is of the first category (Section IV-1). If the periodic function is of the second category (Section IV-1), the sawtooth wave becomes a triangular wave. The proof is as follows:

$$\cos\{w_c t F\,[x(t)]\} = o \qquad 7\text{-}1$$

$$w_c t + F\,[x(t)] = (2k + 1)\,\frac{\pi}{2}$$

$$t_o = \frac{1}{4f_c} - \frac{F\,[x(t)]}{2\pi f_c}$$

$$\vdots$$

$$t_m = \frac{2m + 1}{4\,f_c} - \frac{F\,[x(t)]}{2\pi f_c} \qquad 7\text{-}2$$

A comparison of the above equation with equation 4-7' shows that the zero crossings at t_m's are the intersection of a sawtooth wave with $F[x(t)]$ for the intersection of a sine wave with $x(t)$, Equation 4-7 and Equation 7-2 show that this intersection can be represented as the intersection of a triangular wave with $\sin^{-1}[x(t)]$.

In summary, any intersection with a periodic function can be represented as the intersection of a sawtooth or triangular with $z^{-1}x(t)$. Any kind of intersection, periodic or nonperiodic, can be represented as the zero crossings of an angle modulated signal.

2. F.M. Signal

The information of an F.M. signal lies in the zero crossings or the level crossings of the signal. Hence, we should be able to reconstruct the baseband signal from the impulses at the zero crossings. The intersection problem becomes the impulses at the intersection of the F.M. signal and the horizontal axis. The zero crossings are related to the baseband signal in the following (Figure 7-1)

$$A \cos \left[w_c t + 2 f_d \int_o^t dt\, x(t)\right] = o \qquad 7\text{-}3$$

or

$$w_c t + 2\pi f_d \int_o^t x(t)\, dt = (2k + 1)\, \frac{\pi}{2}$$

$$t_o = \frac{1}{4f_c} - \frac{f_d}{f_c} \int_o^{t_1} x(t)\, dt$$

$$t_1 = \frac{3}{4f_c} - \frac{f_d}{f_c} \int_o^{t_1} x(t)\, dt$$

.

.

.

$$t_m = \frac{2m+1}{4f_c} - \frac{f_d}{f_c} \int_o^{t_m} x(t)\, dt \qquad 7\text{-}4$$

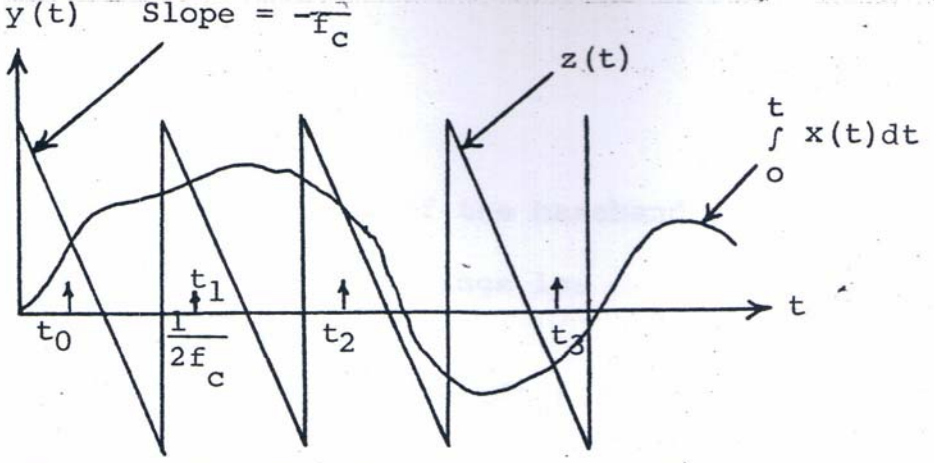

Figure 7-1: The Zero Crossings of an FM Signal Depicted as the Intersection of Two Signals

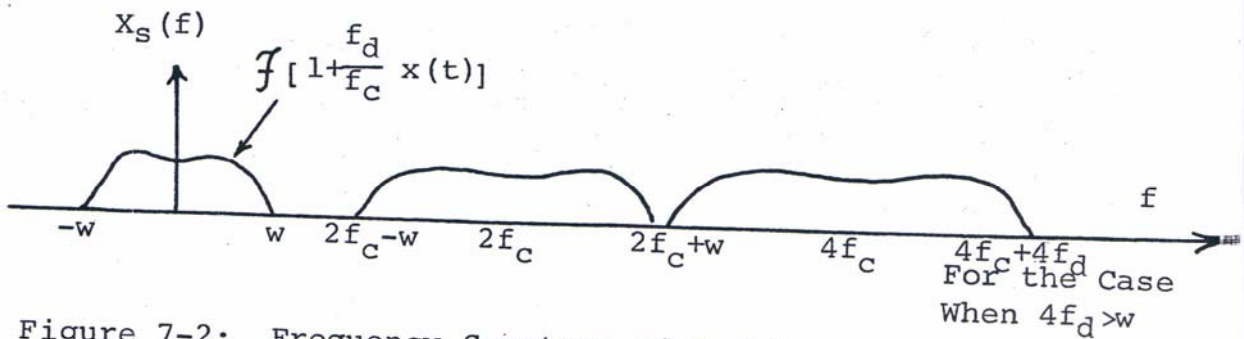

Figure 7-2: Frequency Spectrum of $x_s(t)$

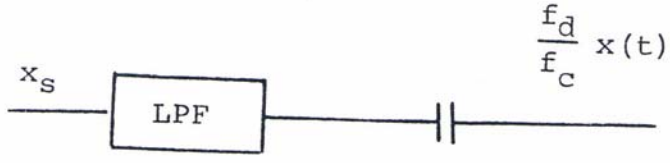

Figure 7-3: Reconstruction of the Signal by Low Pass Filtering

The reconstruction of the baseband signal from the impulses at the zero crossings is:

$$x_s = \sum_{m=o}^{\infty} \delta(t-t_m) = \sum_{m=o} \delta \left| \dot{g}(t_m) \right| \delta[g(t)] \qquad 7\text{-}5$$

where

$$g(t) = t-t_m = t - \frac{2m+1}{4f_c} + \frac{f_d}{f_c} \int_o^t x(h)\,d(h)$$

and

$$g(t_m) = o \text{ and } g(t \neq t_m) \neq o$$

$$\dot{g}(t) = 1 + \frac{f_d}{f_c} x(t)$$

thus

$$x_s = \left[1 + \frac{f_d}{f_c} x(t) \right] \sum_{m=o}^{\infty} \delta \left[t - \frac{2m+1}{4f_c} + \frac{f_d}{f_c} \int_o^t x(h)\,dh \right] \qquad 7\text{-}7$$

where it is assumed that

$$\left| \frac{fd\ x(t)}{f_c} \right| < 1 + \frac{fd}{f_c} x(t) > o \qquad 7\text{-}8$$

The Fourier series equivalent is:

$$x_s = \left[1 + \frac{fd}{f_c} x(t) \right] \sum_{m=o} e^{j2\pi n (2f_c) \left[t + \frac{f_d}{f_c} \int_o^t x(h)\,dh \right]}$$

7-9

The spectrum of x_s is sketched in Figure 7-2.

Figure 7-3 is a simple method to retrieve the baseband signal. The zero crossings of the F.M. signal convey redundant information because the carrier frequency (w_c) is much greater than the bandwidth of the F.M. signal, which is about 2W. This redundancy implies that the zero crossings of an F.M. signal is higher than the Nyquist rate. Therefore as long as there are N samples in each NT interval (where T is the Nyquist rate equal to $\frac{1}{2W}$ for narrow band F.M. and $\frac{1}{4f_d}$ for wideband FM), the baseband signal can be retrieved. Instead of the zero crossings, the level crossings could have been transmitted. The analysis is slightly different and is given below.

Suppose the level is located at the level α A, where α is a fraction of one. The time intervals of the impulses are as follows:

$$A \cos \left(w_c t + w_d \int_o^t x \, dt\right) - \alpha A = o \qquad 7\text{-}10$$

thus,

$$\cos \left(w_c t + w_d \int_o^t x \, dt\right) = \alpha \qquad 7\text{-}11$$

or

$$w_c t + w_d \int_o^t x\,dt = B\pi\ ,\ (2-B)\pi\ ,\ B\pi + 2\pi\ ,\ (4-B)\pi\ ,\ldots \quad 7\text{-}12$$

where $\cos B\pi = \alpha$ and $o \leq B \leq 1$

Hence,

$$t_o = \frac{B}{2f_c} - \frac{f_d}{f_c} \int_o^{t_o} x\,dt$$

$$t_1 = \frac{2-B}{2f_c} - \frac{f_d}{f_c} \int_o^{t_1} x\,dt$$

$$t_2 = \frac{B+2}{2f_c} - \frac{f_d}{f_c} \int_o^{t_2} x\,dt$$

$$\vdots$$

$$t_2 = \frac{B+2m}{2f_c} - \frac{f_d}{f_c} \int_o^{t_{2m}} x\,dt$$

$$t_{2m+1} = \frac{(2m+2-B)}{2f_c} - \frac{f_d}{f_c} \int_o^{t_{2m+1}} x\,dt$$

The reconstruction procedure is as follows:

$$x_s = A \sum_{m=o}^{\infty} \delta(t-t_m) - A \sum_{m=even} \delta(t-t_m) + A \sum_{m=odd} \delta(t-t_m) =$$

$$= A \sum_{m=even} \dot{g}(t_m)\,\delta[g_m(t)] - A \sum_{m=odd} |\dot{g}(t_m)|\,\delta[g_m(t)]$$

where

$$g_m(t) = \begin{cases} t - \dfrac{B + m}{2f_c} - \dfrac{f_d}{f_c} \int_o^t x\,dt & \text{if } m = \text{even} \\ t - \dfrac{m+1-B}{2f_c} - \dfrac{f_d}{f_c} \int_o^t x\,dt & \text{if } m = \text{odd} \end{cases} \qquad 7\text{-}15$$

The above $g_m(t)$ is a valid function because:

$$g_m(t_m) = 0 \qquad m = \text{odd or even}$$

$$g_m(t \neq t_m) \neq 0 \qquad m = \text{odd or even}$$

$$\dot{g}_m(t) = 1 - \frac{f_d}{f_c} x(t) \qquad m = \text{odd or even}$$

$$\dot{g}_m(t_m) \neq 0 \qquad 7\text{-}16$$

Substituting Equation 7-15 in Equation 7-14 and applying the Fourier series equivalent, we can derive at

$$x_s = \left[1 - \frac{f_d}{f_c} x(t)\right] \sum_{n=-\infty}^{\infty} e^{j2\pi n f_c \left[t - \frac{f_d}{f_c} \int_o^t x\,dt\right]} +$$

$$+ \left[1 - \frac{f_d}{f_c} x(t)\right] \sum_{n=-\infty}^{\infty} e^{j2\pi n f_c \left[t - \frac{f_d}{f_c} \int_o^t x\,dt\right]}$$

The extraction of the baseband signal from Equation 7-17 is done by low pass filtering as in Figure 7-3. The main difference

between the zero crossings reconstruction and the level crossings is that the spectrum of x_s in the first case is repeated at a rate of $2f_c$ while the spectrum of the latter has a repetition rate of f_c.

The above analysis gives a better insight about the F.M. signal. it shows clearly how the information of the F.M. signal lies in its zero crossings. It also shows that some of the zero crossings of the F.M. signal are redundant, that is, the baseband signal can be reconstructed from some of the zero crossings as long as it satisfies the Nyquist rate. The analysis also implies a different approach for the reconstruction of an F.M. signal. This unique approach has some similarities and differences with the conventional limiter discriminator. Besides, it has the advantage of simpler hardware implementation plus the fact that unlike a discriminator it does not produce any clicks.[46] Clicks are produced in a conventional discriminator because the discriminator differentiates the phase of the F.M. signal. Our scheme does not differentiate the phase of the signal and therefore does not produce any clicks. In order to show the similarities and differences of these two demodulators, their block diagrams are depicted in Figure 7-4 and Figure 7-5.

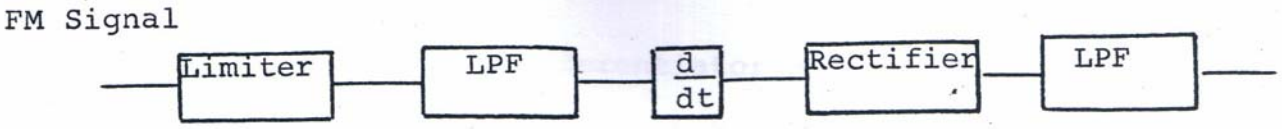

Figure 7-4: Limiter Discriminator for FM Demodulation

Figure 7-5: The Zero Crossing Demodulator

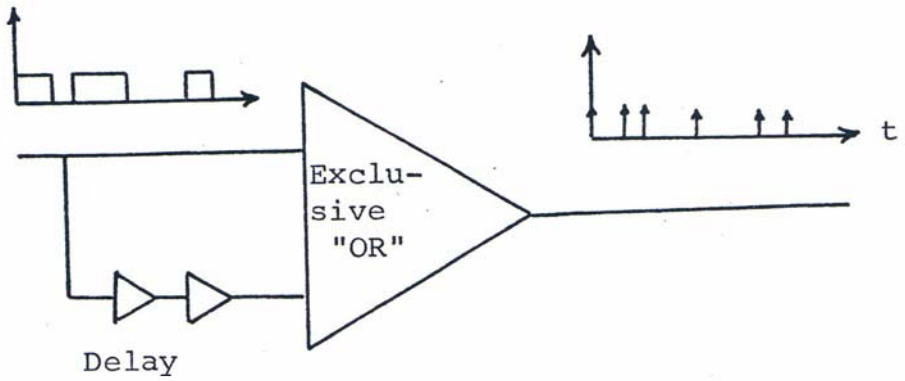

Figure 7-6: The Replaced Block of the Diffrentiator and the Rectifier in Figure 7-5 by an Exclusive "OR"

To avoid the clicks, the differentiator and the rectifier in Figure 7-5 is replaced by the block diagram in Figure 7-6. A literature survey showed that there is a zero crossing detector similar to the Figure 7-6. However, the zero crossing detector has been used in binary F.M.[48] and analog F.M.[49] and has not been analyzed as such. The analog zero crossing detector is more complicated than our circuit. This method can also be used for the synthesis of linear transversal filters.[50]

3. P.M. Signal

The analysis of a P.M. signal is similar to the analysis of an F.M. signal, which is given below:

$$A \cos \left[w_c t + \frac{d}{w_d} x(t) \right] = o$$

$$w_c t + \phi_d x(t) = (2k + 1)\frac{\pi}{2} \qquad 7\text{-}18$$

thus,

$$t_o = \frac{1}{4f_c} - \frac{\phi_d}{w_c} x(t)$$

$$t_1 = \frac{3}{4f_c} - \frac{\phi_d}{w_c} x(t)$$

$$\vdots$$

$$t_m = \frac{2m+1}{4f_c} - \frac{\phi_d}{w_c} x(t) \qquad 7\text{-}19$$

The reconstruction of the baseband signal from the impulses at the zero crossings is:

$$x_s = \sum_{m=o}^{\infty} \delta(t-t_m) = \sum_{m=o}^{\infty} |\dot{g}(t_m)| \delta[g(t)] \qquad 7\text{-}20$$

where

$$g(t) = t - \frac{2m+1}{4f_c} + \frac{\phi_d}{w_c} x(t), \quad g(t_m) = o, \quad g(t \neq t_m) \neq o \qquad 7\text{-}21$$

$$\dot{g}(t) = 1 + \frac{\phi_d}{w_c}\dot{x}(t) \qquad g(t_m) \neq o$$

$$x_s = [1 + \frac{\phi_d}{w_c}\dot{x}(t)] \sum_{n=-\infty}^{\infty} e^{j2\pi n(2f_c)[t + \frac{\phi_d}{w_c}x(t)]} \qquad 7\text{-}22$$

where it is assumed that:

$$[1 + \frac{\phi_d}{w_c}x'(t)] > o$$

The baseband signal is reconstructed as shown in Figure 7-7.

A comparison of Equation 7-19 to Equation 4-8 reveals that the zero crossings of a PM signal are the intersection of x(t) with a sawtooth wave, i.e., nonuniform PPM (Figure 7-8). Hence all the analysis for the reconstruction of PPM signal holds true for a PM signal.

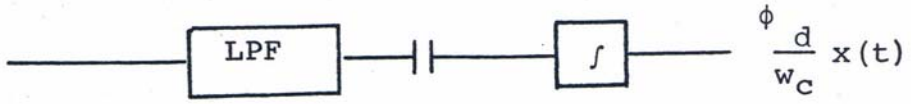

Figure 7-7: The Reconstruction of a PM Signal

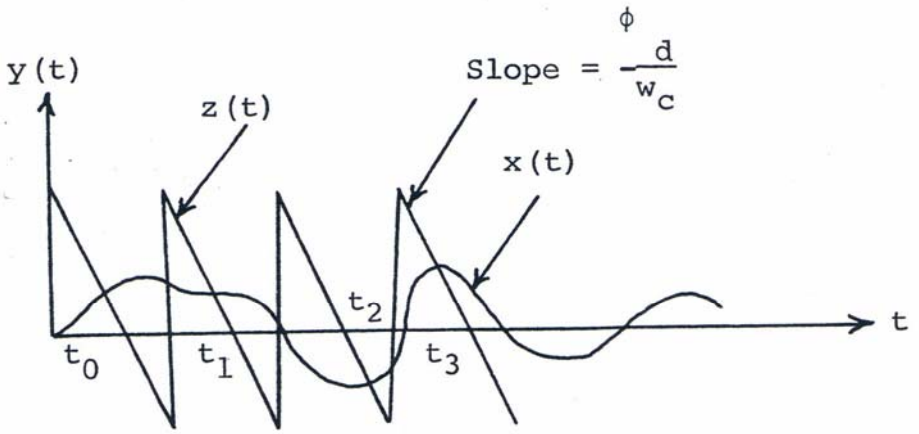

Figure 7-8: The Zero Crossings of a PM Signal as the Intersection of Two Signals

4. F.S.K. Signal

The analysis of an F.S.K. signal is essentially the same as an F.M. signal, which is given in the following:

$$A \cos\left[w_c t + \int_o^t w_d(t)\,dt\right] = o$$

where $w_d(t) = x(t)$ is a binary random variable

$$w_c t + \int_o^t w_d\,dt = (2k + 1)\,\frac{\pi}{2}$$

$$t_o = \frac{1}{4f_c} - \frac{1}{w_c} \int_o^{t_o} w_d\,t$$

$$t_1 = \frac{3}{4f_c} - \frac{1}{w_c} \int_o^{t_1} w_d\,dt$$

$$t_m = \frac{2m+1}{4f_c} - \frac{1}{w_c} \int_o^{t_m} w_d\,dt \qquad 7\text{-}23$$

$$x_s = A \sum_{m=o}^{\infty} \delta(t-t_m)$$

$$g(t) = t - \frac{2m+1}{4f_c} + \frac{1}{w_c} \int_o^t w_d\,dt$$

$$g(t_m) = o, \quad g(t \neq t_m) \neq o$$

$$\dot{g}\,(t) = 1 + \frac{w_d}{w_c}$$

$$\dot{g}(t_m) \neq o$$

Hence,

$$x_s = A \sum_{m=o}^{\infty} |1 + \frac{w_d}{w_c}| \delta [\frac{t-2m+1}{4f_c} + \frac{1}{w_c} \int_o^t w_d \, dt]$$

$$= A (1 + \frac{w_d}{w_c}) \sum_{n=-\infty}^{\infty} e^{j2\pi n(2f_c)[t + \frac{1}{w_c} \int_o^t w_d \, dt]}$$

It is assumed in the above that low pass filtering yields the information signal provided that there is no spectrum overlapping. This assumption is reasonable since $2w_c$ is much greater than w_d. The reconstruction scheme is similar to that of a zero crossing detector.

A comparison of Equation 7-22 with Equation 4-8 reveals that the zero crossings of FSK is, like F.M., the intersection of the integral of $x(t) = w_d(t)$ with a sawtooth generator (Figure 7-9).

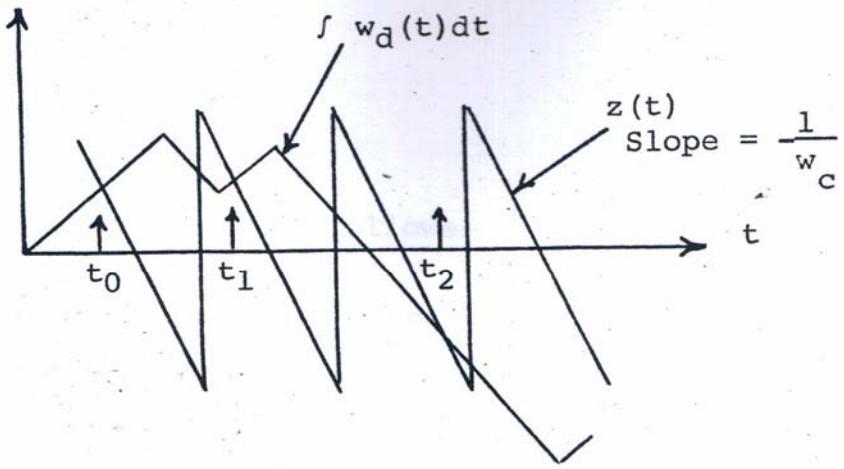

Figure 7-9: Intersection of Two Signals to Generate the Zero Crossings of an FSK Signal

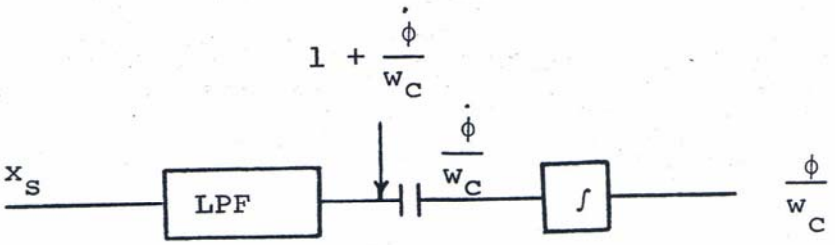

Figure 7-10: PSK Demodulator

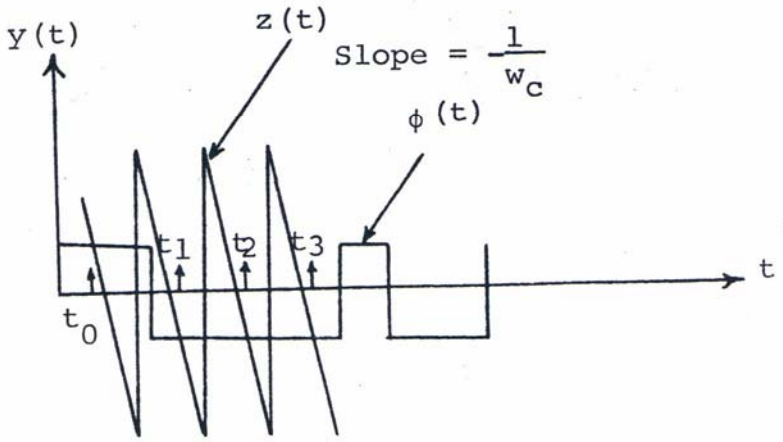

Figure 7-11: Zero Crossings of PSK Depicted as the Intersection of Two Signals

5. P.S.K. Signal

The analysis is as follows:

$A \cos [w_c t + \phi] = o$ where $\phi(t)$ is a binary random phase

$$w_{ct} + \phi = (2R + 1)\frac{\pi}{2}$$

$$t_1 = \frac{1}{4f_c} - \frac{\phi(t_1)}{w_c}$$

$$t_2 = \frac{3}{4f_c} - \frac{\phi(t_2)}{w_c}$$

$$t_m = \frac{2m+1}{4f_c} - \frac{\phi(t_m)}{w_c}$$

$$x_s = A \sum_m \delta(t - t_m)$$

$$g(t) = t - \frac{2m+1}{4f_c} + \frac{\phi(t)}{w_c} \quad \text{where } g(t_m) = o; \quad g(t \neq t_m) \neq o$$

$$\dot{g}(t) = 1 + \frac{\phi(t)}{w_c} \quad \text{where } \dot{g}(t_m) \neq o$$

thus,

$$x_s = [1 + \frac{\phi}{w_c}] \sum_{n=-\infty}^{\infty} e^{\frac{j2\pi n}{1}(2f_c)[t + \frac{\phi(t)}{w_c}]}$$

The reconstruction scheme is illustrated in Figure 7-10

The zero crossings of P.S.K., like P.M., is the intersection of two signals (Figure 7-11), which is a P.P.M. signal.

PART VIII

NONUNIFORM SAMPLING RECONSTRUCTION

1. Zero Order Hold and Low Pass Filtering

All the techniques that have been discussed previously introduce nonuniform samples, which have to be reconstructed at the receiver. Some simple techniques were developed in Section II-3 to reconstruct the nonuniform samples by a combination of low pass filtering and integration. However, the reconstruction is based on the assumption that there is only one sample per interval T; the spectrum aliasing is ignored. If these conditions are not satisfied, other techniques have to be considered. Nonuniform samples can be reconstructed theoretically provided that certain conditions are satisfied. The theorems regarding reconstruction of nonuniform samples are summarized in Appendix A. Unfortunately, the conventional reconstruction scheme of nonuniform samples is not practical. For the first approximation, zero order hold and low pass filtering are tried. It has been shown previously that this method is quite efficient if the nonuniform samples are at the zeros of the signal and the derivative of the signal[5]. In order to test this reconstruction technique on the Adaptive Quantizer, the Adaptive Quantizer has been simulated on a computer (Section IX-1). The nonuniform samples derived from the computer are then reconstructed accordingly to the above scheme.

The reconstructed nonuniform samples, together with the original signal, is illustrated in Figure 8-1. This Figure 8-1 shows that the reconstructed signal is distorted. To reduce this error, the sampling rate has to be increased above that of the Nyquist rate. The computer results show that the error on nonuniform sampling is the same as the error of the uniform sampling if the zero order reconstruction method is used in both cases. However, zero order hold and low pass filtering method requires 2 to 4 times the Nyquist rate in order to have the same fidelity as the method of low pass filtering the uniform samples. One way of reducing the sampling rate requirement for the zero order hold technique is discussed in reference 51.

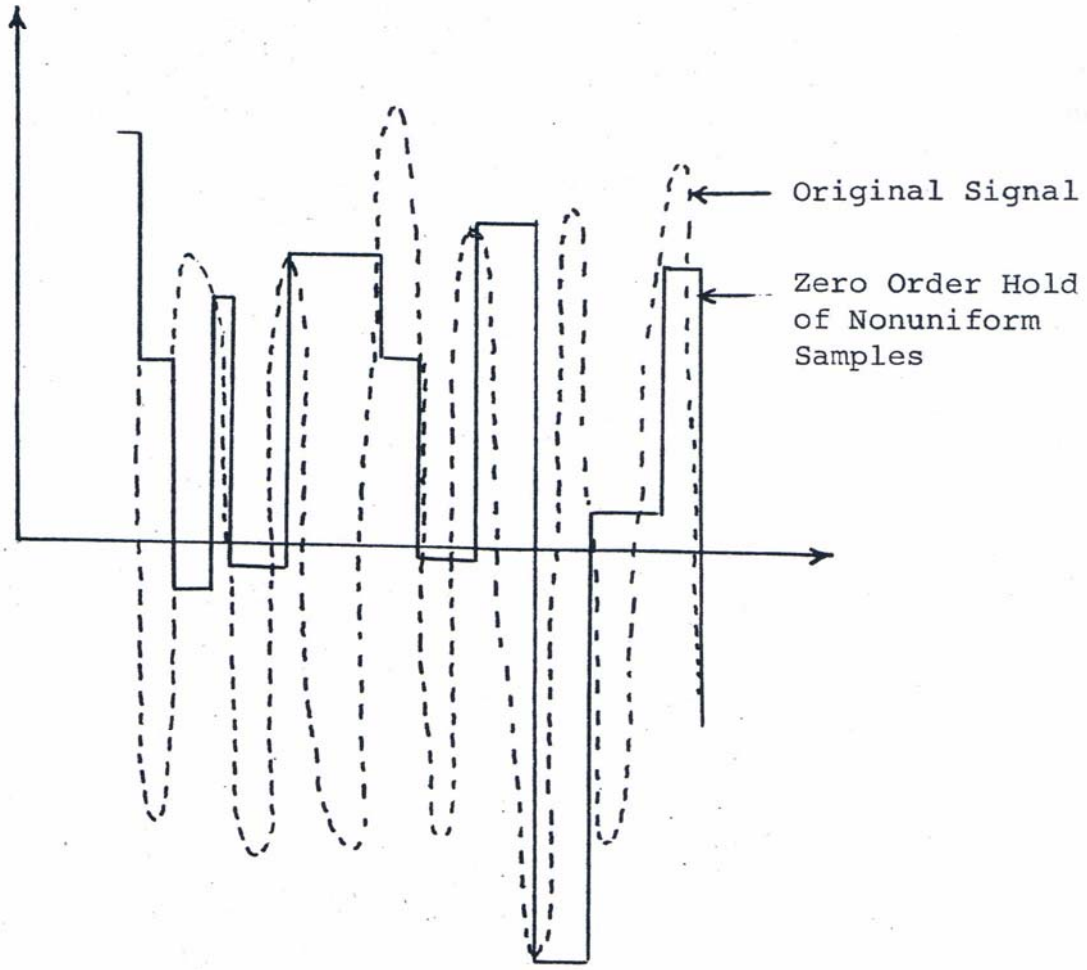

Figure 8-1: Reconstruction of Nonuniform Samples at the Nyguist Rate by Zero Order Hold

2. Some Other Practical Reconstruction Techniques

a. Window function technique

According to the ideal nonuniform sampling reconstruction described in Appendix A, all the samples are needed before the reconstruction of the samples can start. Besides, the filter representing the scanning function of the nonuniform samples is a time varying adaptive one. In order to combat this problem, suitable time window functions are used (Figure 8-2). The length of the window function is chosen as nT where T is the Nyquist interval, and there are n nonuniform samples in each interval, nT. The samples in each interval, nT are then reconstructed separately. The window function has to be designed so that the bandwidth of the window function convolved with the signal is not appreciably increased. From the reconstruction formulas in Appendix A, each window is reconstructed by calculating the n uniform samples from the n nonuniform samples and then by low pass filtering.

In case there are not n samples in each interval nT, e.g., the nonuniform samples of the Adaptive Quantizer, a window of a fixed length can be chosen. If the signal is inactive (low frequency content) in an interval, there will

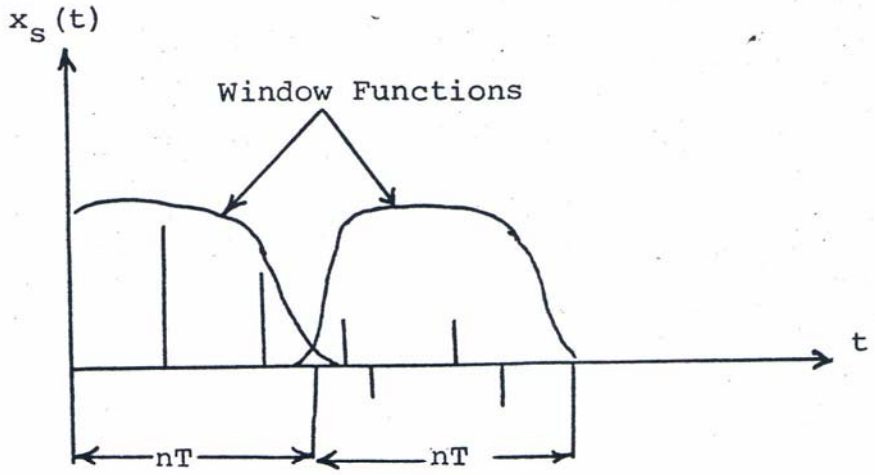

Figure 8-2: Window Functions for Nonuniform Samples

Figure 8-3: Changing Nonuniform Samples into Uniform Samples and then Reconstructing the Signal by Low Pass Filtering

be less samples in that window. The number of nonuniform samples should be doubly proportional to the frequency content of the signal in that window so that it can be reconstructed approximately by the ideal reconstruction method. The above procedure would optimize the number of samples required to reconstruct the signal since in each interval the number of samples is less than or equal the Nyquist rate. In other words, instead of applying the frequency spectrum of the signal as a whole, the instantaneous frequency content of the signal in each window has been utilized. An example of the application of the aforementioned concept is the reconstruction of the nonuniform samples at the zeros of the derivative of the signal.[51] The average number of samples in that case is less than the Nyquist rate.

b. Reconstruction by uniformizing the samples

A method was discussed in Section V-2-b to uniformize the nonuniform samples. The uniform samples are then low pass filtered to reconstruct the signal. The block diagram of the technique is depicted in Figure 8-3. The actual block diagram of the processor is illustrated in Figure 8-4.

Wherever a nonuniform sample enters the processor, a uniform sample emerges from its output (Figure 8-5)

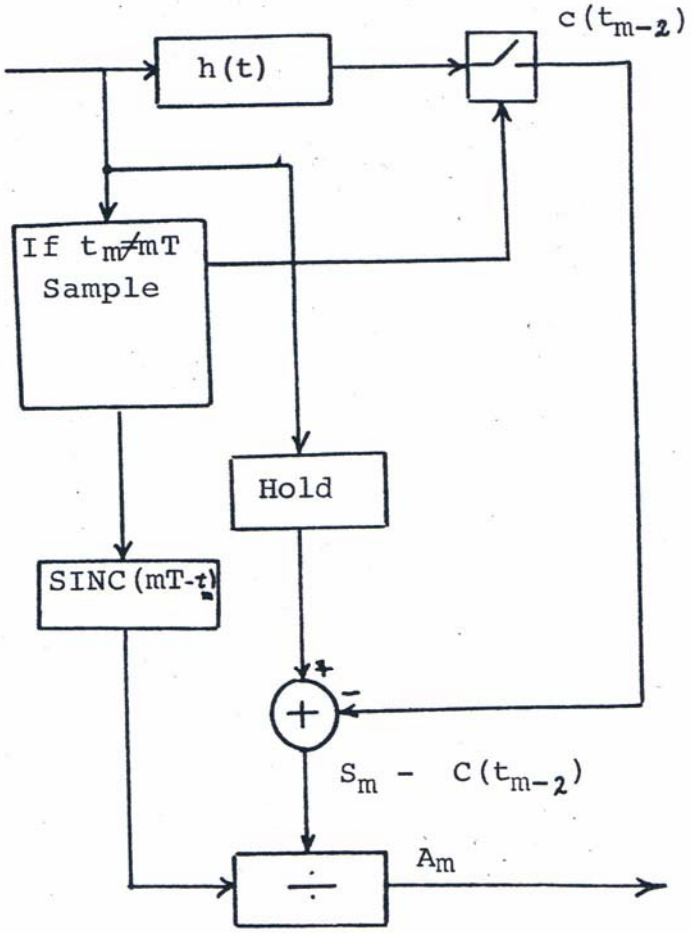

Figure 8-4: The Uniformizer in Figure 8-3

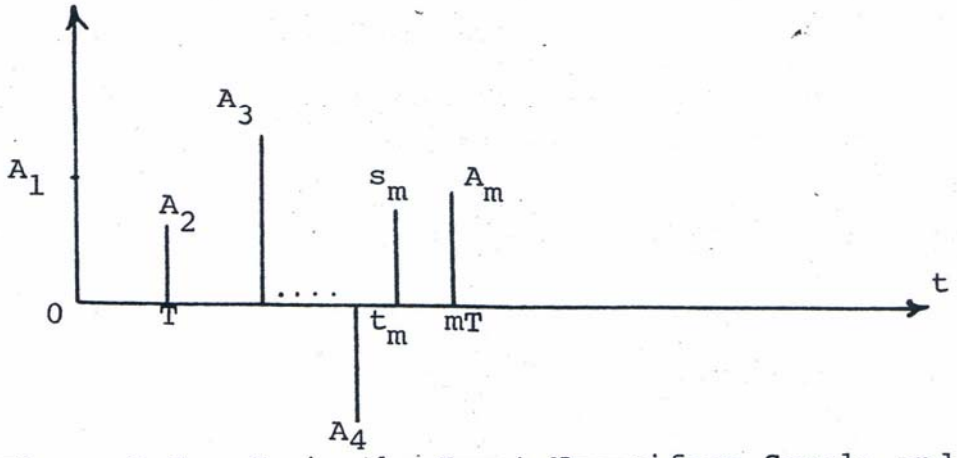

Figure 8-5: S_m is the Input Nonuniform Sample and A_m is the Output Uniform Sample

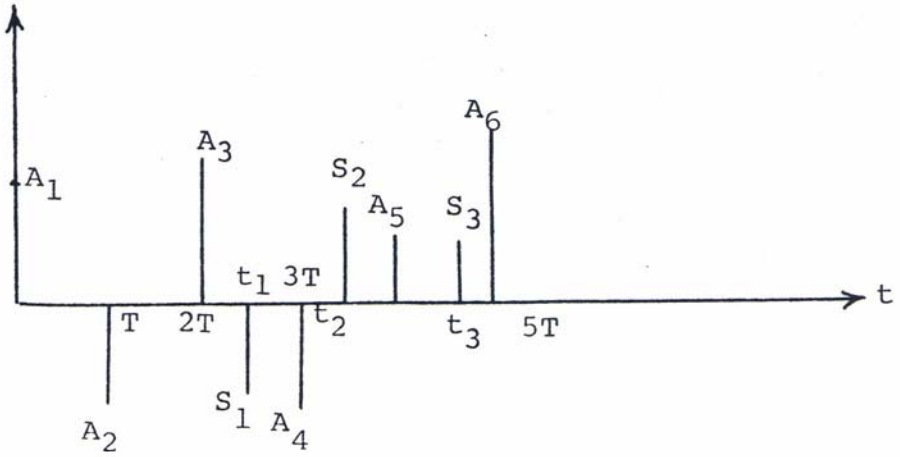

Figure 8-6: s_1, s_2 and s_3 are the Input Nonuniform Samples and A_4 is the Output Uniform Sample (m=4)

The uniform sample A_m is calculated from the nonuniform sample S_m by reconstructing the signal from the uniform samples, assuming A_m is known. The reconstructed signal is then sampled at t_m, which should be equal to S_m. If the reconstructed signal is denoted by R(t), we have the following equations:

$$R(t_m) = S_m \qquad 8\text{-}1$$

$$R(t_m) = \underbrace{\sum_{k=o}^{m-2} A_{m+1} \operatorname{sinc}(t_k - kT)}_{= C(t_{m-2})} + A_m \operatorname{sinc}(mT - t_m) = \qquad 8\text{-}2$$

From the above two equations, we can deduce that:

$$C(t_{m-2}) + A_m \operatorname{sinc}[mT - t_m] = S_m \qquad 8\text{-}3$$

$$A_m = \frac{S_m - C(t_{m-2})}{\operatorname{sinc}(mT - t_m)} \qquad 8\text{-}4$$

where $C(t_{m-2})$ is updated for each incoming nonuniform sample S_m. The block diagram in Figure 8-4 is a circuit realization of the above equation. This technique can be modified in order to reduce the resultant error. The error

is produced due to the dependence of the reconstruction technique on the future samples. Hence a few of the future samples can be clocked into the processor in Figure 8-4 before the first uniform sample A_m is clocked out of the same processor. In other words, there is a delay between the input and output of the processor. This fact is reminiscent to the delay of the impulse response of a low pass filter to approximate an ideal low pass filter. The analysis is as follows:

The next m future nonuniform samples are received before the uniform sample A_m is generated (Figure 8-6). The equations relating to the samples are as follows:

$$\sum_{n=o}^{m-2} A_{n+1}\,\mathrm{sinc}(t_1-nT) + \sum_{n=m-1}^{2m-3} A_{n+1}\,\mathrm{sinc}(nT-t_1) = S_1$$

$$\sum_{n=m-1}^{2m-3} A_{n+1}\,\mathrm{sinc}(nT-t_1) = S_1 - \sum_{n=o}^{m-2} A_{n+1}\,\mathrm{sinc}(t_1-nT)$$

and likewise

$$\sum_{n=m-1}^{2m-3} A_{n+1}\,\mathrm{sinc}(nT-t_2) = S_2 - \sum_{n=o}^{m-2} A_{n+1}\,\mathrm{sinc}(t_2-nT)$$

$$\sum_{n=m-1}^{2m-3} A_{n+1}\,\mathrm{sinc}(nT-t_3) = S_3 - \sum_{n=o}^{m-2} A_{n+1}\,\mathrm{sinc}(t_3-nT)$$

$$\vdots$$

$$\sum_{n=m-1}^{2m-3} A_{n+1}\,\mathrm{sinc}(nT-t_m) = S_m \sum_{n=o}^{m-2} A_{n+1}\,\mathrm{sinc}(t_m-nT) \qquad 8\text{-}5$$

where A_1 through A_{m-1} are known and A_m through A_{2m-3} are unknown. The m unknown A_k's can be found from the above m equations.

For m = 4, A_4 is found as follows:

$$A_4 = \frac{\begin{vmatrix} S_1 - \sum_{n=o}^{2} A_{n+1}\,\mathrm{sinc}(t_1-nT) & \mathrm{sinc}(4T-t_1) & \mathrm{sinc}(5T-t_1) \\ S_2 - \sum_{n=o}^{2} A_{n+1}\,\mathrm{sinc}(t_2-nT) & \mathrm{sinc}(4T-t_2) & \mathrm{sinc}(5T-t_2) \\ S_3 - \sum_{n=o}^{2} A_{n+1}\,\mathrm{sinc}(t_3-nT) & \mathrm{sinc}(4T-t_3) & \mathrm{sinc}(5T-t_3) \end{vmatrix}}{\begin{vmatrix} \mathrm{sinc}(3T-t_1) & \mathrm{sinc}(4T-t_1) & \mathrm{sinc}(5T-t_1) \\ \mathrm{sinc}(3T-t_2) & \mathrm{sinc}(4T-t_2) & \mathrm{sinc}(5T-t_2) \\ \mathrm{sinc}(3T-t_3) & \mathrm{sinc}(4T-t_3) & \mathrm{sinc}(5T-t_3) \end{vmatrix}} \qquad 8\text{-}6$$

A_5 and A_6 can also be found from the above equations because A_5 and A_6 also depend on the future samples, A_5 is calculated after a new nonuniform sample is received. Equation 8-6 is

then updated to find A_5. The procedure is then repeated as shown on the preceding page. This technique is more accurate than the previous method. Each uniform sample is derived from the previous uniform samples and the new incoming nonuniform samples. The error in the previous uniform samples propagate, it might grow up or it might be cancelled out. This fact can only be verified by either a hardware realization or a computer simulation. The advantage of the above technique unlike the nonuniform sampling reconstruction method discussed in Appendix A is that it is easily implementable.

There are other reconstruction methods like polynomial interpolation and spline functions, which is recently developed and need not be discussed here.[52] Some other practical circuits to reconstruct some special nonuniform samples are discussed in literature.[50,53]

3. Nonuniform Sampling Reconstruction as an Intersection Problem

We now try to reconstruct the nonuniform samples by the intersection method developed in the previous sections.

Uniform samples are represented by:

$$x_s = x(t) \sum_{m=o}^{\infty} \delta(t-mT) \qquad 8\text{-}7$$

$$\text{choose } g(t) = t - mT \quad \text{where } g(mT) = o \qquad 8\text{-}8$$

$$\text{and } \dot{g}(t) = 1 \qquad 8\text{-}9$$

Hence

$$x(t) \sum_{m=o}^{\infty} |\dot{g}(t_m)| \, \delta[g(t)] = x(t) \sum_{m=o}^{\infty} \delta(t-mT) =$$

$$= x(t) \sum_{n=-\infty}^{\infty} e^{\frac{j2\pi nt}{T}}$$

Therefore low pass filtering results in the baseband signal.

If there is a nonuniform sample in each interval T as shown in Figure 8-7, the analysis is as follows:

$$x_s = \sum_{m=o}^{\infty} x(t_m) \, \delta(t-t_m) = \sum_{n=-\infty}^{\infty} \delta(t-t_m) \qquad 8\text{-}11$$

$$t_m = (m-1)T + \phi \qquad 8\text{-}12$$

where ϕ is a uniform random phase defined in the region $o \leq \phi < T$.

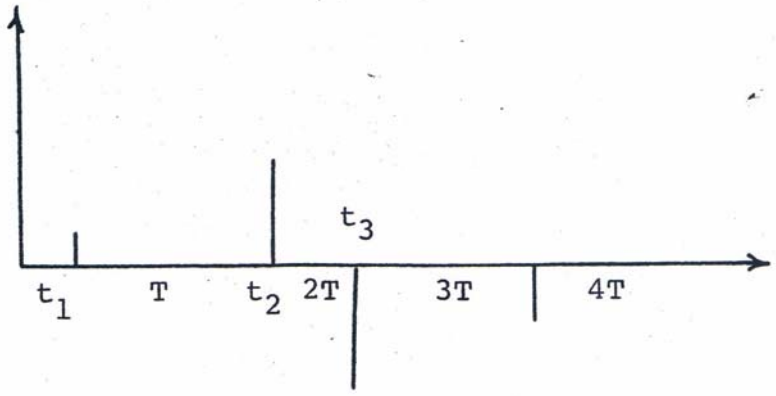

Figure 8-7: Nonuniform Samples

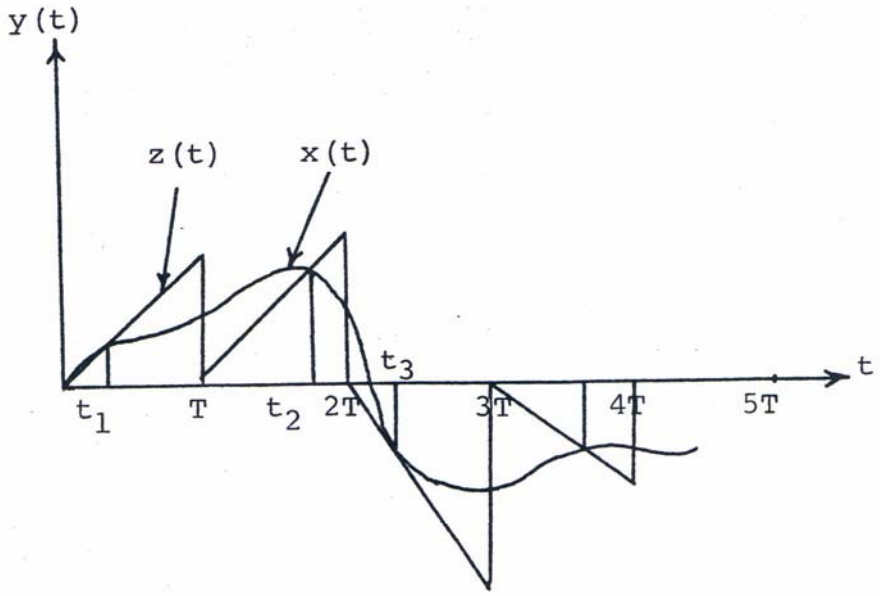

Figure 8-9: Nonuniform Samples Generated by Intersection of Two Signals

We thus have:

$$g(t) = t - (m-1)T - \phi \qquad 8\text{-}13$$

$$\dot{g}(t) = 1$$

$$x_s = x(t) \sum_{m=o}^{\infty} \delta [t - (m-1)T - \phi] = x(t) \sum_{n=-\infty}^{\infty} e^{\frac{j2\pi n(t-\phi)}{T}} \qquad 8\text{-}14$$

The spectrum of $y = \cos[\frac{2\pi t}{T} - \frac{2\pi\phi}{T}]$ is found as follows:

$$R(\tau) = Ey(\phi)\ y\ (\phi-\tau) = \int_o^T d\phi [\cos(\frac{2\pi t}{T} - \frac{2\pi\phi}{T})$$

$$\cos \frac{2\pi}{T} t - \frac{2\pi}{T} \tau - \frac{2\phi}{T}]=$$

$$= \frac{1}{2} \int_o^T \cos(\frac{4\pi}{T} t - \frac{4\pi\phi}{T} - \frac{2\pi\tau}{T}) d\phi + \frac{1}{2} \int_o^T \cos \frac{2\pi\tau}{T} d\phi =$$

$$= \frac{T}{2} \cos \frac{2\pi\tau}{T} \qquad 8\text{-}15$$

Hence the energy of the signal is concentrated on the frequency $\frac{2\pi}{T}$. The same result would have been achieved if ϕ was within the range $0 \leq \phi < \frac{T}{2}$. However, this result does not mean that low pass filtering would result in the baseband signal. The spectrum of $x(t) \cos (\frac{2\pi}{T} t - \frac{2\pi\phi}{T})$

would interfere with the low pass filtering. This fact is shown by the experimental simulation of this problem on computer.[52] The results are shown in Figure 8-8, which includes two different density functions for the random phase.

The nonuniform samples can be treated as the intersection of a train of sawtooth waves and the baseband signal as represented in Figure 8-9. The analysis is as follows:

$$t_1 = t_o x(t_1)$$

$$t_1 = t_o^{1} x(t_2) + T$$

$$\vdots \qquad \vdots$$

$$t_m = t_o^{m-1} x(t_m) + (m-1)T \tag{8-16}$$

$$g(t) = t - t_o^{m-1} x(t) - (m-1)T \tag{8-17}$$

$$g(t_m) = o, \quad g(t \neq t_m) \neq o$$

$$\dot{g}(t) = 1 - t_o^{m-1} \dot{x}(t) \qquad \dot{g}(t_m) \neq o \text{ (in general)} \tag{8-18}$$

$$x_s = A \sum_{m=o}^{\infty} \left| 1 - t_o^{m-1} \dot{x}(t_m) \right| \delta \left[t - t_o^{m-1} x(t) - (m-1)T \right] \tag{8-19}$$

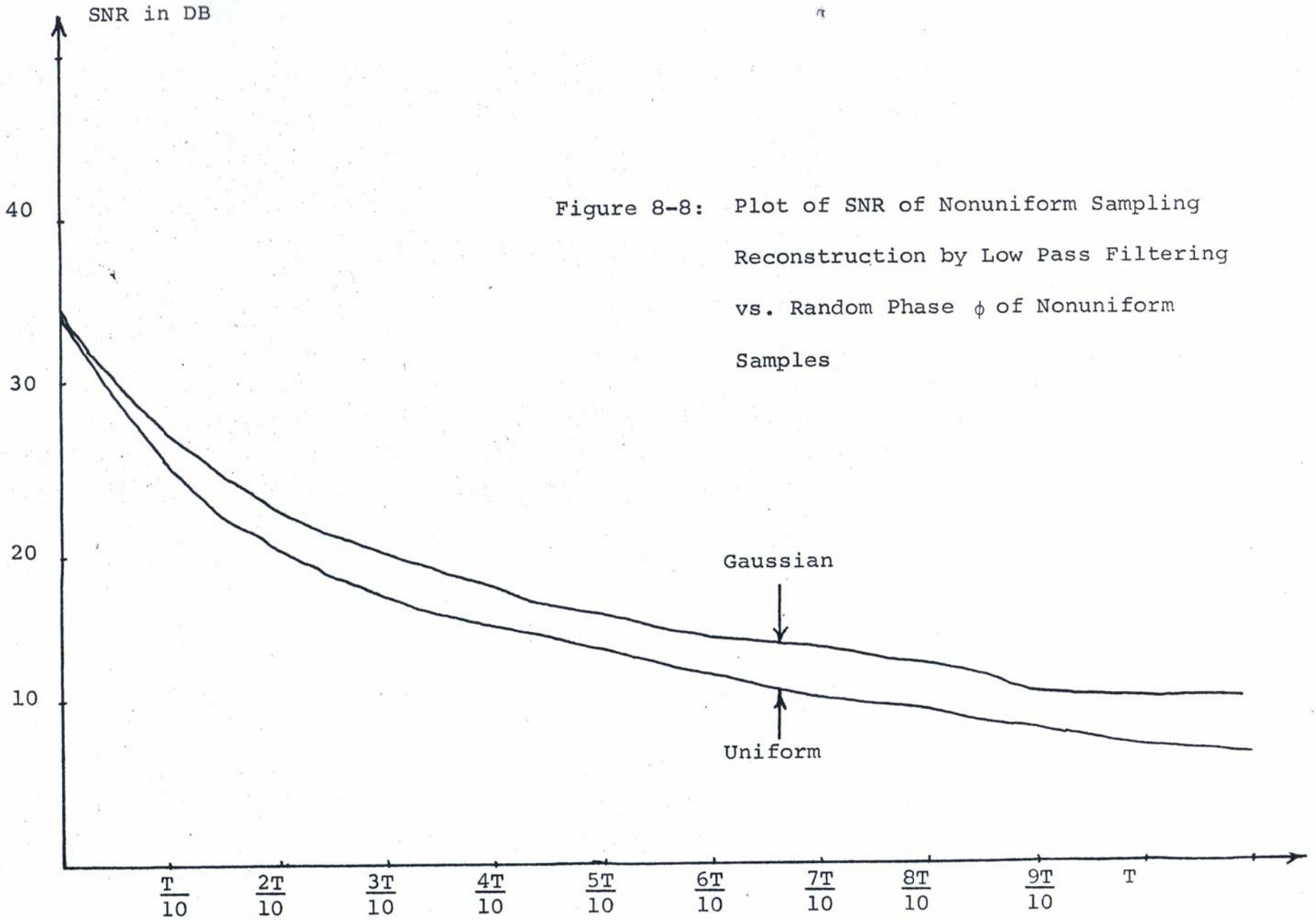

Figure 8-8: Plot of SNR of Nonuniform Sampling Reconstruction by Low Pass Filtering vs. Random Phase ϕ of Nonuniform Samples

In order to use Fourier series for the train of impulses, $g(t_m)$ has to be taken out of the summation in Equation 8-19. Thus, t_o^{m-1} has to be independent of m. There are two ways to solve this problem. The first method is to make t_o^{m-1} periodic, i.e., the slope of the sawtooth waveform repeats itself after p intervals. We thus separate the identical slopes in Equation 8-19 and rewrite the equation in the following:

$$x_s = A[1 - t_o\dot{x}(t)] \sum_{m=1,p+1,2p+1...} \delta[t-t_o x(t) - (m-1)T] +$$

$$+ A[1 - t_o^1 x(t)] \sum_{m=2,p+2,2p+2,...} \delta[t-t_o^1 x(t) - (m-1)T] +$$

$$+ A[1 - t_o^{p-1} x(t)] \sum_{m=p,2p,3p,...} [t-t_o^{p-1} x(t) - (m-1)T] \qquad 8\text{-}20$$

It is assumed that $[1 - t_o^{m-1}\dot{x}(t)] > 0$. The Fourier series equivalent is:

$$x_s = A[1 - t_o\dot{x}(t)] \sum_{n=-\infty}^{\infty} e^{\frac{j2\pi n}{PT}[t - t_o x(t)]} + \ldots$$

$$+ A[1 - t_o^{m-1}\dot{x}(t)] \sum_{n=-\infty}^{\infty} e^{\frac{j2\pi n}{PT}[t - t_o^{m-1} x(t)]} \qquad 8\text{-}21$$

Low pass filtering would yield the baseband signal provided that there is no aliasing effect, which is true if the sampling rate is P times that of the Nyquist rate. The reconstruction

scheme is depicted in Figure 8-10.

The above nonuniform samples are assumed to have been derived by the intersection of the baseband signal and a periodic signal. However, nonuniform samples, in general, are not derived this way. In order to have periodic t_o^{p-1}'s, each block of p nonuniform samples can be reconstructed independently by assuming that each block of p nonuniform samples (Figure 8-11-a) are repeated, which generates a pseudo periodic nonuniform samples. Thus, each block is reconstructed according to Figure 8-10. After the first block is fed into the circuit of Figure 8-10, the same block is fed into the circuit. The output of the circuit in Figure 8-10 is a periodic waveform, which is that portion of the baseband signal contained in the block (Figure 8-11-b). Since there is a transient response, there is a time delay before a good representative of the block is reconstructed (Figure 8-11-c). This fact points the necessity of having two reconstruction blocks in parallel as depicted in Figure 8-12 and Figure 8-11,d,e,f.

A different approach to the above problem would be to make t_o^{m-1} dependent on t rather than on m in Equation 8-19.

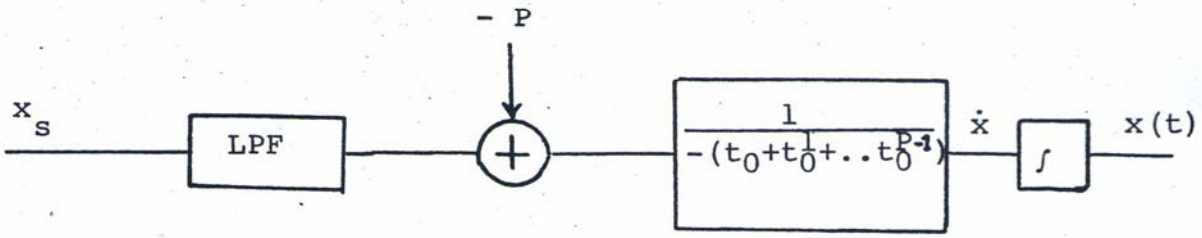

Figure 8-10: Reconstruction of Nonuniform Samples by Low Pass Filtering

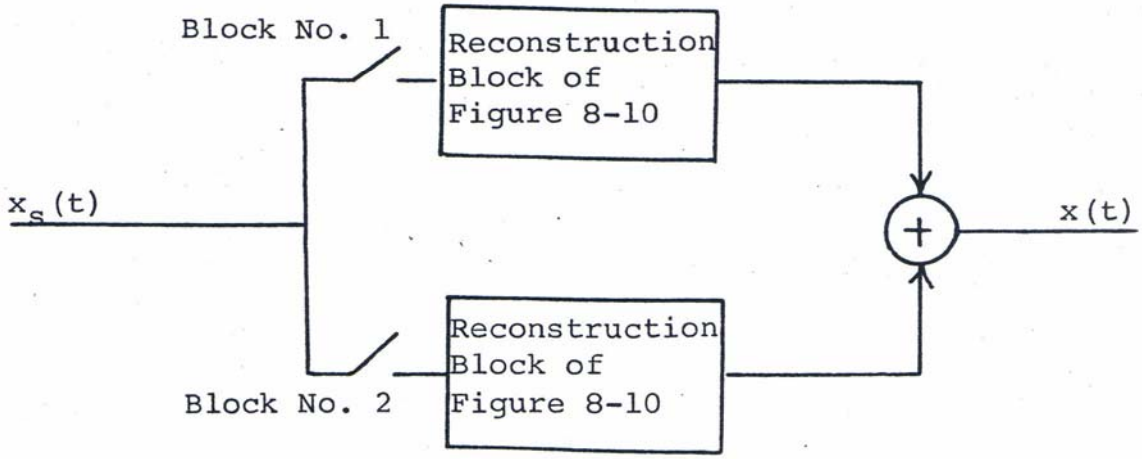

Figure 8-12: General Reconstruction for Any Nonuniform Samples

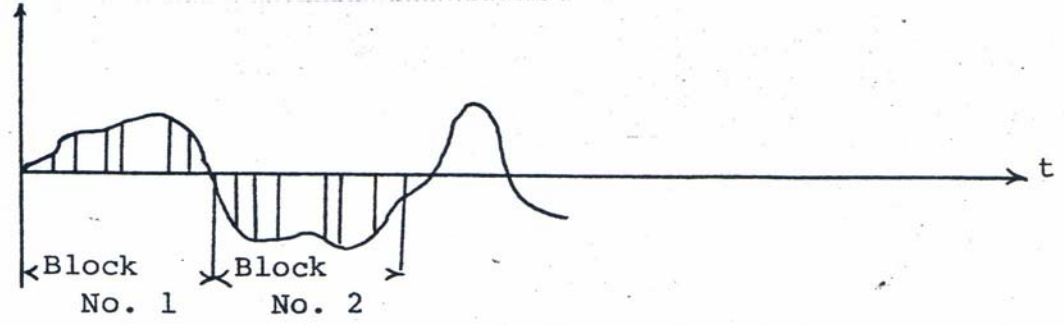

a.

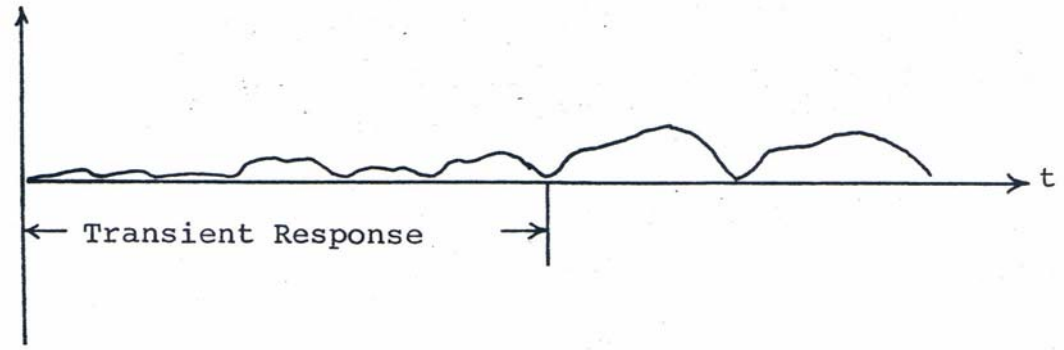

b. Output of Figure 5-10 for Block No. 1

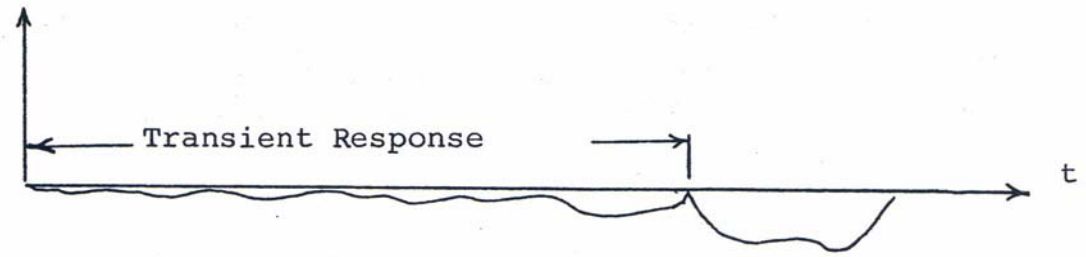

c. Output of Figure 5-10 for Block No. 2

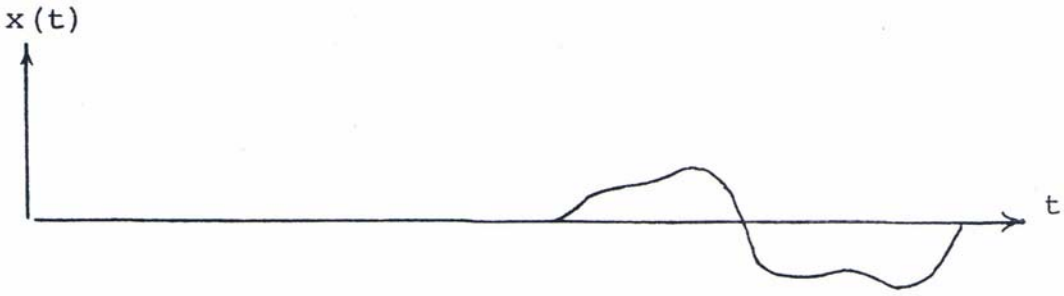

d. Output of Figure 8-12

Figure 8-11: Reconstruction of Nonuniform Samples Block by Block

This can be done by rearranging Equation 8-16 as follows:

$$t_o^{m-1} = \frac{t_m-(m-1)T}{x(t_m)} = \frac{\phi(t_m)}{x(t_m)} \qquad 8\text{-}22$$

where $\phi(t_m) = t_m-(m-1)T$. Equation 8-17 is redefined as in the following:

$$g(t) = \frac{\phi(t)\ x(t)}{y(t)} - (m-1)T \qquad 8\text{-}23$$

where $y(t_m) = x(t_m)$ and $y(t\neq t_m)\neq x(t) \Rightarrow g(t_m) = o$ and $g(t\neq t_m)\neq o$. $\phi(t)$ and $y(t)$ are plotted in Figures 8-13 and 8-14. $\phi(t)$ and $y(t)$ are chosen for minimum bandwidth (See Appendix A for details).

$$\dot{g}(t) = 1 - [\frac{\phi(t)}{y(t)} x(t)]'$$

where

$$\dot{g}(t_m) \neq o$$

thus,

$$x_s = A \sum_{m=o}^{\infty} \delta(t-t_m) = A\{1 - \frac{\phi(t)x(t)}{y(t)}]'\} \sum_{m=o}^{\infty} \delta[t- \frac{\phi x}{y} - (m-1)T]$$

where

$$[\frac{(t)x(t)}{y(t)}] < 1$$

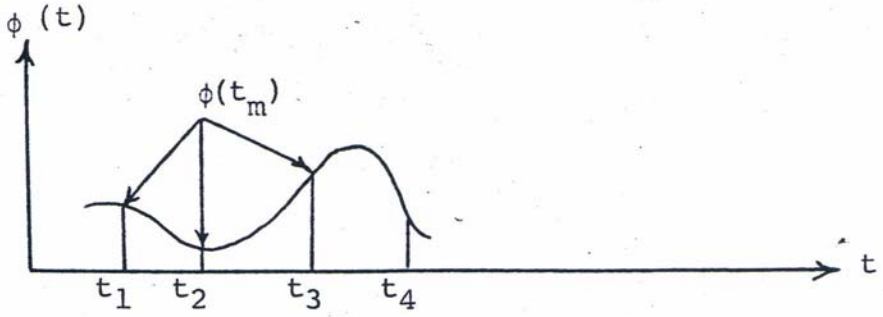

Figure 8-13: The $\phi(t)$ is chosen for Minimum Bandwidth (Appendix A)

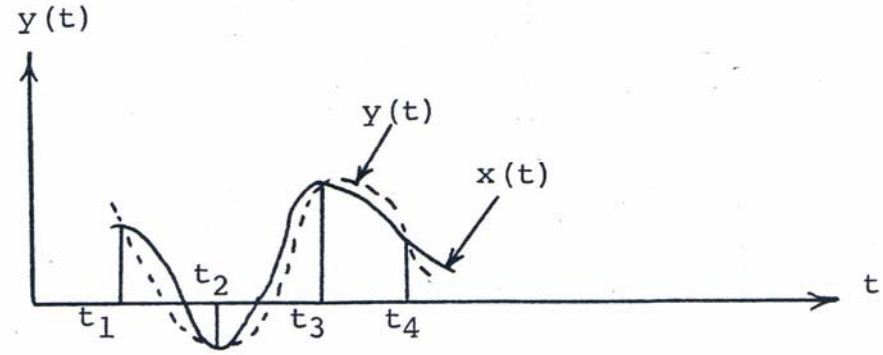

Figure 8-14: $y(t)$ is generated Such that $y(t_m) = x(t_m)$

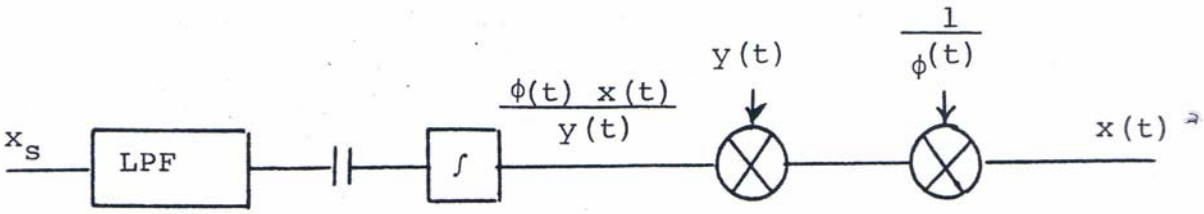

Figure 8-15: Reconstruction of Nonuniform Samples

thus,

$$x_s = A\,1 - \{[\frac{\phi(t)x(t)}{y(t)}]' \} \sum_{n=-\infty}^{\infty} e^{\frac{j2\pi n}{T}[t - \frac{(t)\cdot x(t)}{y(t)}]} \qquad 8\text{-}24$$

Assuming $\frac{\phi(t)x(t)}{y(t)}$ is bandlimited to W and $T \leq \frac{1}{2w}$, 8-25

there is no aliasing effect if x_s is low pass filtered at a cut off frequency of W. The block diagram of the reconstruction technique is depicted in Figure 8-15.

The zeros of y(t) are made as the zeros of ϕ (t) so that the function $\frac{\phi(t)x(t)}{y(t)}$ does not blow up at the zeros of y(t). y(t) is the estimated baseband signal that carries the amplitude information of the nonuniform samples ($y(t_m) = x(t_m)$) and ϕ (t) carries the time information of the nonuniform samples ($\phi(t_m) = t_m - (m-1)T$). Thus, if the function $\frac{\phi(t)x(t)}{g(t)}$ is a bounded and bandlimited function, the nonuniform samples can be exactly reconstructed by the above practical technique.

4. Improving Aliased Signals by Feedback Techniques

If the sampling rate is below the Nyquist rate, the frequency spectrum of the uniform samples are aliased (Figure 8-16). The original signal is approximated as follows:

$$X(f) = [X_s(f) - X(f-f_c) - X(f+f_c)] \times H(f) \qquad 8\text{-}26$$

where H(f) is the transfer function of a low pass filter with a passband equal to the bandwidth of the baseband signal (W). In time domain the equation is written as:

$$x(t) = (x_s - x \cos w_c t) * h(t) \qquad 8\text{-}27$$

x(t) is estimated and a new estimate of x(t) is found from the above equation. This iteration is repeated until the estimate of x(t) coverages to x(t). The iterative procedure is depicted in Figure 8-17. After the third iteration, the procedure converges into two stable states (Figure 8-17-e,f). The sum of these two states yield a better estimate of the original signal (Figure 8-16-g). A block diagram of the system is illustrated in Figure 8-18. Any iteration after x_4 will not change anything due to the symmetry of x_4.

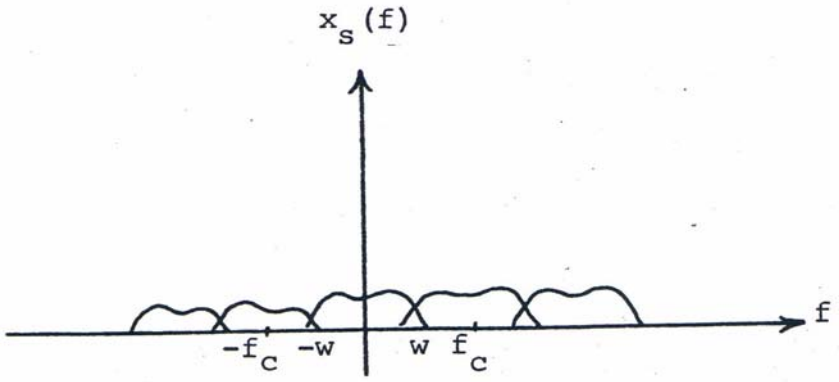

Figure 8-16: The Spectrum of Uniform Samples when the Sampling Rate is Below the Nyguist Rate.

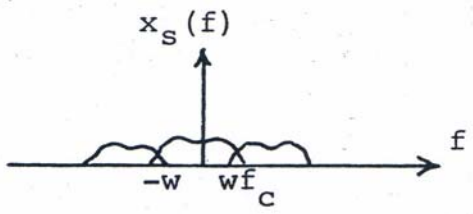

a. Aliased Samples

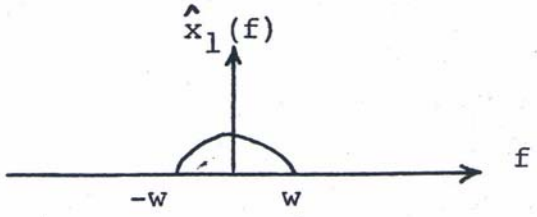

b. First Estimate of x(t)

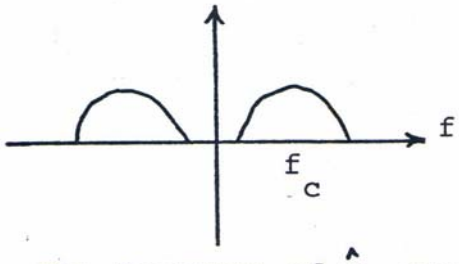

c. The Spectrum of $\hat{x}_1 \cos w_c t$

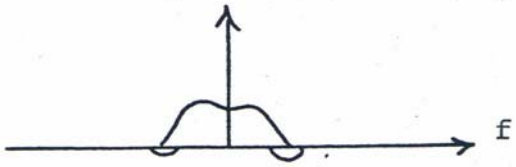

d. The Spectrum of $x_s - \hat{x}_1 \cos w_c t$

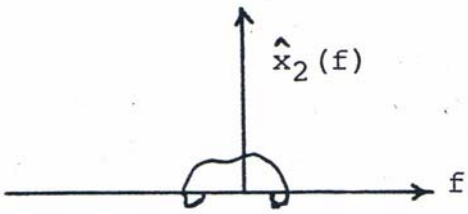

e. The Second Estimate of x(t)

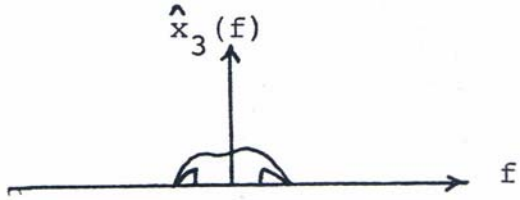

f. The Third Estimate of x(t)

$$\hat{x}_4 = \frac{\hat{x}_2 + \hat{x}_3}{2}$$

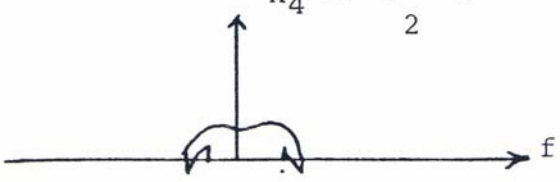

g. The Fourth Estimate of x(t)

Figure 8-17: Iteration Technique

The same procedure can be extended to nonuniform pulses derived by the intersection of two signals. The original signal is approximated from the Equation 4-7 and the reconstruction schemes shown in Section IV as follows:

$$1 + \frac{df}{dt}^{-1} [x(t)] = \{ x_s - \{ 1 + \frac{df}{dt}^{-1} [x(t)] \} \cos \{ \frac{2\pi t}{T} + f^{-1} [x(t)] \} \} * h(t)$$

where $h(t)$ is the impulse response of a low pass filter with a passband equal to the bandwidth of the baseband signal $\frac{df^{-1}[x(t)]}{dt}$. By an initial estimate of the random signal, $x(t)$, a better estimate can be found by an iterative procedure from the above equation. The block diagram of the iterative procedure is shown in Figure 8-19, which is similar to the feedback technique of uniform samples in Figure 8-18.

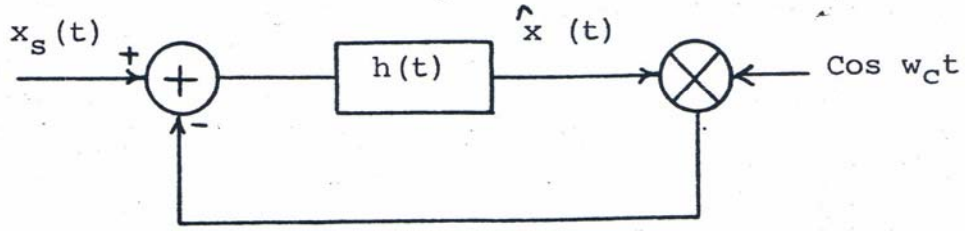

Figure 8-18: Improvement of an Aliased Signal

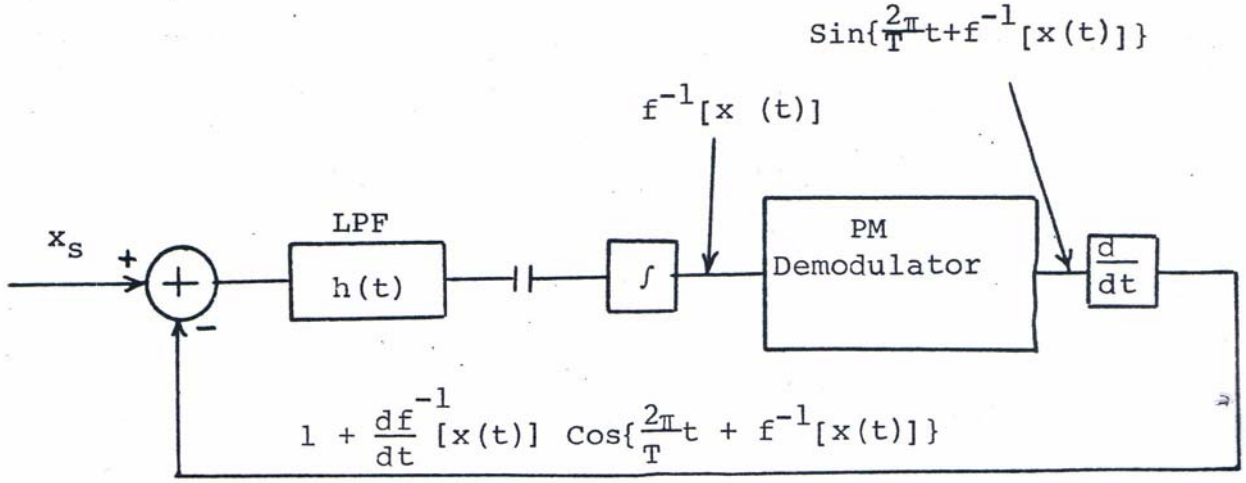

Figure 8-19: Reconstruction of an Aliased Signal for Nonuniform Pulses by a Feedback Technique

PART IX

EXPERIMENTAL RESULTS

1. Computer Program for the Adaptive Quantizer

The Adaptive Quantizer was simulated on a G.E. Pac. Computer. The simulated programme is depicted in page A signal is first sampled uniformly and then the intersectin levels are adapted on the samples. The closest sample to one of the levels is chosen as the intersecting sample.

Henc, the programme produces some quantization noise. The uniform samples of a signal and the intersecting samples found by the adaptive technique are shown in page .

The signal to noise ratios for the reconstruction of uniform and nonuniform samples using a zero order hold and low pass filtering were calculated on the G.E. Pac. Computer. The signal to noise ratio is the same for both uniform and nonuniform samples on the average.

Due to the limitation of the sampling rate of the A/D converter of the computer, together with the introduction of quantization error and phase jitter in the simulated Adaptive Quantizer, the computer simulation of the adaptive technique was abandoned for a circuit implementation.

```
* LI
          95  J=KK+1
* LI
              TYPE 'QA GOES TO F'
* DE
              CALL F
* END
← #
← SUBR AA
← LI
              SUBR AA
              DO 9 I=1,DD
              READ X,@B
              AM(I)=AD
           9  CONT
              END
← SUBR FD
← LI
              SUBR FD
              RM=O+[illegible]/MM
              CALL C
              RN=RM-MA/2
              CALL D
              IF (KQ-KK) 32,32,33
          33  L(KK)=LL(KK)
              O=L(KK)
              GO 35
          32  L(KQ)=SL(KQ)
              O=L(KQ)
          34  IF (KQ+2-DD) 35,36,36
              GO 38
          35  IF [illegible]
          30  IF (KP-KK) 33,33,[illegible]
          [illegible]
```

Computer Program for the

Adaptive Quantizer

```
          O=L(KK)
          GO 9
        4 L(KQ)=SL(KQ)
          O=L(KQ)
        6 IF (KQ+2-DD) 9,23,23
          GO 90
        9 IF (KK+2-DD) 90,23,23
       90 IF (KQ-KK) 93,93,95
       93 J=KQ+1
          CALL E
          GO 96
       95 J=KK+1
          CALL F
          GO 96
       23 CALL H
       96 CONT
          RETU
          END
← SUBR TA

← LI

          SUBR TA
          DO 8 M=1,DD
          TYPE AM(M)
        8 CONT
          END
← SUBR ZA

← LI

          SUBR ZA
          DO 7 I=1,DD
          SL(I)=0
          AM(I)=0
          L(I)=0
          LL(I)=0
        7 CONT
          END
← SUBR A

← LI

          SUBR A
          O=MA/2
          M=1
          X=AM(M)-O
          X=AM(M+1)-O
          IF (O-Y) 39,2,49
       49 Y=-Y
       39 IF (O-X) 59,1,59
       69 X=-X
       59 IF (X-Y) 1,1,2
        1 P=X
          K=0
          GO 3
        2 P=Y
          K=1
        3 CONT
          J=3
          CALL B
          RETU
          END
```

```
      SUBR B
      DO 92 M=J,J+NJ
      Z=AM(M)-C
      IF (0-Z) 24,6,27
27    Z=-Z
24    IF (P-Z) 6,6,7
 6    P=P
      GO 92
 7    P=Z
      K=M
92    CONT
      L(K)=AM(K)
      J=K+1
      RETU
      END
```

← SUBR C

← LI

```
      SUBR C
      NQ=0
      IF (J+NJ-DD)      76,76,78
78    PO=DD
      GO 74
76    PO=J+NJ
74    CONT
      DO 50 M=J,PO
      IF (AM(M)-RM) 10,20,20
10    NQ=NQ+1
      GO 50
20    CONT
50    CONT
      IF (NQ+J-PO-1) 30,40,40
40    KQ=PO
      GO 60
30    CONT
      P=AM(J)-RM
      KQ=J
      ID (0-P) 55,80,77
77    P=-P
55    DO 70 M=J+1,PO
      Z=AM(M)-RM
      IF (0-Z) 87,67,29
29    Z=-Z
87    IF (P-Z) 80,80,67
80    P=P
      GO 70
67    P=Z
      KQ=M
70    CONT
      CL(KQ)=AM(KQ)
60    CONT
      RETU
      END
```

← SUBR B

← LI

```
      SUBR D
      NQ=0
      IF (J+NJ-DD) 37,37,46
41    PI=DD
      GO 36
```

```
37  CONT
    DO 51 M=J,PT
    IF (AM(M)-RN) 21,21,11
11  NQ=NQ+1
    GO 51
21  CONT
51  CONT
    IF (NP+J-PT-1) 31,41,31
41  KK=PT
    GO 61
31  CONT
    P=AM(J)-RN
    KK=J
    IF (O-P) 64,31,88
88  P=-P
64  DO 71 M=J+1,PT
    Z=AM(M)-RN
    IF (O-Z) 99,91,98
98  Z=-Z
99  IF (P-Z) 81,81,91
81  P=P
    GO 71
91  P=Z

    K

     K=M
71  CONT
    LL(KK)=AM(KK)
61  CONT
    RETU
    END
← SUBR E

← LI

    SUBR E
    RN=O-MA/MN
    CALL D
    RM=RN+MA/2
    CALL C
    IF (KQ-KK) 22,22,33
33  L(KK)=LL(KK)
    O=L(KK)
    GO 35
22  L(KQ)=LL(KQ)
    O=L(KQ)
32  IF (KQ+O-DD) 35,36,3[illegible]
    GO 37
35  IF ([illegible]) 37,[illegible],[illegible]
37  IF ([illegible]) 45,[illegible],5[illegible]
45  J=[illegible]+1
    CALL [illegible]
[illegible]
    CALL [illegible]
    GO [illegible]
    CALL [illegible]
[illegible]
    RETU
    END
← [illegible]
```

```
      RM=0+MA/MN
      CALL C
      RN=RM-MA/2
      CALL D
      IF (KQ-KK) 12,12,13
13    L(KK)=LL(KK)
      O=L(KK)
      GO 14
12    L(KQ)=SL(KQ)
      O=L(KQ)
24    IF (KQ+2-DD) 14,15,15
      GO 16
14    IF (KK+2-DD) 16,15,15
16    IF (KQ-KK) 17,17,18
17    J=KQ+1
      CALL E
      GO 25
18    J=KK+1
      CALL FD
      GO 25
15    CALL H
25    CONT
      RDTU
      END
```

← SUBR H

← LI

```
      SUBR H
      DO 11 I=1,DD
      TYPD L(I)
11    CONT
      END
```

← SUBR W

← LI

```
      SUBR W
      DO 88 K=1,DD
      L(K)=0
88    CONT
      END
```

← C

```
CALL TA

 -72
 -61
 -38
 -3
 22
 49
 67
 71
 61
 39
 9
 -23
 -50
 -68
 -72
 -62
 -39
 -10
 21
 48
 66
 71
 62
 40
 10
 -22
 -50
 -67
 -72
 -62
 -40
 -11
 20
 47
 66
 71
 [illegible]
 41
 11
 -[illegible]
 -[illegible]
 -[illegible]
 -72
 -[illegible]
 [illegible]
 -11
 [illegible]
 [illegible]
 [illegible]
 [illegible]
```

Uniform Samples Representing the Random Signals x(t)

-22
-50
-67
-72
-62
-40
-11
20
47
66
71
62
41
11
-22
-50
-63
-72
-62
-40
-11
20
47
66
71
62
41
11
-22
-50
-67
-72
-62
-40
-11
20
47
66
71
62
41
11
-22
-50
-67
-72
-62

,NQ=5
QA GOES TO F
C,NQ=6
F,RN=-16RM=44
F,KK=9SL(KK)=-22
F GOES TO FD
C,NQ=4

0
0
0
0
0
0
0
0
61
39
0
-23
0
0
0
0
0
-10
0
48
0
0
0
40
0
-22
0
0
0
0
0
-11
0
47
0
0
0
41
0
-22
0
0
0
0
0
-11
0
47
0
0
0
-1
0
-22
0
0

The Nonuniform Samples Derived from the Random Signal, x(t), by the Adaptive Quantizer

Nyguist Rate = 15 Samples/100

27 Samples out of 100

```
47
0
0
0
41
0
-22
0
0
0
0
0
-11
0
47
0
0
0
41
0
-22
0
0
0
0
0
-11
0
47
0
0
0
41
0
-22
0
0
0
0
```

2. Selected Experimental Verification of the Intersection Technique

a. Procedure

From the theoretical point of view, we have shown that sampling at the intersection of a random signal and any periodic wave will result in the original signal after intergration, low pass filtering and appropriate inverse transformations. The information lies in the zero crossing of the nonuniform samples that have fixed amplitudes. An experimental set up, to check various selected aspects of the intersection problem is depicted in Figure 9-1 and 9-2 using a periodic waveform.

The output of the transmitter is the integral of the alternate positive and negative impulses. The frequency of the periodic wave is, hence, twice the Nyquist rate (See Section IV-1-6).

In the actual experiment, a triangular and sine waveform has been used for the periodic signal in Figure 9-1. The level of the Schmitt trigger can be varied from zero all the way to the highest amplitude of the periodic waveform.

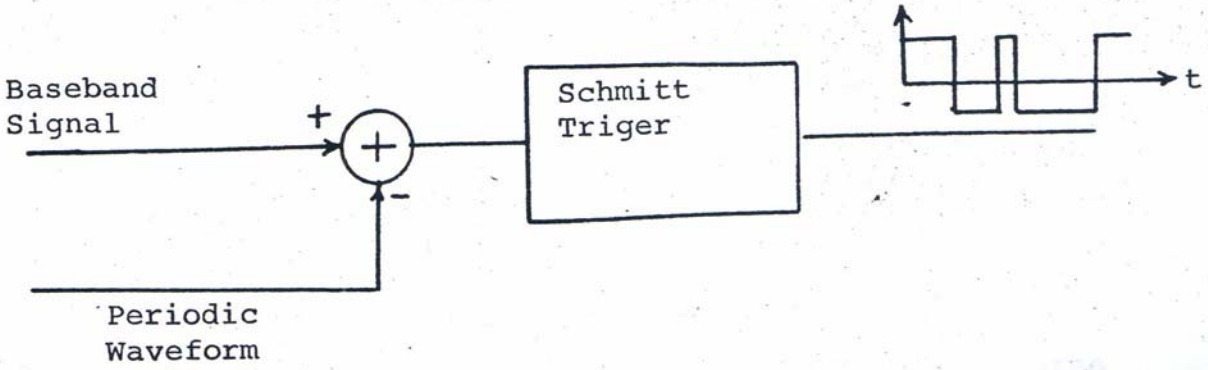

Figure 9-1: Transmitter

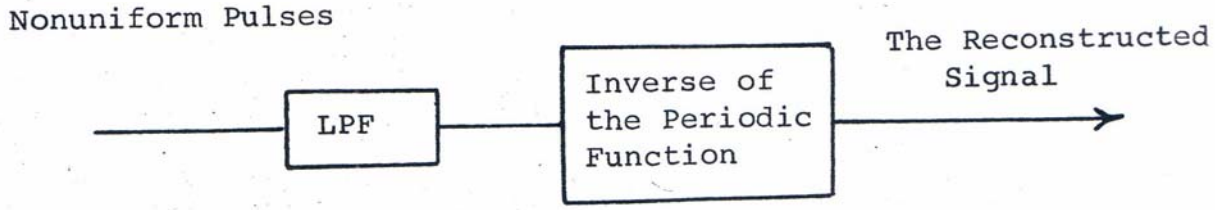

Figure 9-2: Receiver

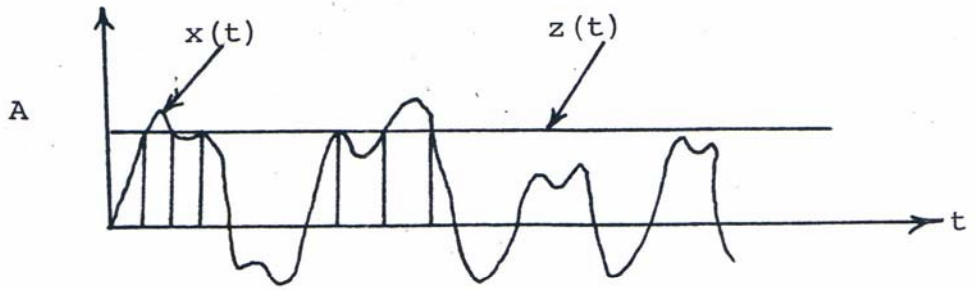

Figure 9-3: Sampling at Level A

If the amplitude of the sine wave is high enough (as a result its slope is large enough so that the condition $\uparrow t_o \dot{x} | < 1$ is satisfied (Section IV-1-c), then the sine of an angle is approximately equal the angle in radians. Thus, the inverse transform at the receiver is just a gain factor. But if the threshold is at a high level, the curvature of the sine and the missing samples are the cause of distortion (Figure 9-3). This phenomenon has been verified experimentally. The triangular wave has a better performance than the sine wave at high level thresholds due to lack of curvature. The analysis of the samples at high level thresholds is similar to the zero crossing analysis.

Nonuniform PPM, being the product of a sawtooth generator, resembles our case with the exception that the impulses cannot be integrated first and then low pass filtered. The output of the Schmitt trigger resembles a pulse duration modulation (PDM) of the transmitted impulses. PDM is for uniform samples but the above modulation is for nonuniform samples.

b. Experimental Data and Results

The baseband signal can be any bandlimited signal.

In the experiment, both a deterministic and an audio signal has been used. The original signal and the reconstructed signal can be compared either on an oscilloscope or they can be recorded on a paper and have a visual comparison. Due to the lack of availability of high speed recorders at the time of experimentation, there are two other alternatives for the comparison of voice signals. One method is to take a snap shot of the original signal and the reconstructed signal on the scope. The second method is to listen to both voice signals and have a subjective comparison. Some experimental results for the subjective comparison of the voice signals are given in Table 9-1. A tape for the subjective analysis of human voice is included with the dissertation.

Type of the Periodic Signal	Ratio of Sine Amplitude over input Signal	Sampling Rate	Cut Off Frequency of the Reconstruction Low Pass Filter	Comments Based on Listening to the Voice Reconstructed Voice
1. Sinusoidal Threshold at Zero	4	5 KHz	1 KHz	Voice is intelligible but noisy
2. Sinusoidal Threshold at Zero	4	5 KHz	2 KHz	Clearer but noisy
3. Sinusoidal Threshold at Zero	4	10 KHz	2 KHz	Clearer but noisy
4. Sinusoidal Threshold at Zero	4	15 KHz	4 KHz	Perfectly clear plus background noise
5. Sinusoidal Threshold is not at Zero	4	15 KHz	4 KHz	Voice is Slightly Distorted.
6. Triangular Threshold at Zero	3 to 4	4 KHz	1 KHz	Very Clear plus background noise
7. Triangular Threshold not at Zero	3 to 4	4 KHz	1 KHz	Very clear plus background noise
8. Triangular Threshold not at Zero	3 to 4	8 KHz	4 KHz	Clear plus a Periodic hum
9. Triangular Threshold not at Zero	3 to 4	15 KHz	4 KHz	Clear Noise is reduced
10. Triangular Threshold not at Zero	3 to 4	20 KHz	4 KHz	Clear less noisy

In general, better results have been obtained with a triangular wave than a sinusoidal wave. This can be explained from the fact that, from the theoretical point of view, there is a need for an inverse transform of sine wave while the triangular wave can be reconstructed ideally by low pass filtering. The parameters that affect the experimental results are as follows:

1. Volume of the input signal
2. Amplitude of the periodic waveform
3. The period of the periodic waveform (sampling rate)
4. The pass-band of the low pass filter
5. The threshold level
6. Type of the periodic waveform

The reason for getting a periodic hum, in addition to the voice signal when sampling at the Nyquist rate (#8 in Table 9-1) is due to the fact that the input of the low pass filter is a square wave. So if the bandpass of the low pass filter is large enough, the principal harmonic will pass through the filter and hence causing background hum. If we place the threshold level at the top of the amplitude of the periodic waveform, the hum disappears since there are no samples when there is no voice signal.

3. The Circuit Realization of the Adaptive Quantizer and Some Experimental Results

a. Hardware Realization

There are many ways to show the validity of the ideas mentioned in Section V-2. The easiest method is to sketch a curve and apply the adaptive technique on the curve to get nonuniform samples as described in Section V-2-a. The second method is the computer simulation of the Adaptive Quantizer (Section IX-1). Another method is the actual circuit realization of the Adaptive Quantizer. The block diagram of the two level Adaptive Quantizers is illustrated in Figure 9-4. As it can be noticed, the circuitry is easy to implement and econmical. The adaptive quantization levels is either moving upward or downward. If it is going upward, adder A is (a-1) and adder B is -1 otherwise adder A is 1 and adder B is (1-a). In the actual circuit realization of the block diagram of Figure 9-4 four adders are used (Figure 9-5). The block diagram depicted in Figure 9-4 works as follows: To start with, the upper quantization level q_u is set at (a-1), and the lower level q_L at -1. q_u and q_L are compared to the signal by the comparators A and B, respectively.

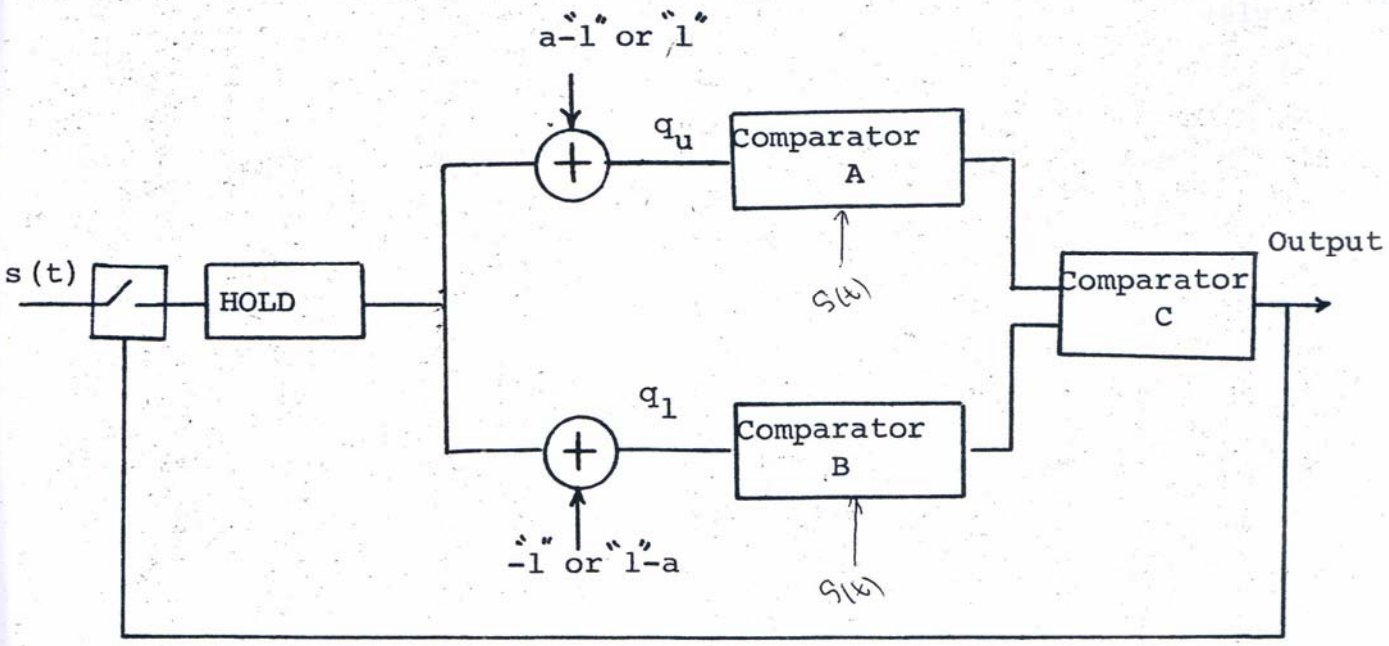

Figure 9-4: Adaptive Quantizer at the Transmitter

The Parameters, a and "1", are Defined in

Figure 5-1

As soon as one of the levels intersects the signal, the switch of the sample and hold closes, and a new sample is generated and is hold. The new q_u and q_l are found by adding (a-1) and -1 to the amplitude of the new sample, respectively. If q_l intersects the signal first, q_u and q_l are found by adding 1 or(1-a) respectively. The block diagram of the receiver is depicted in Figure 9-6. At the receiver the analog samples are reconstructed from the transmitted positive and negative pulses.

b. Experimental Results

The circuit depicted in Figure 9-5 was actually built and tested sucessfully. This circuit can accept any signal as long as its bandwidth is in the range of 0-8 KHz. The average samples per second depends on the parameters of the Adaptive Quantizer, a and 1, is tabulated in the Table 9-2 and depicted in Figure 9-7 through 9-17.

	Input Signal	Frequency	Amplitude	l	a=	Average Samples Per Period
Figure 9-7	Sine Sign	1 K Hz	± 1 volt	.8	"l"/2= .4	8.5 samples per period
Figure 9-8	Sine Sign	1 K Hz	± 1 volt	.9	"l"/2= .45	6.5 samples per period
Figure 9-9	Sine Sign	1 K Hz	± 1 volt	1.0	"l"/2= .5	4.25 samples per period
Figure 9-10	Sine Sign	1 K Hz	± 1 volt	1.1	"l"/2= .55	4 samples per period
Figure 9-11	Sine Sign	1 K Hz	± 1 volt	1.4	"l"/2= .7	2 samples per period
Figure 9-12	Sine Sign	1 K Hz	± 1 volt	1.4	.5	4 samples per period
Figure 9-13	Sine Sign	1 K Hz	± 1 volt	1.4	.25	4 or 2 samples per period depending on the initial condition
No figures shown	Sine Sign	1 K Hz	± 1 volt	1.4	.2	2 samples per period
Figure 9-14	Triangular	1 K Hz	± 1 volt	.2	"l"/2= .1	26 samples per period
Figure 9-15	Triangular	1 K Hz	± 1 volt	.6	"l"/2= .3	8 samples per period
Figure 9-16	Triangular	1 K Hz	± 1 volt	1.6	"l"/2= .8	4 samples per period
Figure 9-17	Triangular	1 K Hz	± 1 volt	1.8	"l"/2= .9	2 samples per period
No figures shown	Triangular	1 K Hz	± 1 volt	1.8	0 < a < .9	2 samples per period
No figures shown	Triangular	2 K Hz	± 1 volt	1.8	.9	2 samples per period
No figures shown	Triangular	3 K Hz	± 1 volt	1.8	.9	2 samples per period
No figures shown	Any Signal	Any frequency	Increasing the amplitude is similar to decreasing a and l proportionally			Table 9-2

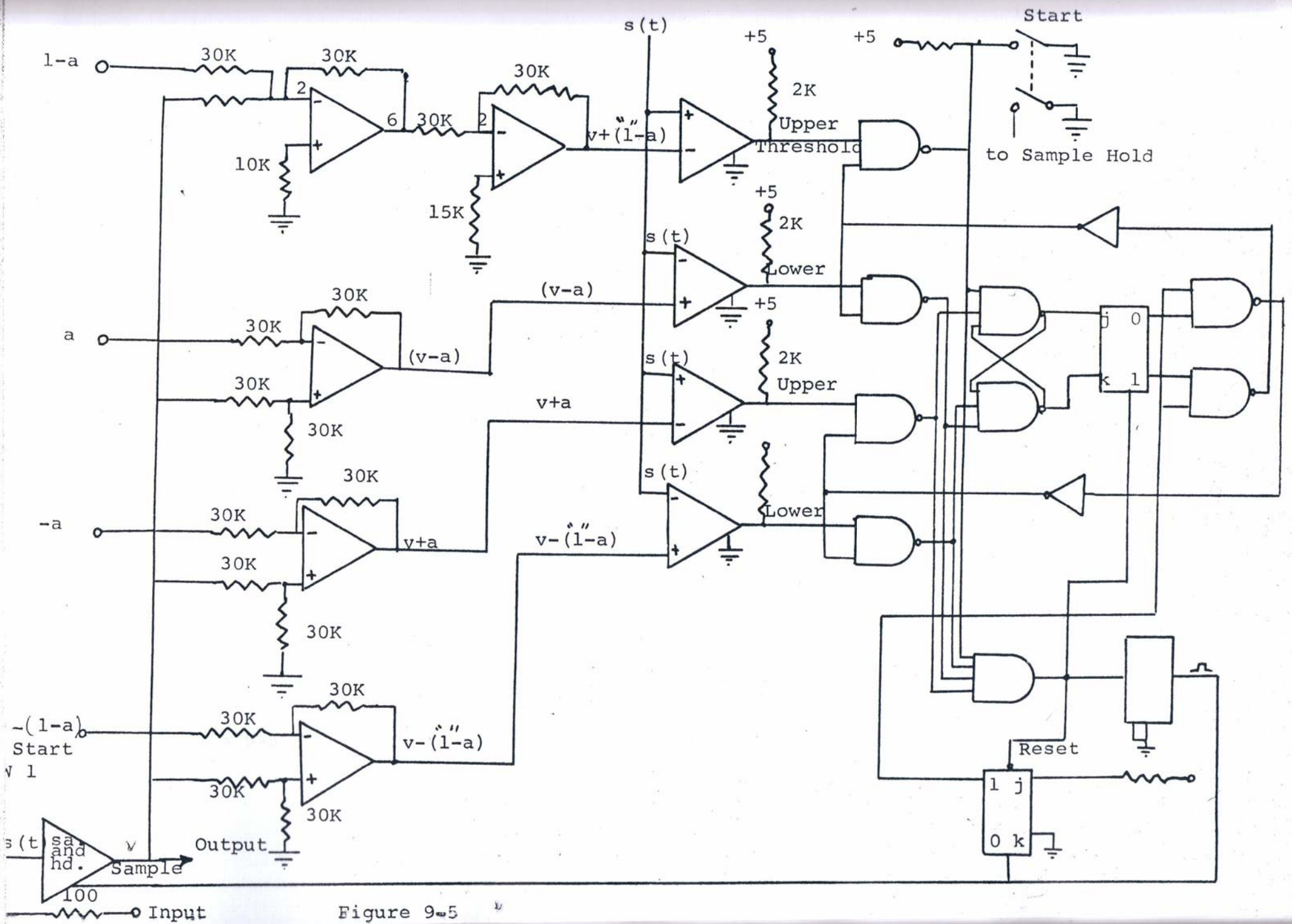
1-a
30K
30K
30K
2
6
10K
15K
v+(1-a)
s(t)
+5
2K
Upper
Threshold
Start
to Sample Hold
Lower
a
(v-a)
v+a
-a
v-(1-a)
-(1-a)
Start
Reset
Output
Sample
100
Input
s(t) sa and hd.

Figure 9-5

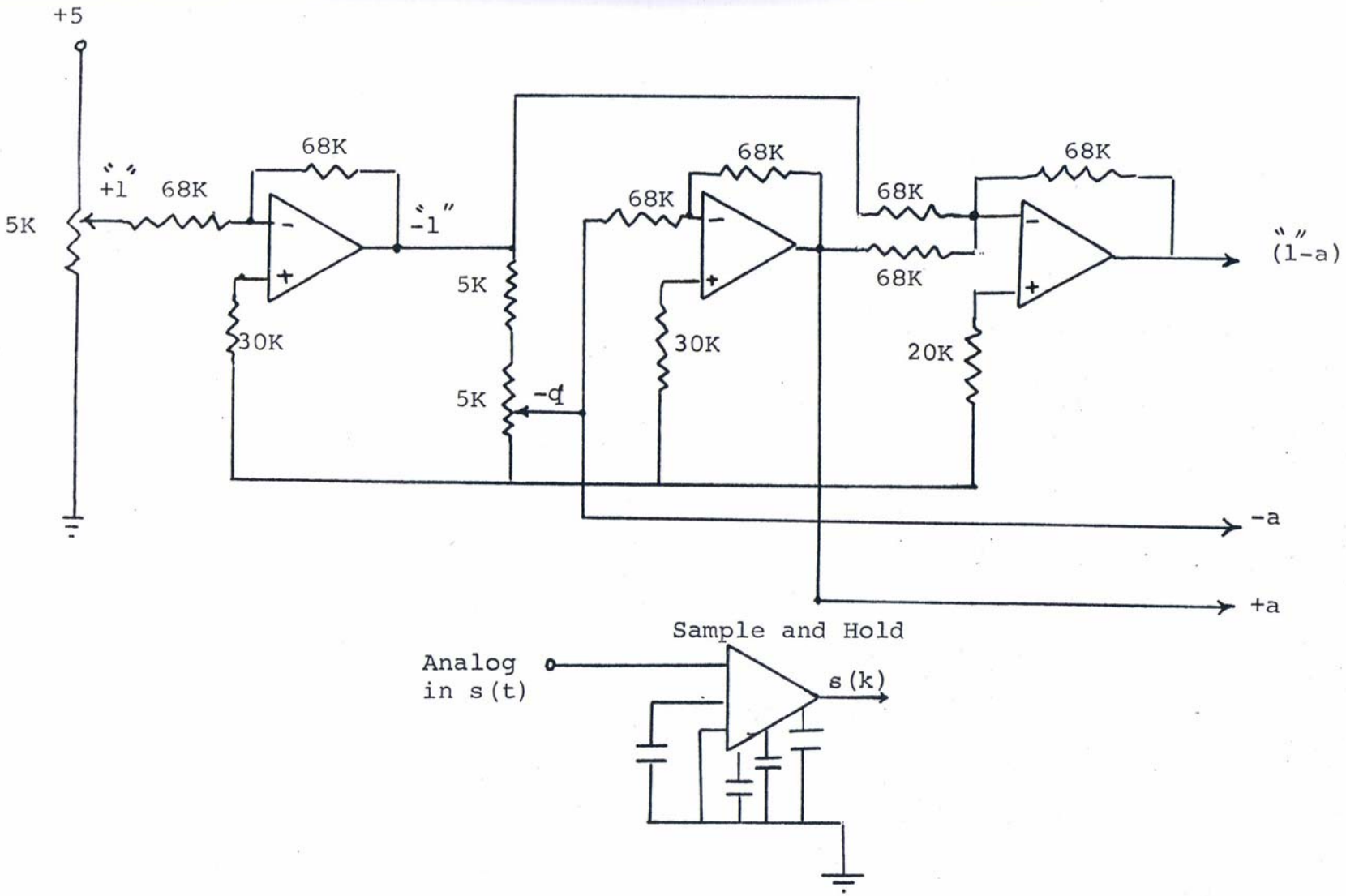

Figure 9-5 (Continued): The Circuit Implementation of the Adaptive Quantizer

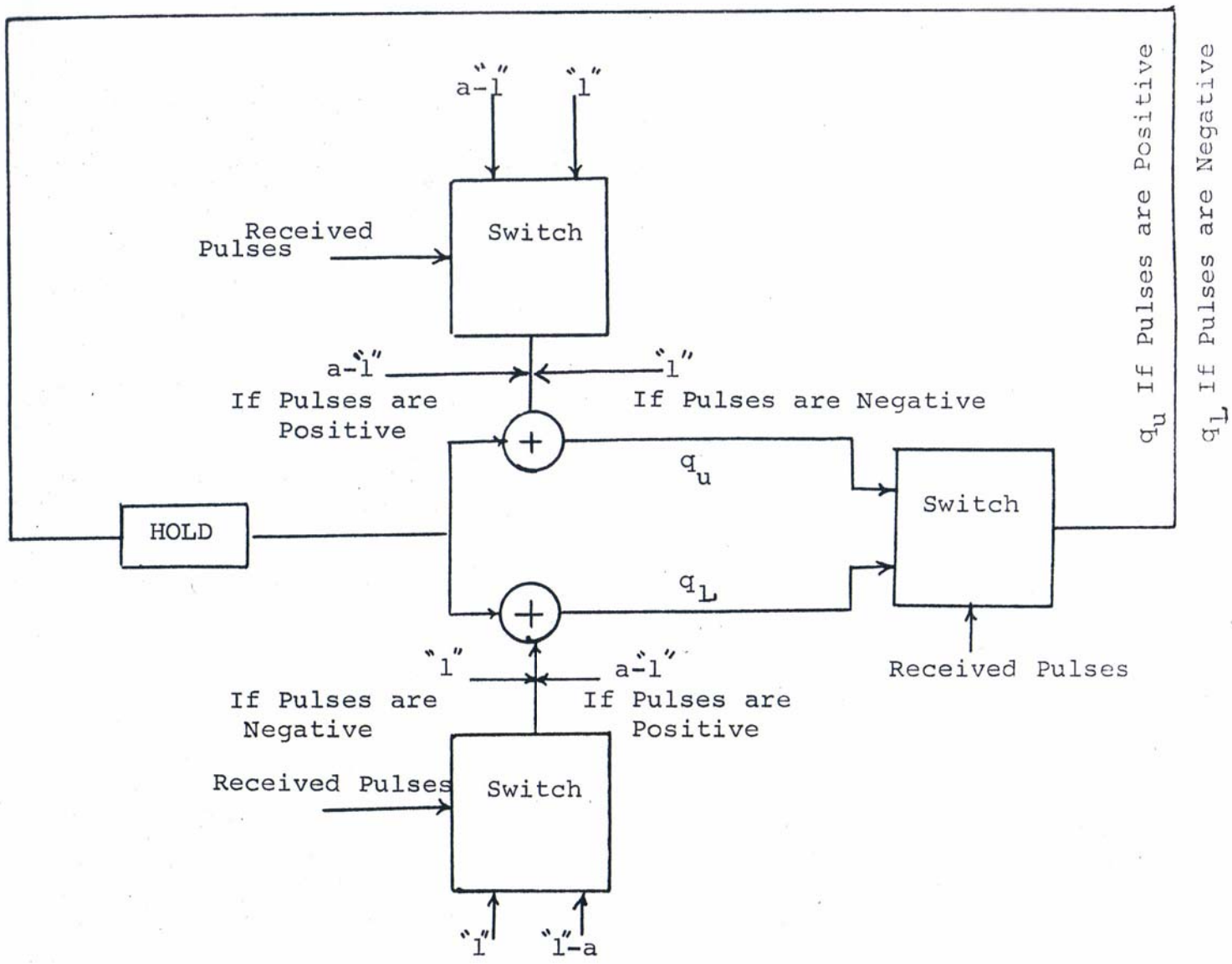

Figure 9-6: Reconstruction of the Analog Samples at the Receiver

For a Detailed Description of the Pictures, See Table 9-2

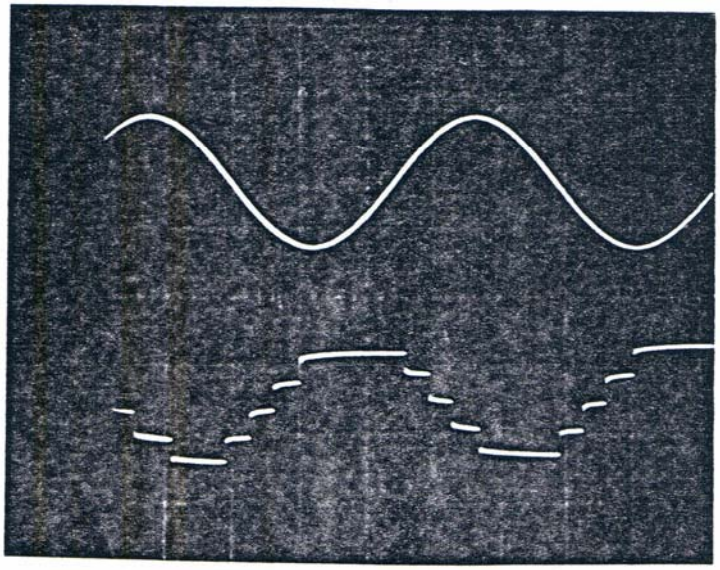

1

Figure 9-7: The Input Signal and the Nonuniform Samples Derived by the Adaptive Quantizer $a = \frac{"1"}{2} = .4$

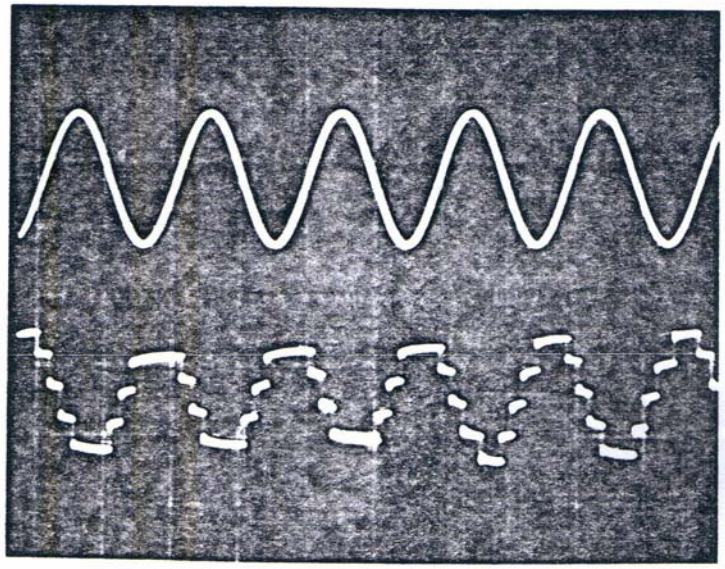

Figure 9-8: $a = \frac{"1"}{2} = .45$

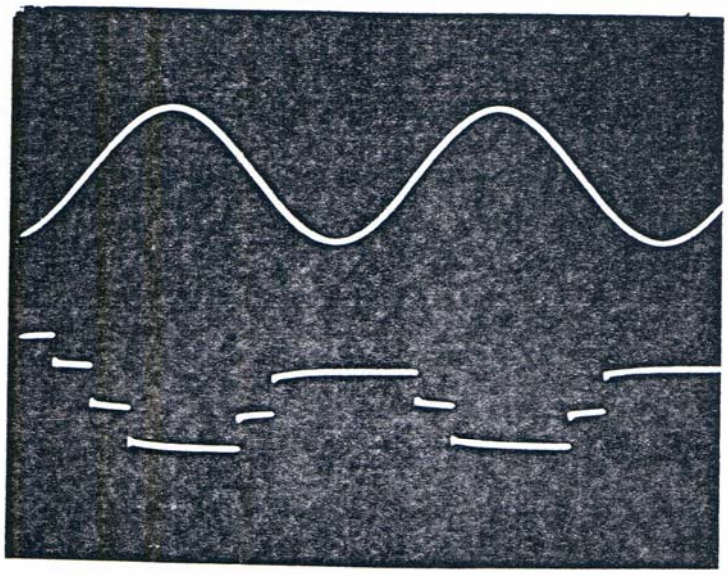

3

Figure 9-9: a = "$\frac{1}{2}$" = .5

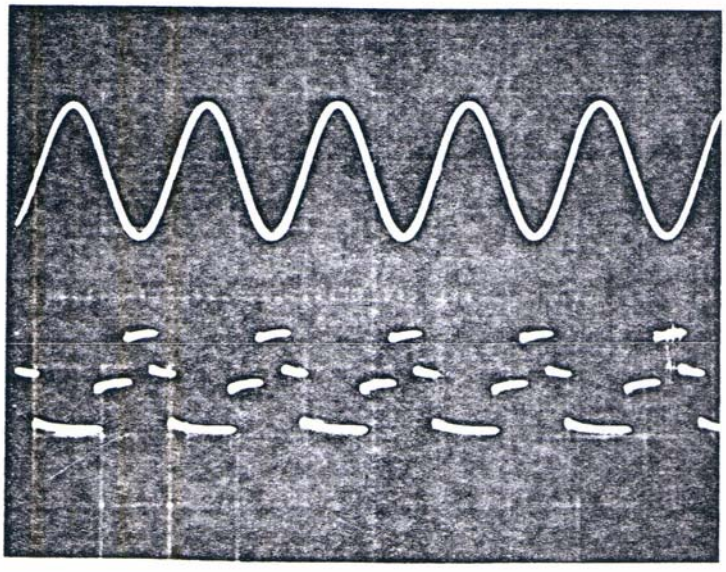

Figure 9-10: a = "$\frac{1}{2}$" = .55

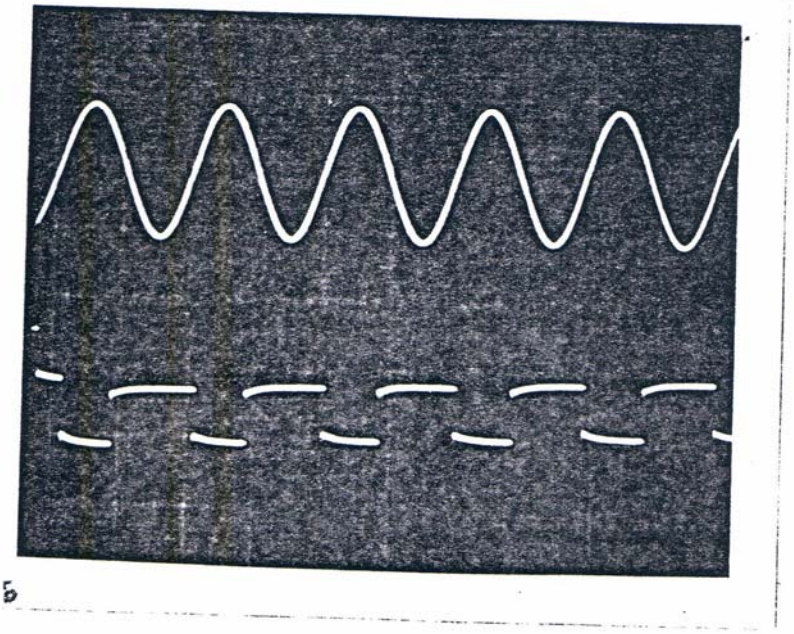

Figure 9-11: a = $\frac{1}{2}$ = .7

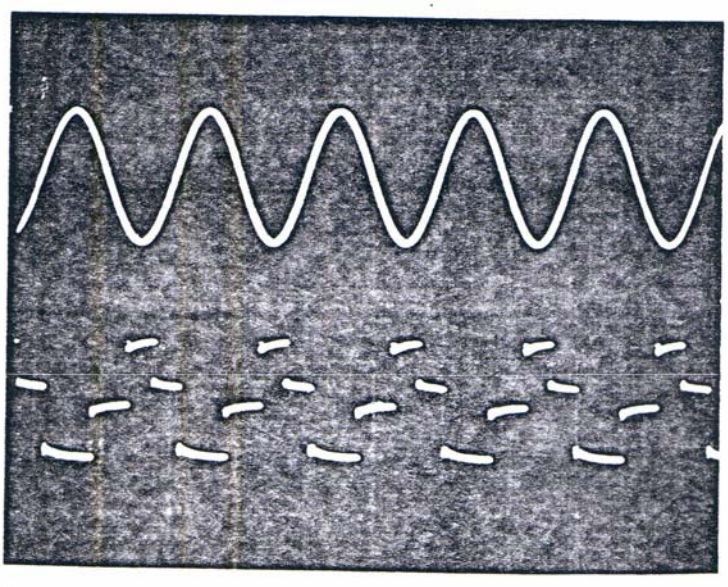

Figure 9-12: $\frac{1}{2}$ = .7 a = .5

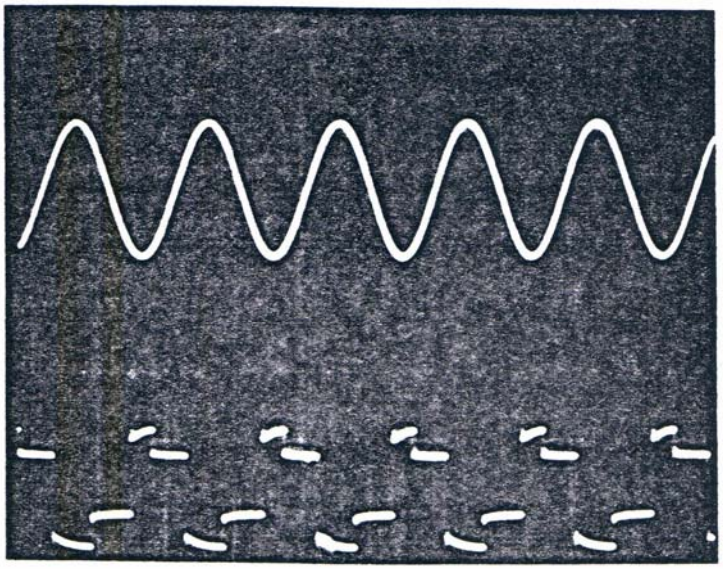

Figure 9-13: $\frac{\text{"1"}}{2} = .7 \quad a = .25$

Depending on the Initial Condition,

either 2 or 4 Samples per Period

are Produced

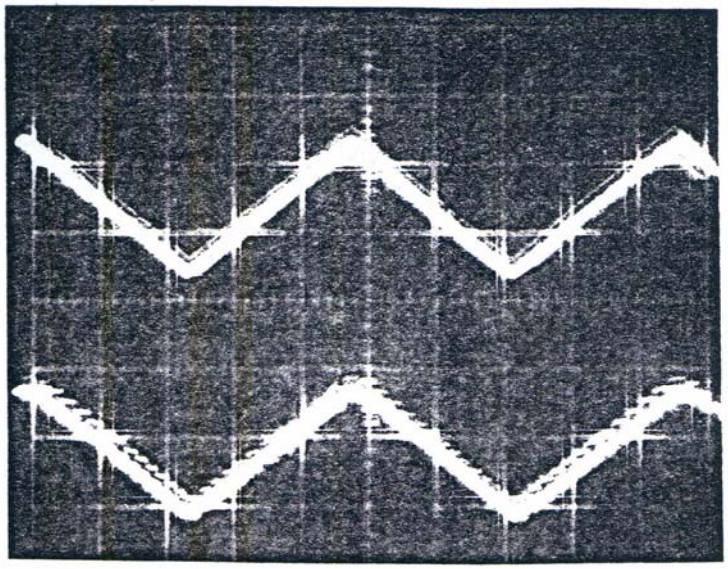

Figure 9-14: $a = \frac{1}{2} = .1$

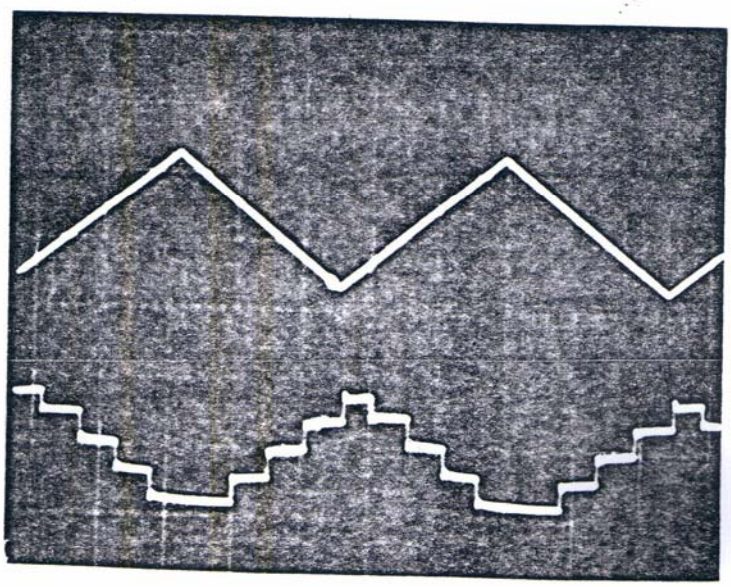

Figure 9-15: $a = \frac{1}{2} = .3$

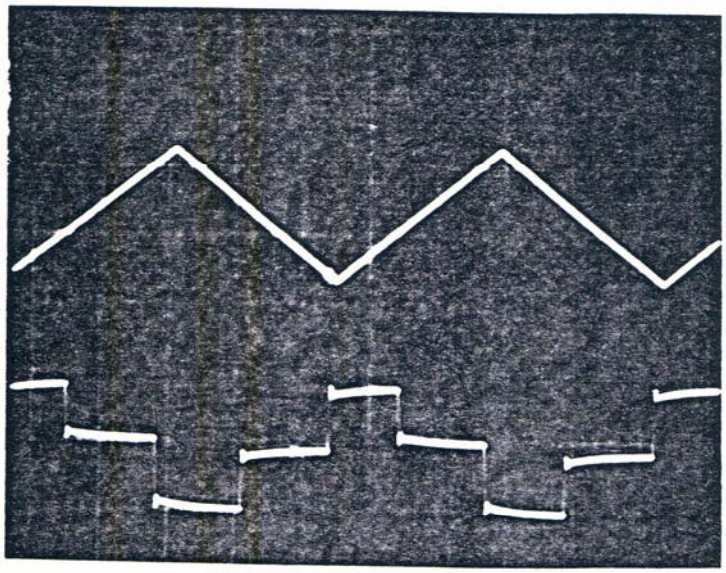

Figure 9-16: $a = \frac{\text{"1"}}{2} = .8$

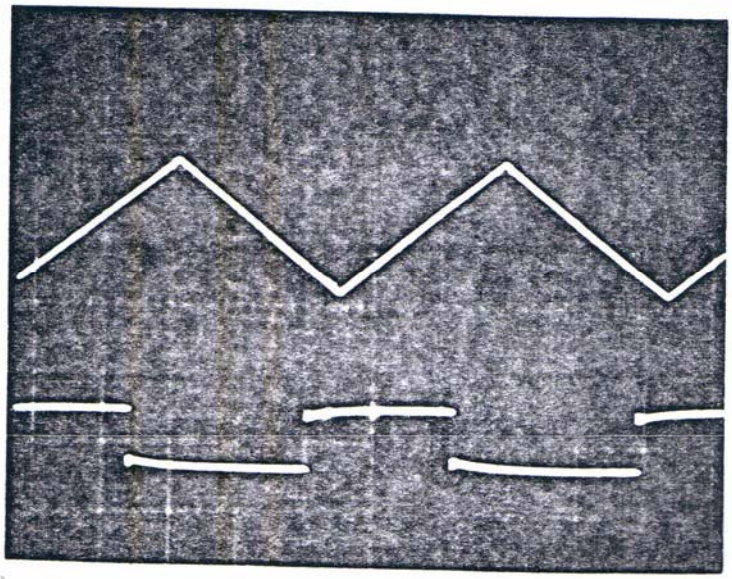

Figure 9-17: $a = \frac{\text{"1"}}{2} = .9$

Figures 9-7 through 9-13 show the adaptive technique on a sine wave. As "l" increase and the ratio a/l remains constant, the average number of samples per period decreases. The exact numbers are given in Table 9-2. When "l" remains constant and "a" changes, the average number of samples per period remans the same or is doubled depending on the initial conditions, (Figure 9-12 and 9-13). Figures 9-14 through 9-17 show the adaptive technique on a triangular wave. As "l" increases, and the ratio a/l remains constant, the average number of samples per period decrease (Table 9-2)

In summary, Section IX-1 and IX-3 show that the Adaptive Quantizer discussed in Section V is practical and the results are promising. Section IX-2 verifies the intersection theory for the intersection of voice signals with periodic waveforms. The experimentation proves the feasibility of designing simple encoders that transmit digital information at one bit per sample at equal or less than the Nyquist rate with a simple reconstruction technique at the receiver.

PART X

CONCLUSION AND RECOMMENDATIONS

Different pulse time modulations can be viewed as the intersection of a random signal with a deterministic signal. The deterministic signal can be a periodic, non-perioic, adaptive or a function of the random signal. If the intersections produce one pulse per interval, the train of pulses can be analyzed by a Fourier series expansion. The analysis shows that the baseband signal can be reconstructed from the nonuniform pulses by either lowpass filtering, integration and appropriate inverse transformation or by bandpass filtering and PM demodulations. The first technique is easier to implement while the second method takes advantage of the noise immunity of PM signals due to bandwidth to noise reduction. Using intersection techniques, transmission is at one bit per sample at equal or less than the Nyquist rate with no quantization error in the sampler. Noise analysis shows that if the amplitude of noise is small compared to the transmitted pulses, the intersection modulated pulses have the same noise immunity as angle modulated techniques.

Different intersecting deterministic signals have been analyzed. The zero and level crossings for a Gaussian signal were discussed. A novel technique was developed in the same section for fixed quantization levels. The transmission rate is at one bit per sample. The receiver consists of a low pass filter and an integrator. The periodic signals as intersecting waves can all be regarded as the intersection of a sawtooth or a triangular wave with a function of the random signal. That function is the inverse of the periodic wave. Hence, the spectrum and noise analysis of nonuniform PPM holds for periodic signals with some modifications. A comparison of different periodic signals was discussed based on the ease of reconstruction.

Intersection with adaptive signals were analyzed from both the adaption and intersection point of view. A novel Adaptive Quantizer was discussed in full. It has the advantages of one bit per sample transmission, and zero quantization noise. Also the active regions (high frequency content) of random signal, $x(t)$, are sampled more frequently than the passive regions (low frequency content). This characteristic

allows reduction of transmission time by any kind of run length coding. The Adaptive Quantizer compares favorably to other adaptive techniques. An actual circuit was successfully built and tested.

A modified asynchronous delta modulator and pulse frequency modulation were discussed and analyzed as the intersection of two signals. The intersection point of view was expanded to other unique modulation techniques such as flipping and the intersection of a signal with its derivative.

One of the main advantages of intersection pulse modulations, besides its noise immunity, is time domain multiplexing.

The pulse time modulations viewed as the intersection of two signals can also be regarded as the zero crossings of an angle modulated signal. At the same time exponential modulated signals can be viewed as the intersection of two signals. The zero crossings of FM, PM, PSK, and FSK were analyzed from the intersection point of view and some reconstruction methods were proposed.

Although the reconstruction from the intersection point of view is satisfactory in many cases, some conditions may not be satisfied and hence the general nonuniform sampling

reconstruction has to be considered. The standard and some original reconstruction methods were discussed.

Experimentally, the intersection of voice signals with triangular and sinusoidal waves verifies the mathematical analysis for the intersection technique. The computer simulation and the circuit realization of the Adaptive Quantizer verified the feasibility and the intuitive observations of the technique.

Due to the generality ofthe intersection techniques, a broad range of topics in digital communication, biomedical engineering and automatic control were included. Naturally, quality was sacrifieced for the sake of quantity. Therefore, I recommend for future work a deeper analysis of the intersection techniques. The noise and spectrum analysis of the distortion of the reconstruction techniques remain to be discussed further.

Different algorithms have to be studied for the adaptive techniques for the optimizationof the transmission rate.

The ideas developed in Section VIII regarding nonuniform sampling reconstruction have to be implemented and tested experimentally. More experimental results can lead to better

insight of the intersection techniques. The intersection of random signals with periodic signals that have adaptive periodicity is another interesting project.

A more reliable and simpler reconstruction technique for nonuniform samples is also recommended for future work.

The effect of channel distortion on the nonuniform pulses is another topic for futher research.

An experimental verification of the feedback techniques for the improvement of an aliased signal is another interesting project for future work.

APPENDIX A

THEOREMS AND EQUATIONS REGARDING THE UNIFORM AND NONUNIFORM SAMPLES

Theorem 1: Uniform samples are uniquely reconstructable at the Nyquist rate.

$$S(t) = \sum_{k=-\infty}^{\infty} S(kT)\ \text{sinc}\ W(t - kT) \qquad \text{A-1}$$

Where $S(t)$ is bandlimited at $\frac{W}{2}$.

Theorem 2: A function $s(t)$ bandlimited to the interval $-\frac{W}{2} < w < \frac{W}{2}$ can be uniquely recovered from a set of samples $s(t_{ki})$ obtained at instants $t = t_{ki} = kT + t_i$, spaced according to a periodically recurring, nonuniform pattern.

We may write

$$s(t) = \sum_{k=-\infty}^{\infty} \sum_{i=o}^{m} s(t_{ki})\phi_{xi}(T) \qquad \text{A-2}$$

where

$$\phi_{ki} = \frac{\prod_{j=o}^{m} \sin \frac{W(t - kT - t_i)}{2}}{\frac{KW(t - kT - t_i)}{2}} \quad \text{and} \quad K = \prod_{\substack{r=o \\ r \neq i}}^{m} \sin \frac{W(t_i - t_r)}{2}$$

A-3

Theorem 3: A function S(t), bandlimited to $-\frac{W}{2} < w < \frac{W}{2}$, can be uniquely reconstructed from a set of samples which are nonuniformly spaced but satisfy the condition that there be precisely N distinct samples to every interval of length NT, where N is some finite integer. The interpolation formula will be of the form

$$S(t) = \sum_{\substack{k=-\infty \\ k\neq k_p}}^{\infty} S(kT)\,\phi_a(k,T) + \sum_{p=1}^{m} S(t_p)\,\phi_b(k_p,t) \qquad \text{A-4}$$

where

$$\phi_a(k,T) = \frac{K_1 \sin\frac{W(t-kT)}{2} \prod_{p=1}^{m}(t-t_p)}{\frac{W(t-kT)}{2} \prod_{p=1}^{m}(t-k_pT)}$$

$$K_1 = \frac{\prod_{p=1}^{m}(kT - k_pT)}{\prod_{p=1}^{m}(kT - t_p)}$$

$$\phi_b(k_p,t) = \frac{K_2 \sin\frac{Wt}{2} \prod_{\substack{q=1 \\ q\neq p}}^{m}(t-t_q)}{\prod_{p=1}^{m}(t-k_pT)}$$

$$K_2 = \frac{\prod_{p=1}^{m} (t_p - k_p T)}{\sin \frac{Wt_p}{2} \prod_{\substack{q=1 \\ q \neq p}}^{m} (t_p - t_q)}$$

Theorem 4: Uniform Sampling

Suppose a signal is sampled uniformly at the Nyquist rate. Any other signal passing through the samples has a higher bandwidth than the original signal.

Proof: If the latter signal has equal or less than the bandwidth of the original signal, then two different signals can be reconstructed from the samples at the Nyquist rate. This is contradictory to the uniqueness.

Corrollary A: No sine wave can be generated to pass the uniform samples with a frequency equal or less than the highest frequency content of the signal. Therefore the intersection of a sine signal with any other signal will not result in uniform samples. This fact also holds true for the principal frequency of a triangular waveform.

Corrollary B: Suppose there are uniform samples at the sampling rate $\frac{1}{T}$. There are many curves that can be fit on these samples. The curve (signal) with the lowest bandwidth

that fits the samples is derived by low pass filtering the samples by a filter with a passband of $\frac{1}{2T}$. Any other low pass filters with lower bandwidth do not fit the samples.

Theorem 5: Nonuniform Sampling

Suppose a signal is sampled nonuniformly at the Nyquist rate. Any other signal passing through the samples has a higher bandwidth than the original signal.

Proof: Otherwise, it will contradict the uniqueness of the nonuniform sampling (Theorem 3).

Corrollary C: Unlike the uniform samples, a sine wave can be generated to fit the nonuniform samples with a frequency equal to half of the Nyquist rate or the bandwidth of the original signal. This can be shown by the intersection of a signal with a sine wave with large amplitude at the Nyquist rate. Both the signal and the sine wave fit the nonuniform samples. This fact does not contradict Theorem 5 since the sampling theorems are for the energy signals only.

APPENDIX B

FOURIER SERIES REPRESENTATION OF NONUNIFORM PULSES

In the Section II, nonuniform impulses were represented by a Fourier series equivalent. In this Appendix, the Fourier Series expansion of nonuniform pulses (Figure B-1) is discussed. These pulses are derived from the intersection of a random signal, x, and a periodic signal, z(t). The nonuniform pulses are made uniform through the following transformation:

$$t_m = (m-1)T + f^{-1}x(t_m) \quad \Rightarrow x_s(t) = \frac{1}{p}\sum_{m=o}^{\infty} \Pi\{\frac{t-(m-1)T-f^{-1}[x(t)]}{p}\} \qquad \text{B-1}$$

$$Q(t) = t - f^{-1}[x(t_m)] \text{ where } Q(t_m) = (m-1)T \qquad \text{B-2}$$

The nonuniform pulses in Q domain is represented in Figure B-2. The periodic function x_s is represented by the Fourier series expansion in terms of Q

$$x_s(Q) = \frac{C_o}{2} + \sum_{n=1}^{\infty} C_n(Q) \cos \frac{(2n\pi Q)}{T} \qquad \text{B-3}$$

where

$$C_n = \frac{2}{T} \int_o^T x_s(Q) \cos\left(\frac{2n\pi Q}{T}\right) dq \qquad \text{B-4}$$

which yields:

$$C_o = \frac{2}{T}$$

$$C_N = \frac{T}{P_\pi n} \sin \frac{\pi np}{T} = \text{sinc} \frac{np}{T} \qquad \text{B-5}$$

Thus,

$$x_s(Q) = \frac{2}{T} + \sum_{n=1}^{\infty} \text{sinc} \frac{np}{T} \cos\left(\frac{2\pi nQ}{T}\right) \qquad \text{B-6}$$

or in time domain

$$x_s(t) = \frac{2}{T} + \sum_{n=1}^{\infty} \text{sinc} \frac{np}{T} \cos\left\{\frac{2\pi n\{t - f^{-1}[x(t_m)]\}}{T}\right\} \qquad \text{B-7}$$

As P approaches zero, the train of the pulses approach a train of impulses. Equation B-7 becomes:

$$x_s(t) = \frac{2}{T} + \sum_{n=1}^{\infty} \cos\left\{\frac{2n\{t - f^{-1}[x(t_m)]\}}{T}\right\} \qquad \text{B-8}$$

Where $\lim_{p \to 0} (\text{sine} \frac{np}{T}) \to 1$

Comparing Equation B-8 to the Equation 4-7, we have

$$\lim_{\rho \to o} [x_s(t)] = \{1 - \dot{x} \frac{df}{dx}^{-1} [x(t)]\} \sum_{n=1}^{\infty} \{1+2 \cos [nwt-nwf^{-1}[x(t)]]\}$$

APPENDIX C

PHASE JITTER ANALYSIS OF NONUNIFORM PULSES

Noise analysis has been done extensively on PPM and PFM signals.[45,46,24,61,62] Some of the analysis can be used for any intersecting modulation pulses. The phase jitter analysis of nonuniform pulses follows:[46]

A convenient type of pulse to use as means of analysis is the "raised cosine" as shown in Figure C-1. Its equation is given by:

$$g(t) = \frac{A}{2}(1 + \cos \pi f_b t), \quad -T \quad t < T, < f_b = \frac{1}{T} \qquad \text{C-1}$$

For practical purposes the bandwidth required for transmission of the pulse can be taken as $2f_b$.

A noise wave of relatively small instantaneous value v_n displaces the time of detection by τ, where

$$\frac{v_n}{-} = g'(-\frac{T}{2}) = \frac{\pi f_b A}{2} \qquad \text{C-2}$$

The peak to peak position swing is represented by 2λ. A sine wave signal modulates the pulse position by $\pm\lambda$ and has mean-square deviation $\lambda^2/2$. The mean-square deviation is:

$$E\tau^2 = \frac{4Ev_n^2}{(\pi f_b A)^2} \qquad \text{C-3}$$

The mean-square value of the nonuniform pulses is

$$P_s = \frac{1}{2\lambda} \int_{-T}^{T} g^2(t)\, dt = \frac{3A^2}{8\lambda f_b} \qquad \text{C-4}$$

Hence the signal to noise ratio is given by

$$S/N = \frac{\pi^2 f_b^2 \lambda^2 A^2}{6 w_o} = \frac{\pi^2 f_b^2 \lambda^3 P_s}{6 w_o} \qquad \text{C-5}$$

The signal to noise ratio of the nonuniform pulses is similar to that obtained by FM in that the improvement follows the square of the transmission bandwidth. As the bandwidth is increased indefinitely, the accompanying increase in total noise power eventually causes a sufficient number of false pulses to prevent further improvement by band widening.

APPENDIX D

THRESHOLD DETECTION OF NONUNIFORM PULSES WITH ADDITIVE GAUSSIAN WHITE NOISE

If phase jitter (Appendix C) of nonuniform pulses are neglected and false and missing pulses are predominant, the analysis is as follows:

Let the instantaneous pulse frequency $f_p = T$, $f_{p(min)} \leq f_p \leq f_{p\ (max)}$ (Figure 2-9 and 2-10). The effect of channel noise may be evaluated by considering the number of false pulses per unit time at this pulse frequency and then averaging this with respect to the pulse frequency range. The pulse duration is τ and the space interval is $T - \tau$. Pozin[36] studied the case $\tau = \frac{T}{2}$. His basic method is adopted here.

Let e_n be the channel noise assumed Gaussian white noise with zero mean value and standard deviation E_N, which is independent in each interval. The probability of a missing pulse in each interval is:

$$P_p\left(\frac{e_n}{E_n} - \frac{E_f - E_o}{E_n}\right) = \frac{1}{\sqrt{2\pi}} \int_{-\infty}^{\frac{E_o}{E_n}} e^{-\delta^2/2}\, dz =$$

$$\frac{1}{\sqrt{2\pi}} \int_{\frac{E_o}{E_N}}^{\infty} e^{-z^2/2} dz = V\left(\frac{E_o}{E_n}\right) \qquad \text{D-1}$$

Where E_f is the amplitude of the transmitted pulses and $E_o = \frac{E_f}{2}$ is the threshold level. The probability of a false pulse (P_s) is equal P_p in Equation D-1.

Let k_p be a binary random variable representing the number of false pulses in a signal pulse duration τ. If a pulse is missing, $k_p = -1$, otherwise $k_p = o$. Let

$$P_p(k_p = -1) = P_p = V\left(\frac{E_o}{E_n}\right)$$

and

$$P_p(k_p = o) = 1 - P_p = 1 - V\left(\frac{E_o}{E_n}\right) \qquad \text{D-2}$$

The average of false pulses in the interval is equal to

$$Ek_p = (-1)P_p + o\,(1-P_p) = -P_p = -V\left(\frac{E_o}{E_n}\right)$$

The standard deviation k_p is

$$E(k_p^2) - (Ek_p)^2 = (-1)^2 P_p = V\left(\frac{E_o}{E_N}\right) \qquad \text{D-3}$$

where Ek_p is assumed to be very small. Let n_s = number of elementry time segments (τ) in one space interval = $\frac{T-\tau}{\tau} = \frac{1}{\tau f_p} - 1$, and k_s be defined as the number of false pulses in a space interval $T - \tau$. A false pulse occurs only when it is isolated from the neighboring false pulses and signal pulses by the amount τ. Hence, the number of false and lost pulses (m) in each interval is less than or equal to n_s. One lost pulse is assumed to be -1 false pulse.

The probability of m out of n_s elementary time segments being distorted is

$$P_{sm} = C_{n_s}^{m} (P_s)^m (1 - P_s)^{n_s - m}$$

where

$$C_{n_s}^{m} = \frac{n_s!}{m!\ (n_s - m)\ !} \qquad \text{D-4}$$

At a given number $m(o \leq m \leq n_s)$, the probability of k_s false pulses for $k_s < m$ (Figure D-1) is given as follows:

$$P_{sm}(k_s) = A_{sm}(k_s) \ (P_s)^m (1-P_s)^{n_s-m} \qquad \text{D-5}$$

where $A_{sm}(k_s)$ = a coefficient for forming k_s false pulses by m false and lost pulses in a space interval T - .

Hence

$$P_{sm} = \sum_{k_s=-1}^{m} P_{sm}(k_s)$$

with

$$C_{n_s}^{m} = \sum_{k_s=-1}^{m} A_{sm}(k_s) \qquad \text{D-6}$$

However, a given number of false pulses, k_s, may result from a different number of false and lost pulses (Figure D-1) in the space interval for all possible values of m in the range $k_s \leq m \leq n_s - (k_s+1)$ is:

$$P_s(k_s) = \sum_{m=k_s}^{n_s-(k_s+1)} P_{sm}(k_s) = \sum_{m-k_s}^{n_s-(k_s+1)} A_{sm}(k_s) (P_s)^m (1-P_s)^{n_s-m} \qquad \text{D-7}$$

Let $k_s(max)$ be the maximum number of false pulses that

may occur over a space interval $T - \tau$.

$$k_s(\max) = \frac{n_s - 2}{2} \quad \text{for even } n_s > 2$$

$$= \frac{n_s - 1}{2} \quad \text{for odd } n_s > 2$$

$$= -1 \qquad \text{for } n_s = 1, 2 \qquad \text{D-8}$$

The mean number of false pulses over a given space interval $T - \tau$ at a signal pulse frequency f_p is

$$E(k_s) = \sum_{k_s=-1}^{k_s(\max)} k_s \, P_s(k_s) =$$

$$= \sum_{k_s=-1}^{k_s(\max)} k_s \sum_{m=k_s}^{n_s-(k_s+1)} A_{sm}(k_s) (P_s)^m (1-P_s)^{n_s-m} \qquad \text{D-9}$$

The standard deviation is

$$\sigma^2 = E(k_s^2) - (Ek_s)^2 = \sum_{k_s=-1}^{k_s(\max)} (k_s - Ek_s)^2 P_s(k_s) \qquad \text{D-10}$$

The rigorous evaluation of $A_{sm}(k_s)$ is rather complicated.[36] An approximate method of determining Ek_s due to Pozin[36] can be applied with much ease. Consider the case that there is only one false pulse occurring in the space interval for $n_s > 2$. The probability of occurrence of such a false pulse is $(n_s - 2)\ P_s$. When there is more than one false pulse, the mean number of false pulses in the space interval may be approximated as:

$$E(k_s) \simeq (n_s-2)P_s = (n_s-2)v\left(\frac{E_o}{E_n}\right),\ n_s \leq 1 \qquad \text{D-11}$$

$$\sigma^2 = E(k_s^2) - (Ek_s)^2 \simeq \sum_{k_s=-1}^{k_s(max)} (k_s-o)^2\ P_s(k_s),\ \text{where } E(k_s) \simeq o \qquad \text{D-12}$$

Assume again that the probability of forming only one false pulse by one lost or false pulses in a space interval is $(n_s-2)\ P_s$ for $n_s > 2$,

$$\sigma^2 = (1-o)^2\ P_s(k_s=1) = (n_s-2)\ P_s, \qquad \text{for } n_s > 2$$

Also,

$$\sigma^2 = \sum_{k_s=-1}^{o} (k_s-o)^2\ p_s(k_s) = (-1-o)^2\ P_s(k_s=-1)P_s, \text{ for } n_s-1$$

Hence,

$$\sigma^2 = |n_s - 2| V \left(\frac{E_o}{E_n}\right) \text{ for } n_s \geq 1 \qquad \text{D-13}$$

The mean number of false pulses in one period, T, is $Ek = E(k_s) + E(k_p)$. The mean error Δ_{av} at the signal pulse frequency f_p is defined as the mean number of false pulses per unit time at the pulse frequency f_p; from Equations D-3 and D-11

$$\Delta_{av} = \frac{Ek}{T} = f_p(Ek_s + Ek_p) \simeq f_p(n_s - 3)\, V\left(\frac{E_o}{E_n}\right) \text{ Pulses/Section}$$

$$\simeq f_p \left(\frac{1}{\tau f_p} - 4\right) V\left(\frac{E_o}{E_n}\right) \qquad \text{for } n_s > 1,\ f_p > \frac{1}{2\tau} \qquad \text{D-14}$$

The average absolute mean error over the pulse frequency range $\Delta f_p = f_p(\max) - f_p(\min)$ is:

$$E\Delta_{av} = \frac{1}{\Delta f_p} \int_{f_p(\min)}^{f_p(\max)} |\Delta_{av}|\, d \quad \text{pulses/sec.}$$

$$= \frac{2}{\Delta f_p} V\left(\frac{E_o}{E_n}\right) \left\{ \left[f_p(\max) - \frac{1}{4\tau} \right]^2 + \left[\frac{1}{4\tau} - f_p(\min) \right] \right\}^2$$

pulses/sec. D-15

The standard deviation of the number of false pulses in one period T at a signal pulse frequency f_p is:

$$E(k_s - Ek_s)^2 + E(k_p - Ek_p)^2.$$

The mean square error $\Delta^2_{me.sq.}$ mean square is defined as

$$f_p^2\{ E(k_s - Ek_s)^2 + E(k_p - Ek_p)^2 \qquad \text{D-16}$$

Substituting Equations D-3 and D-13 in the Equation D-16 we have

$$\Delta^2_{me.sq.} = f_p^2 \left[\left| \frac{1}{\tau f_p} - 3 \right| + 1 \right] V\left(\frac{E_o}{E_n}\right) =$$

$$= \left[\left| \frac{1}{\tau} f_p - 3 f_p^2 \right| + f_p^2 \right] V\left(\frac{E_o}{E_N}\right) \quad \text{for } f_p < \frac{1}{2\tau}$$

The average mean square error over the frequency range f_p is

$$E\,\Delta^2_{me.sq.} = \frac{1}{\Delta f_p} \int_{f_p(min)}^{f_p(max)} \Delta^2_{me.\,sq.}\, d_{fp}\,(\text{Pulses/sec.})^2$$

$$V\left(\frac{E_o}{E_n}\right) = \frac{}{5\ 4\ \Delta f_p}\ [\ 36(f_p^{\ 3}(\max) + f_p^{\ 3}(\min) - \frac{27}{\tau}\ (f_p^{\ 2}(\max) +$$

$$+ f_p^{\ 2}\ (\min) + \frac{2}{\tau^3}]\ \ (\text{pulses/sec.})^2$$

APPENDIX E

NOISE ANALYSIS FOR THE TRANSMISSION OF NONUNIFORM PULSES AT THE ZERO CROSSINGS OF A SQUARE WAVE

If a square wave passing through the nonuniform pulses is transmitted, a perfect clipper at the receiver is used. The output of the limiter is a new square wave with zeros displaced(Figure F-1). The crosscorrelation between the transmitted and clipped received waveforms compared to the autocorrelation of the transmitted signal is a measure of the zeros displacement.[4] Assume s(t) to be the transmitted random signal that is stationary with zero mean, and n(t) the stationary, zero-mean, Gaussian, additive and independent noise. s(t) is the output of the perfect clipper. Relying on the Fourier transform pair $\operatorname{sgn} v \longleftrightarrow \frac{2}{jw}$, we describe the relation between the input and the output of this device by:[4]

$$\hat{s}(t) = [R_{\hat{s}\hat{s}}(o)]^{\frac{1}{2}} \frac{1}{\pi j} \int_{-\infty}^{\infty} w^{-1} e^{jw[s(t) + n(t)]}\, dw$$

then with $s(t + \tau) = s_1$ and $s(t) = s_2$

$$R_{s\hat{s}}(\tau) = E[s(t+\tau)\,\hat{s}(t)] =$$

$$[R_{s\hat{s}}(o)]^{\frac{1}{2}} \frac{1}{\pi i} \int_{-\infty}^{\infty} w^{-1} \{ [\int_{-\infty}^{\infty}\int_{-\infty}^{\infty} s_1 e^{jws_2} f(s_1,s_2)\, ds_1 ds_2] \times$$

$$\times \int_{\infty}^{\infty} e^{jwn} f(n)\, dn \}\, dw$$

where $f(s_1,s_2)$ is the joint density of $s(t)$ and $s(t+\tau)$, and $f(n)$ is the density of the noise. The characteristic function of the zero-mean Gaussian noise is

$$\phi(w) = \int_{\infty}^{\infty} e^{jwn} f(n)\, dn = e^{\frac{-N}{2} w^2}$$

where N is the noise power. With $P_{ij}(\tau)$ the transition probabilities of the original rectangular waveform ($P_{12}(\tau)$ is the probability that the transmitted signal is positive at t and negative at $t+\tau$, etc.), we have with $A = \sqrt{R_{ss}(o)}$,

$$f(s_1,s_2) = \delta(s_1-A)\,[P_{11}(\tau)\,\delta(s_2-A) + P_{12}(\tau)\,\delta(s_2+A)]$$

$$+ \delta(s_1+A)\,[P_{21}(\tau)\,\delta(s_2-A) + P_{22}(\tau)\,\delta(s_2+A)]$$

Thus,

$$\frac{1}{A} \iint s_1 e^{jws_2} f(s_1,s_2)\, ds_1\, ds_2 = P_{11}(\tau)\, e^{jwA} +$$

$$+ P_{12}\, e^{-jwA} - P_{21}\, e^{jwA} - P_{22}\, e^{-jwA}$$

and since

$$P_{11} + P_{12} = .5$$

$$P_{21} + P_{22} = .5$$

$$P_{12} = P_{21}$$

$$P_{11} = P_{22}$$

$$\frac{R_{ss}(\tau)}{R_{ss}(o)} = P_{11}(\tau) + P_{22}(\tau) - P_{12}(\tau) - P_{21}(\tau)$$

we have

$$P_{11}(\tau) = P_{22}(\tau) = \tfrac{1}{4}\left[1 + \frac{R_{ss}(\tau)}{R_{ss}(o)}\right]$$

$$P_{21}(\tau) = P_{12}(\tau) = \tfrac{1}{4}\left[1 - \frac{R_{ss}(\tau)}{R_{ss}(o)}\right]$$

and finally

$$\frac{1}{A}\int_{-\infty}^{\infty}\int_{-\infty}^{\infty} s_1 \, e^{jws_2} \, f(s_1, s_2) \, ds_1 \, ds_2 = j \frac{R_{ss}(\tau)}{R_{ss}(o)} \sin wA$$

Thus

$$\frac{R_{s\hat{s}}(\tau)}{R_{ss}(o)} \left[\frac{R_{ss}(o)}{R_{\hat{s}\hat{s}}(o)}\right]^{\frac{1}{2}} = \frac{1}{\pi}\int_{-\infty}^{\infty} w^{-1} \sin w\sqrt{R_{ss}(o)}\; e^{\frac{N}{2}w^2}\, dw$$

with $v = w\,[R_{ss}(o)]^{\frac{1}{2}}$, $\alpha = R_{ss}(o)/N$ (the signal to noise ratio), and the normalized correlations.

$$\rho_{s\hat{s}}(\tau) = \frac{R_{s\hat{s}}(\tau)}{[R_{ss}(o)\; R_{\hat{s}\hat{s}}(o)]^{\frac{1}{2}}}$$

$$\rho_{ss}(\tau) = R_{ss}(\tau) \;/\; R_{ss}(o)$$

we get

$$\frac{\rho_{s\hat{s}}(\tau)}{\rho_{ss}(\tau)} = \frac{1}{\pi}\int_{-\infty}^{\infty} v^{-1} \sin(v)\; e^{-v^2/2\,\delta}\, dv$$

Expanding sin v in series:

$$\frac{\rho_{s\hat{s}}(\tau)}{\rho_{ss}(\tau)} = \frac{2}{\pi}\sum_{n=o}^{\infty} \frac{(-1)^n}{(2n+1)!}\int_{0}^{\infty} u^{2n}\; e^{-v^2/2}\, dv =$$

$$= \sqrt{\frac{2}{\pi}}\sum_{n=o}^{\infty} (-1)^n\; \frac{(2n-1)!}{(2n+1)!}\; \delta^{n+\frac{1}{2}}$$

We note that for high values of

$$\lim_{\delta \to \infty} \frac{\rho_{s\hat{s}}(\tau)}{\rho_{ss}(\tau)} \simeq \frac{2}{\pi} \int_0^{\infty} \frac{\sin v}{v} \, dv = \frac{2}{\pi} \, si(\infty) = 1$$

For the signal to noise ratio = 9dB, $\frac{\rho_{s\hat{s}}(\tau)}{\rho_{ss}(\tau)} = .99.$

Thus, it can be seen that even with moderate signal to noise ratio the crosscorrelation $P_{s\hat{s}}(\tau)$ between the transmitted and clipped received signals is close to the autocorrelation $\rho_{ss}(\tau)$. This indicates a slight change of the zero crossings position. The noise acts in two quite different ways on the transmitted signal:

i) It adds or eliminates some zero crossings.

ii) It displaces the zero crossings.

Obviously, when $\delta >> 1$, the probability of the first phenomenon is very small.

The analysis for the zero crossings displacement shows that it has the same characteristics as phase jitter (Appendix C). Fawe[4] has shown that by using the zero crossing reconstruction, the zero crossing displacement of the random square wave due to the noise behaves like an FM signal, i.e. bandwidth to noise reduction.

PART XI

LITERATURE CITED

1. J. Max, "Quantizing for Minimum Distortion", IRE Transaction on Information Theory, PP. 7-12, March 1960.

2. J.Y. Huang, "Quantization of Correlated Random Variables" Ph. D. Dissertation, Yale University, New Haven, Ct., 1962.

3. L. S. Golding and Schultheiss, "Study of an Adaptive Quantizer", Proc. of the IEEE, PP. 293-297, March 1967.

4. A. L. Fawe, "The Use of Zero-Crossings in Signal Processing", Master of Science Thesis, Poly. Inst. of Brooklyn, Brooklyn, N.Y., 1968.

5. S.O. Rice, "Mathematical Analysis of Random Noise", BSTJ, July 1948.

6. S.S. Bendat, "Principles and Applications of Random Noise Theory", John Wiley & Sons, 1958

7. B. Carlson " Communication Systems: An Introduction to Signals and Noise in Electrical Communications", McGraw - Hill, 1968

8. B. Friedman, "Principles and Techniques of Applied Math", John Wiley, New York, 1956.

9. J. D. Bruce, "Optimum Quantization", MIT. Research Lab. of Electronics, Cambridge, Mass., Tech. Report 429.

10. V.R. Algazi, "Useful Approximation to Optimum Quantization", MIT Electronics Research Lab. Quart. Prog. Rep. 79, PP. 185, October 1965.

11. R.C. Wood, "On Optimum Quantization", IEEE Trans. on Information Theory, Vol. lT-15, No. 2 March 1969.

12. P.F. Panter and W. Rite, "Quantization Distortion in Pulse Count Modulation with Nonuniform Spacing of Levels", Proc. IRE, Vol. 39, PP. 44-48, January 1951.

13. T. Berger, "Optimum Quantizers and Permutation Codes", IEEE Trans. on Information Theory, Vol. IT-18, No. 6, November 1972.

14. L.S. Golding, "A Study of Adaptive Quantization Techniques", Ph.D. Dissertation, Yale University, New Haven, Ct. 1970.

15. R.M. Wilkinson, "An Adaptive Pulse Code Modulation for Speech Signals", Procurment Executive, Ministry of Defense. Signals Research and Development Establishment. Report No. 72001, January 1972.

16. L.S. Butler, "The Rating of Deltasigma and Adaptive PCM Speech Coding Systems", Signals Research and Development Establishment, Report No. 72017.

17. D. Weber and F.J. Wynhoff, "The Concept of Self Adaptive Data Compression," PGSET Rec., Sec. 4.1, 1962

18. S.S. Bendat, OP. CIT., P. 382

19. H.E. Rowe, "Signals and Noise in Communication Systems" D. Van Nostrand Company, Inc., Princeton, New Jersey, 1965.

20. L.W. Gardenhire, "Redundancy Reduction the Key to Adaptive Telemetry, "Proc. of the Nat'l Tel. Conf., 1964.

21. C.M. Kortman, "Redundancy Reduction - A Partial Method of Data Compression, "Proc. of IEEE, Vol. 55, No. 3, March 1967

22. C.A. Andrews, J.M. Davies and G.R. Schwarz, "Adaptive Data Compression", Proc. of IEEE, Vol. 55, No. 3, March 1967

23. A. Papoulis, "Probability Random Variables and Stochastic Processes", McGraw-Hill, PP. 242-243, 1965.

24. D. Middleton, "An Introduction to Statistical Communication Theory", McGraw-Hill PP. 697, 1960.

25. J.L. Yen, "On Nonuniform Sampling of Bandwidth Limited Signals", IRE Trans. on Circuit Theory, PP. 253, 1956

26. P.M. Derusso, R.J. Roy and C.M. Close, "State Variables for Engineers", John Wiley and Sons, Inc., P. 292, 1965

27. F. Reza, "An Introduction to Information Theory", McGraw-Hill, pp. 258, 1961.

28. W.R. Bennett, "Spectra of Quantized Signals", B.S.T.J., pp. 448-472, July 1948.

29. S. Narayano and L.E. Franks, "The Spectra of Digitally Encoded Video Signals", IEE Trans. on Comm. Tech. Vol. Com-19, No. 4, August 1971.

30. B.D. Stavron, "Data Compression for Documents Using Run Length Coding", A Technical Note, PHILCO-FORD Corporation, Willow Grove, Penn. 1969

31. J.R. Oswald, "CODEST: A New Pulse-Code Modulation System for Telegraph and Data Transmission", IEEE Trans. on Comm. Tech., Vol. Com-18, No. 3, June 1970.

32. A.E. Ross, "Theoretical Study of Pulse Frequency Modulation", Proc. IRE, Vol. 37, No. 71, PP. 1277-86, November 1949.

33. J.C. Rock, "Rucursive Plane Analysis", Ph.D. Dissertation The Ohio State University, 1972.

34. C. Li, "Integral Pulse Frequency Modulated Systems", Ph.D. Dissertation, Northwestern University, June 1961

35. J.C. Rock, OP. CIT. , PP. 133-135.

36. N.V. Pozin, "Concerning the Noise Stability of Pulse-Frequency Telemetry", Automation and Remote Control, Vol. 19, No. 10, PP. 948-956, October 1956.

37. A.M. Pschenichnikov, "A Static Transmitter Unit for Pulse-frequency Telemetry Systems", Automation and Remote Contro1 Vol. 18, No. 5, PP. 485-490, May 1957.

38. J.C. Rock, OP. CIT., PP. 4-5.

39. A.V. Meyer, "Pulse-Frequency Modulation and its Effect In Feedback Systems", Ph.D. Dissertation, Northwestern University, 1961.

40. M. Davidson; H. Josph and N. Zucher," Using Markless Pulse Train to Communicate", Electronics, 31: 89-91, November 1958.

41. J.C. Rock, OP. CIT. P. 135.

42. K. Horiuchi, "A Note on Sampling Principles for Continuous Signals with Time Varying Spectra", Elec. and Comm. in Japan, Vol. 51, No. 1, P. 122, 1968.

43. C. Li, OP. CIT., P. 15.

44. B. Carlson, OP. CIT. P.

45. H.E. Rowe, OP. CIT., P. 304.

46. M. Schwartz; W.R. Bennet and S. Stein, "Communication Systems and Techniques", McGraw-Hill, 1966.

47. A. L. Fawe, OP. CIT. P. 24.

48. J. Cohn, "A New Approach to the Analysis of F.M. Threshold Detection", Proc. NEC, Vol. 12, PP. 221-236, 1956.

49. D. Shilling, "Theory of Operation of An All-Digital FM Discriminator, "IEEE Trans. on Comm. Tech., PP. 1160-1165, December 1972.

50. C. Atzeni and L. Masotti, "A New Sampling Procedure for the Synthesis of Linear Transversal Filters", IEEE Trans. on Aerospace and Electronic Systems, Vol. AES-7, No. 4, July 1971.

51. Regula, "

52. B. Sankur, and L. Gerhardt, "Reconstruction of Nonuniform Samples", International Conference on Comm., June 1973.

53. T. Fjallbrant and L. Bengisson, "A Network for the Recovery of Nonuniformly Sampled Signals", 5th Hawaii International Systems Conference.

54. M.R. Schroeder and J. L. Flanagan, "Bandwidth Compression of Speech by Analytic Signal Rooting", Proc. of IEEE, Vol. 55, No. 3, March 1967.

55. A. Macoski, "Bandwidth Reduction Technique", United States Patent Office, Ser. No. 731, 162, November 1970.

56. H. Freeman, OP. CIT. PP 77-89.

57. D.A. Linden and N.M. Abramson, "A Generalization of the Sampling Theorem", Information and Control, Vol. 3, 26-31, 1960.

58. E. Praffehuber, "Sampling Series for Band Limited Generalized Functions", IEEE Trans. on Information Theory, Vol. lT-17, No. 6, November 1971.

59. D.A. Linden, "A Discussion of Sampling Theorems", Proc. of IRE, July 1959.

60. S. Tazaki and K. Yamashita, "Fixed Difference Sampling Modulation System", Elec. and Comm. in Japan, Vol. 51-B, No. 4, 1968.

61. H.S. Black, "Modulation Theory", D. Van Nostrand Company, Inc. January 1966.

62. J.M. Wozencraft and I.M. Jacobs, "Principles of Communication Engineering", John Wiley and Sons, Inc. 1967.